AN ABSTRACT OF THE THESIS OF

Erin N. Anderson for the degree of Master of Science in Wood Science, and Civil Engineering presented on May 27, 2005.

Title: The Effects of Nail Bending-Yield Stress and Biological Deterioration on the Cyclic Performance of Shearwalls

Abstract approved: Redacted for Privacy

Robert J. Leichti

Key parts of the lateral force resisting system in wood-frame buildings are the shearwalls and the connections. The connections in wooden buildings are the primary source of ductility and energy dissipation; these are essential properties when buildings are exposed to lateral forces, such as wind and earthquakes. Shearwall design is based on new materials and a monotonic testing method, which departs from the actual situation because buildings age and are subjected to cyclic loads during wind and earthquake events. After the property losses experienced in the Loma Prieta and Northridge earthquakes, the engineering community realized there was a need to further investigate wooden shearwall performance especially with respect to condition and cyclic loading.

Individual sheathing-framing connections can be designed with respect to capacity and yield mode by using the yield mode equations. However, the relationship between individual connection characteristics and the performance of a shearwall remains unclear. The objective of this study was to investigate the relationship between individual connections and shearwall performance where nail bending-yield stress (f_{yb}) and biological deterioration of the wood were sources of variation in physical and simulation experiments.

In Part I of this research, it was hypothesized that nail bending-yield stress would affect initial stiffness and capacity of wood shearwalls. Four sets

of sheathing nails were specially manufactured so that each set had a different mean bending-yield stress: f_{yb}= 87 ksi, f_{yb} =115 ksi, f_{yb} =145 ksi and f_{yb}=241 ksi. Each set of nails was used to construct two test shearwalls. The shearwalls were 2×4 framing and sheathed one side with oriented strandboard. The walls were fully anchored and tested using a fully-reversed cyclic test protocol developed by the Consortium of Universities for Earthquake Engineering (CUREE). When the shearwall tests were complete, materials for lateral nail connection tests were removed from each wall. Twelve connections were tested from each shearwall using the CUREE protocol. Ten hysteretic parameters were extracted from the test data for each connector using the SASHFIT preprocessor. This data was used as input for the numerical model Cyclic Analysis of SHEar Walls (CASHEW) to predict the properties of the walls from which the materials came.

The dominant failure mode of the nails in the walls was withdrawal, however, the number of fatigue of fatigue failures increase with increasing bending-yield stress. The shearwall tests showed that the initial stiffness and energy dissipation of the shearwalls were not affected by the bending-yield stress of the nails. In addition, the capacities of the shearwalls were not drastically different. This was also mimicked in the connection tests. The computed shearwall performance matched the shearwall test data.

In Part II of the study, the effect of biological deterioration on shearwall performance was examined by simulation methods. The structural analysis software, CASHEW, was modified to allow multiple nail types. SASHFIT was used to determine the ten hysteretic parameters from nail test data. The nail test data included control nails and nail connections at four levels of increasingly more severe fungal deterioration. The simulation determined that the stiffness and capacity of the shearwall were affected by decay that started at approximately mid-height on one side and progressed downward and across the sill plate. For each temporal decay condition, thirty walls were

simulated where the nail parameters were randomly assigned and the capacity, stiffness, and energy dissipation of the shearwall were determined.

The results of this analysis indicate that the wall capacity and stiffness are not dramatically affected by decay unless a large percentage of the perimeter nails are affected by severe decay. Analysis showed that the distributions of peak capacity and initial stiffness are normally distributed. In addition, the displacement at peak capacity is not affected by the decay.

Two important inferences emerged from this study:

- Shearwall strength and stiffness are insensitive to sheathing nail bending-yield stress.
- Shearwall strength and stiffness are not affected by decay fungi until a large percentage of the perimeter nails are involved.

The Effects of Nail Bending-Yield Stress and Biological Deterioration on the Cyclic Performance of Shearwalls

by
Erin N. Anderson

A THESIS

submitted to

Oregon State University

in partial fulfillment of
the requirements for the
degree of

Master of Science

Presented May 27, 2005
Commencement June, 2006

Master of Science thesis of Erin N. Anderson presented on May 27, 2005.

APPROVED:

Redacted for Privacy

Major Professor, representing Wood Science and Civil Engineering

Redacted for Privacy

Head of the Department Wood Science and Engineering

Redacted for Privacy

Head of the Department of Civil, Construction and Environmental Engineering

Redacted for Privacy

Dean of the Graduate School

I understand that my thesis will become part of the permanent collection of Oregon State University libraries. My signature below authorizes release of my thesis to any reader upon request.

Redacted for Privacy

Erin N. Anderson, Author

ACKNOWLEDGEMENTS

The author expresses sincere appreciation to the following individuals and organizations:

Robert J. Leichti

David V. Rosowsky

Michael H. Scott

Edward G. Sutt, Jr.

Milo Clauson

Cameron Carroll

Jun Hee Kim

Stanley Bostitch

USDA, Center for Wood Utilization and Research

CONTRIBUTION OF AUTHORS

Robert Leicthi, David Rosowsky, and Edward Sutt assisted with writing Chapter 3. Robert J. Leichti assisted with the additional chapters.

TABLE OF CONTENTS

Page

1. Introduction 1
   1.1. Background 1
   1.2. Objectives 3
   1.3. Scope 4
2. Literature Review 6
   2.1. European Yield Mode and Nail Performance 7
   2.2. Shearwall Design 10
   2.3. Shearwall Tests 12
   2.4. Shearwall Models 13
   2.5. Role of Moisture and Decay in Shearwall Performance 16
3. Effect of Nail Bending-Yield Stress on Cyclic Performance of Wood Shearwalls 20
   3.1. Abstract 21
   3.2. Introduction 21
   3.3. Objectives 26
   3.4. Materials and Methods 26
      3.4.1. Single-Fastener Connection Tests 27
      3.4.2. Shearwall Tests 30
      3.4.3. Analysis Programs 31
   3.5. Results and Discussion 32
      3.5.1. Single-Fastener Connection Tests 32
      3.5.2. Shearwall Tests 33
      3.5.3. CASHEW Models and Seismic Analyses 36
   3.6. Conclusions 40
   3.7. References 41
4. Cyclic Performance of Wood Shearwalls as Affected by Decay ... 46
   4.1. Abstract 47
   4.2. Introduction 48

TABLE OF CONTENTS (Continued)

Page

4.3. Analysis and Design Scenario 49
4.4. Methods and Materials 51
4.5. Results 56
4.6. Conclusions 66
4.7. References 67
5. Conclusions 69
5.1. Bending-Yield Stress Analysis 69
5.2. Decayed Shearwall Analysis 70
5.3. Combined Assessment 70
Bibliography 72

TABLE OF APPENDICES

Page

Appendix A – Nail Bending-Yield Stress Data 84

Appendix B – Lateral Nail Connection Tests 86

Appendix C – Shearwall Tests 98

Appendix D – CASHEW Nail Bending-Yield Analysis 111

Appendix E – Decayed Lateral Nail Connection Tests 116

Appendix F – CASHEW Decay Analysis 119

Appendix G – Hysteretic Parameters 137

Appendix H – Revisions to CASHEW 140

Appendix I – Notation 142

LIST OF FIGURES

Figure		Page
3.1	Single nail lateral connection test specimen (a) dimensions and detail, (b) test apparatus	28
3.2	CUREE loading protocol used for single nail and shearwall tests.	29
3.3	Shearwall configuration for cyclic tests and numerical models	30
3.4	Average backbone curves for the two walls at each bending-yield stress value	34
3.5	Average cumulative energy dissipated at the primary cycles for the two walls at each f_{yb} value	34
3.6	Summary of CASHEW backbone curves for each sheathing nail bending-yield stress	37
3.7	Cumulative energy dissipated at the primary cycles from the shearwalls evaluated with CASHEW at each bending-yield stress value	38
3.8	Comparison of predicted peak wall displacements for the life-safety limit state	39
3.9	Comparison of predicted peak wall displacements for the Immediate-occupancy limit state	30
4.1	Structural configuration: shearwall with window where water enters at the window sill and runs down the stud (Zone 1)and along the sill plate (Zone 2 and 3)	50
4.2	CUREE cyclic loading protocol used for lateral nail tests by Kent (2004)	52
4.3	Hysteretic parameters for lateral nail tests or shearwall tests under cyclic loading (Folz and Filiatrault 2000).	54
4.4	Force-displacement response of a single lateral connection under CUREE loading protocol fit with SASHFIT estimated response	55

LIST OF FIGURES (Continued)

Figure — Page

4.5 Average backbone curves at each decay condition, (a) complete backbone curves in quadrant I; (b) backbone curves from 0.3 to 0.5 in. of displacement; (c) backbone curves for decay conditions 1 to 5 at maximum 58

4.6 Box plots for initial stiffness values output from CASHEW 60

4.7 Box plots for displacement at peak capacity output from CASHEW 61

4.8 Box plots for peak capacity values output from CASHEW 61

4.9 Average cumulative energy dissipated at the primary cycle of the CUREE loading protocol for shearwalls at each decay condition 63

4.10 Initial stiffness distributions for shearwalls shown by decay condition 65

4.11 Peak capacity distributions for shearwalls shown by decay condition 65

LIST OF TABLES

Table		Page
3.1	Nail bending-yield stress from tests in compliance with F 1575 (ASTM 2002g), nail diameter 0.113 in., length 2-1/2 in., n=24.	26
3.2	Yield mode calculations for laterally loaded single nail connections constructed with Douglas Fir-Larch and 7/16-in. sheathing materials and four different varying f_{yb} nails.	27
3.3	Single fastener monotonic test results by nail f_{yb}	29
3.4	Hysteretic nail parameters for single lateral nail specimens from SASHFIT, Std & Btr, Douglas fir-Larch and 7/16-in. OSB, parenthetical values are coefficients of variation	32
3.5	Percentage of nail failures for single lateral connections and shearwalls by nail f_{yb} value	33
3.6	Summary of cyclically tested 8 × 8-ft. shearwall results for each nail bending-yield stress	35
3.7	Hysteretic parameters (n=1) from CASHEW for modeled shearwalls	37
4.1	Decay conditions for the shearwall where decay condition is described by Kent (2004)	50
4.2	Description of hysteretic parameters extracted from cyclic data by SASHFIT	53
4.3	Hysteretic parameters for nailed connections, where parenthetical values are coefficients of variation	54
4.4	Hysteretic shearwall parameters from CASHEW (n=30), where parenthetical values are coefficients of variation	59

LIST OF APPENDIX FIGURES

Figures		Page
B1	Modified lateral connection test set-up	87
C1	Shearwall test set-up	98
C2	Hydraulic actuator and set-up	99
C3	Split center stud from the 115 ksi wall before (left) after (right)	100
C4	Wall 1 hysteresis curve f_{yb}=87 ksi	100
C5	Wall 2 hysteresis curve f_{yb}=87 ksi	101
C6	Wall 3 hysteresis curve f_{yb}=115 ksi	101
C7	Wall 4 hysteresis curve f_{yb}=115 ksi	102
C8	Wall 5 hysteresis curve f_{yb}=145 ksi	102
C9	Wall 6 hysteresis curve f_{yb}=145 ksi	103
C10	Wall 7 hysteresis curve f_{yb}=241 ksi	103
C11	Wall 8 hysteresis curve f_{yb}=241 ksi	104
C12	Top plate separation from the studs	104
C13	Nail failure modes (left) OSB separation due to nail withdrawals, (middle) edge tear-out and pull-though, (right) fatigue	105
C14	Sheathing nail failure modes for Wall 1, f_{yb}=87 ksi	106
C15	Sheathing nail failure modes for Wall 2, f_{yb}=87 ksi	106
C16	Sheathing nail failure modes for Wall 3, f_{yb}=115 ksi	107
C17	Sheathing nail failure modes for Wall 4, f_{yb}=115 ksi	107
C18	Sheathing nail failure modes for Wall 5, f_{yb}=145 ksi	108
C19	Sheathing nail failure modes for Wall 6, f_{yb}=145 ksi	108

LIST OF APPENDIX FIGURES (Continued)

Figures		Page
C20	Sheathing nail failure modes for Wall 7, f_{yb}=241 ksi	109
C21	Sheathing nail failure modes for Wall 8, f_{yb}=241 ksi	109
F1	Wall configuration with adjacent window modeled by CASHEW	119
G1	Hysteretic parameters for connections and walls (Modified from Folz and Filiatrault 2000)	137

LIST OF APPENDIX TABLES

Tables		Page
A1	Summary of nail properties, n=24 per box, determined in accordance with method F 1575 (ASTM 2002g)	85
B1	f_{yb}=87 ksi nail hysteretic parameters for 15/32-in. OSB at 0.2 Hz	89
B2	f_{yb}=115 ksi nail hysteretic parameters for 15/32-in. OSB at 0.2 Hz	89
B3	f_{yb}=145 ksi nail hysteretic parameters for 15/32-in. OSB at 0.2 Hz	89
B4	f_{yb}=241 ksi nail hysteretic parameters for 15/32-in. OSB at 0.2 Hz	90
B5	f_{yb}=87 ksi nail hysteretic parameters for 15/32-in. OSB at 0.1 Hz	90
B6	f_{yb}=241 ksi nail hysteretic parameters for 15/32-in. OSB at 0.1 Hz	90
B7	Wall 1, f_{yb}=87 ksi nail hysteretic parameters	91
B8	Wall 2, f_{yb}=87 ksi nail hysteretic parameters	92
B9	Wall 3, f_{yb}=115 ksi nail hysteretic parameters	92
B10	Wall 4, f_{yb}=115 ksi nail hysteretic parameters	93
B11	Wall 5, f_{yb}=145 ksi nail hysteretic parameters	93
B12	Wall 6, f_{yb}=145 ksi nail hysteretic parameters	94
B13	Wall 7, f_{yb}=241 ksi nail hysteretic parameters	94
B14	Wall 8, f_{yb}=241 ksi nail hysteretic parameters	94
B15	Average bending yield nail hysteretic parameters	95
B16	f_{yb}=87 ksi nail hysteretic parameters for 1/2-in. plywood	95

LIST OF APPENDIX TABLES (Continued)

Tables		Page
B17	f_{yb}=115 ksi nail hysteretic parameters for 1/2-in. plywood	95
B18	f_{yb}=145 ksi nail hysteretic parameters for 1/2-in. plywood	96
B19	f_{yb}=241 ksi nail hysteretic parameters for 1/2-in. plywood	96
B20	Average embedment properties and moisture contents	97
B21	Yield mode calculations for laterally loaded single nail connections constructed with wood materials as described and varying f_{yb}	97
C1	Wall Energy Dissipated per Loop (lb·in.)	110
D1	Typical CASHEW Input File for Bending-Yield Stress	111
D2	CASHEW Cumulative Energy Dissipated (kip·in.)	112
D3	Typical SASH1 Input File for Bending-Yield Stress	113
D4	Cumulative distribution function for peak displacement data points for life-safety	114
D5	Cumulative distribution function for peak displacement data points for immediate-occupancy	115
E1	Connection hysteretic parameters for Control Group	117
E2	Connection hysteretic parameters for 0 Weeks Inoculation	117
E3	Connection hysteretic parameters for 5 Weeks Inoculation	117
E4	Connection hysteretic parameters for 10 Weeks Inoculation	118
E5	Connection hysteretic parameters for 20 Weeks Inoculation	118
E6	Connection hysteretic parameters for 30 Weeks Inoculation	118
F1	Randomized nail parameters at each decay condition	121

LIST OF APPENDIX TABLES (Continued)

Tables		Page
F2	Typical CASHEW Input File for Decayed Walls	125
F3	Wall hysteretic parameters for decay condition 1	127
F4	Wall hysteretic parameters for decay condition 2	128
F5	Wall hysteretic parameters for decay condition 3	129
F6	Wall hysteretic parameters for decay condition 4	130
F7	Wall hysteretic parameters for decay condition 5	131
F8	Wall hysteretic parameters for decay condition 6	132
F9	Wall hysteretic parameters for decay condition 7	133
F10	Cumulative distribution function data points for initial stiffness	134
F11	Cumulative distribution function data points for peak capacity	135
F12	Cumulative Wall Energy Dissipated (lb·in.)	136

1. Introduction

1.1. Background

Connections, shearwalls and diaphragms provide wood-frame buildings with a primary lateral force resisting system for wind and seismic loadings. Shearwalls are light weight and ductile and they transfer loads from the roof to the foundation: dead loads, live loads and transverse loads from wind or seismic activity. Timber shearwalls are typically framed with 2×4 (or 2×6) lumber and sheathed with engineered structural panels, such as plywood or oriented strandboard (OSB). The panels are connected to the wood frame with nails. The resistance capacity and stiffness of a shearwall can be changed by altering the nail spacing, increasing the panel thickness or by adding anchorage and hold downs. An extensive body of literature has developed since the 1950's describing the role of the nails and other construction variables such as exterior sheathing, framing, openings, and hold-downs, etc. on the performance of shearwalls.

The engineering design values for shearwalls are based on extensive monotonic testing of new walls made with new materials, which is not representative of the fully reversed cyclic loads that are imposed by earthquakes (Dolan and Madsen 1992a). Despite the differences between design value assignment and use conditions, wood shearwalls have gained a reputation for being highly resistant to earthquakes due to the high strength-to-weight ratio of wood and the ductility of connections used (Filiatrault 1990). However, damage to wood buildings in the Northridge and Loma Prieta earthquakes prompted further investigation of cyclic load effects in shearwalls and connections.

The California Universities for Research in Earthquake Engineering Caltech Woodframe project (CUREE) was established to examine the performance of wood-frame buildings and their connections in earthquake prone regions. This program was later re-named CUREE—The Consortium of

Universities for Earthquake Engineering. Within this study, the investigation team developed the CUREE loading protocol (Krawinkler et al. 2000). The non-near-fault protocol is intended to be more representative of earthquake loading than other cyclic protocols. It is a displacement controlled, fully-reversed cyclic-load protocol with leading and trailing cycles starting at relatively low amplitudes and progressing through a series of increasing amplitude cycles. This protocol is scaled to a reference displacement, which is based on monotonic tests. The protocol was initially devised for shearwalls, but it also has been used to evaluate individual nail and staple connections (Jones and Fonseca 2002; Kent 2004).

The sheathing-to-framing connections in shearwalls are important to the wall performance and in almost all cases these connections are nails or staples. A wall dissipates energy under cyclic loading. The energy introduced into a wall by a load is dissipated through the fasteners in the form of yielding, internal friction or non-recoverable damage (fracture). Typical nails used in wood-frame construction have a bending-yield stress (f_{yb}) of at least 100 ksi if the nominal diameter is 0.135 in. or less (ICC 2004), but they do not have a distinct yield point.

The sheathing nail connections have a nonlinear inelastic load-displacement relationship, so that when subjected to cyclic loading they have a complex hysteretic response of pinched hysteresis loops. Shearwalls exhibit hysteretic behavior similar to the connections. Many attempts have been made to model and understand the hysteretic behavior of the nail using numerical methods, finite-element analysis, and curve fitting procedures with empirical data. Several computer programs have attempted to predict the behavior of shearwalls with numerical methods. For example, Kasal and Leichti (1992) created a model with walls having nonlinear load-displacement characteristics using finite-element methods and superimposed quasi-super-elements. A more recent numerical model is CASHEW (Cyclic Analysis of SHEar Walls) (Folz and Filiatrault 2001).

CASHEW combines several concepts from earlier generation programs and treats the wall system as a single-degree-of-freedom system in order to predict the load-displacement response and energy dissipation of a wall subjected to the CUREE loading. The input parameters of CASHEW are based on the hysteretic response of a single sheathing nail connection and the global and local coordinates of the nails on all of the sheathing panels. The structural and numerical concepts of CASHEW subsequently were extended to whole structure analysis in the Seismic Analysis of Woodframe Structures (SAWS) (Filiatrault and Folz 2002; Folz and Filiatrault 2004b).

Allowable shearwall properties are based on monotonic tests of shearwalls fabricated with typical nails and new materials. Further, the implicit design assumption is that the condition of the structure remains unchanged throughout the life of the structure. However, many wood-frame structures experience water intrusion around wall openings, e.g., doors, windows, and at the sill plates, where the walls are attached to the foundation. The elevated moisture condition can be sufficient to support microbial activity in the form of decay fungi. Wilcox (1978) provides an overview of the effect of decay on solid wood and Kent (2004) summarizes the effect of decay for wood-based engineering materials. Experimental studies by Leichti et al. (2002) examined the effect of flood exposure on shearwalls, and Leichti et al. (2005) reported the effect of water saturated sill plates on cripple wall behavior. The effect of various special decay conditions was reported by Kim et al. (in review) using a CASHEW analysis.

1.2. Objectives

This project incorporates two separate studies that assess the role of nail connections in the performance of wood-frame shearwalls. The objectives of this project are:

1. Evaluate the performance of wood-frame shearwalls as affected by nail bending-yield stress.

2. Evaluate the performance of wood-frame shearwalls as affected by changes in wood condition, specifically the effect of a decay condition.

1.3. Scope

Within this project, the sheathing nail connections of shearwalls are examined. The accepted yield theory for connections assumes that the behavior of a connection is controlled by the properties of the nail and the properties of the wood main and side members, and the thickness of the side members. Since connections govern the behavior of the shearwall, altering the properties of the nail or the wood materials could modify the behavior of the shearwall. The first objective was addressed with a study where bending yield stress (f_{yb}) of the sheathing nail was modified while leaving the properties of the wood members constant. The investigation included lateral nail tests and shearwall tests with specially manufactured nails where nail f_{yb} was the independent variable. Sample connections were conditioned and tested using the CUREE loading protocol. The hysteretic parameters of the connections were extracted from the test data using a curve-fitting program called SASHFIT (Elkins and Kim 2003b). These hysteretic parameters were used in conjunction with CASHEW to model the behaviors of fully-anchored 8×8ft shearwalls sheathed with OSB that were in turn compared with experimental shearwalls.

The second objective is to assess the unknown effects of biological action on structural competence. Moisture intrusion and condensation are common problems in American homes. Millions of dollars are spent every year attempting to fix or prevent water problems (Smulski 1999 and 2000). Although moisture and decay have been identified as problems with connections, very little research has appeared in literature. This study assumes that a window is continually leaking at a corner and that the moisture ingress proceeds down the wall and along the sill plate. The condition creates a plume of moisture as well as decay. As the window continues to leak, decay

is introduced into the wall. First the side of the wall is wet, and the bottom of the wall is dry, then as the moisture spreads, the decay follows until the side and entire bottom of the wall are decayed to an extreme level. In the second part of this project, the wood is exposed to increasing severe levels of decay that alter the mechanical properties of the wood, but does not affect the bending-yield stress of the nail. This study uses previous connection data collected by Kent (2004) and determines the effect the progressive growth of decay on the overall shearwall behavior. This was done using a modified version of the CASHEW software. The results are stated in terms of cumulative distribution functions to provide the information essential to the specific conditional probability analysis using fragility methods.

2. Literature Review

The shearwalls in light-frame wood buildings are the lateral support resisting system, but the connections in the shearwalls provide ductility, damping and energy dissipation through mechanisms such as internal friction, non-recoverable damage, and connection failure and yielding of the metal fasteners, such as nails (Chui et al. 1998; Lam et al. 1997). The stiffness and energy dissipation capacity of a structural lateral load resisting system are important because by altering either can affect the performance of a structure (Shenton et al. 1998). The weakest link in a structure is often the connections (Kalkert and Dolan 1997), therefore, the key to predicting the overall system response through a numerical model is being able to properly model the hysteretic behavior of the nails (Foliente 1995). Wood is a brittle material in tension, so all of the ductility and energy dissipation of the system comes in the form of friction, wood material compression, and metal fastener yielding.

A contemporary wood shearwall consists of four main parts, engineered structural panels such as plywood or oriented strandboard (OSB), a wood stud frame, nails connecting the panels and the stud frame and the foundation that includes bolts and anchorage devices. The most recent numerical models are based on evidence that shows wood structures are controlled by the connections (Dolan 1989; Foliente 1994), particularly the sheathing-framing connection. The nail connections are important to the assembly performance because the sum of the individual nail behaviors equals the load-displacement response of the wall. From the load-displacement curves, the essential parameters including initial stiffness, and peak wall capacity and deflection at peak capacity can be extracted (Gupta and Kuo 1985; McCutcheon 1985; Filiatrault 1990; Dolan and Madsen 1992b). The yield point and ductility of the wall can also be determined from this data.

2.1. European Yield Mode and Nail Performance

Nails became one of the most common fasteners in wooden houses, structural timber constructions, and wooden assemblies after the industrial manufacturing started (Aune and Patton-Mallory 1986b). Yield limit theory (EYM) (Wilson 1917; Johansen 1949; Moller 1950; Larsen 1973; Aune and Patton-Mallory 1986 a, b) emerged as the common method of analysis for dowel-type fasteners. This theory assumes that the wood and the fasteners are rigid-plastic materials, and that the have ductile failure modes where they experience strain hardening rather than true yield stress (Smith et al. 2001).

The EYM analysis is based on the embedment strength of the wood, the bending-yield stress of the nail, and the joint geometry; it calculates the ultimate lateral load of a joint and its failure mode. The embedment strength, also known as the dowel bearing strength, is dependent on the specific gravity of the wood (Wilkinson 1991) and is the primary factor that measures the strength of the wood elements in the connection (Breyer et al. 2003). The bending-yield stress of the fastener predicts the load capacity of a mechanism that involves the formation of a plastic hinge (Breyer et al. 2003). All of the yield modes involve nail bending, wood crushing, or some combination of the two. The yield theory assumes that the joint does not fail at a load below the yield point due to insufficient spacing or end distances, ignores friction, and assumes that there is no joint deformation (Aune and Patton-Mallory 1986a).

Test data can also be used to assign properties to connections. The lateral capacity and yield load of a connection are read from the load-displacement curve. The yield load is approximated as the intersection of the load-deflection curve and a straight line parallel to the initial stiffness offset by 5 percent of the dowel diameter (AFPA 1999) and is between the ultimate load and the proportional limit. Changing the properties of the wood, the thickness of the side member, or the nail in the connection will alter the ultimate lateral load and possibly the controlling yield mode of the joint.

Four common models of failure for sheathing-framing connections can describe sheathing-framing connection failure: withdrawal, pull-through, fatigue and edge tear-out. Nail yielding (fatigue) and withdrawal are ductile modes of failure where as pull-through and tear-out failures, which are more common for overdriven nails, are non-ductile (Jones and Fonseca 2002). Overdriving nails has an effect similar to that of thickness swelling in the sheathing that causes the head of the head of the nail to be embedded into the face of the sheathing. A dominate failure mode is difficult to predict in walls, because the failure mode depends on the load and the materials used. An optimal ductile system would have the sheathing and sheathing nails fail simultaneously (Chai and Hutchinson 2003); however, that does not happen. Monotonically loaded nails show no signs of fatigue failure (Gatto and Uang 2003), and nail fatigue is not common in earthquake damage (He et al. 1998; Rose 1998). Although cyclically loaded nail failure modes are variable, all four modes can be common. Increased load cycles will be indicative of a more common occurrence of fatigue (He et al. 1998) because fatigue tends to occur post-peak capacity and in tests with larger displacements (Langlois et al. 2004). When load cycles are kept small, the dominate failure is arguably pull-through or withdrawal; withdrawal is most common on the edges of the panel around mid height and along the bottom plate, while nails in the corners and along the bottom plate are likely to pull through or tear-out before they fatigue (Dinehart and Shenton 1998). Nails along the bottom plate are also likely to fatigue, and the nails along the interior edge of the sheathing are likely to pull-through or tear-out due to a smaller edge distance (Langlois et al. 2004, Salenikovich and Dolan 2000; He et al. 1999).

The type of wood materials used can also affect the failure mode: thicker sheathing causes nails to be more susceptible to fatigue while thinner panels make nails more susceptible to pull-through (Salenikovich and Dolan 2003). Fatigue is more dramatic in OSB than in plywood (Shenton et al. 1998). The density of the wood studs impacts the type of failure, nails in

higher density studs are more likely to fatigue, while nails in low density studs are more likely to withdraw and sustain resistance longer (Ni and Chui 1994, Salenikovich and Dolan 2003). The load capacity of walls with lower density studs is slightly lower, but the deflection capacity is not affected. Displacements are limited by yielding; systems with less yielding capacity will have premature failures. The large displacements post-peak can be attributed to the loss of restraint due to the failure and fatigue of the nails.

The behavior of nailed connections depends on four interrelated factors: the wood, the nail, the joint characteristics, and the loading (Hunt and Bryant 1990). When the wall is subjected to a cyclic loading, the load-deflection curve is a series of pinched hysteresis loops where each successive loop has a degrading stiffness. The pinching is caused by the loss of stiffness at small joint slips where a cavity around the fastener is formed by the wood crushing. Repeated cycling causes the stiffness of the fastener to degrade due to a reduction of the bearing stiffness of the wood or due to withdrawal; the joint is loosened, and the nail is not fatigued (Dolan and Madsen 1992*b*; Foliente 1995). Similarly, at a repeated displacement there will be a degradation of strength. At small displacements, a nail will behave elastically, while at large displacements the nail behavior is inelastic and nonlinear without a distinct yield point (Filiatrault 1990), which makes the hysteretic response difficult to predict.

A set of hysteresis loops can be divided into four sections (White and Dolan 1995) where each section is defined with an exponential equation. Further research has determined that the positive quadrant hysteretic behavior can be captured with ten extracted parameters to fully describe one connection (Foliente 1995). The first five parameters K_o, r_1, F_o, r_2, Δ_u describe the envelope response of a connector, while the other five parameters r_3, r_4, F_l, α and β describe the hysteretic part of the response due to cyclic loading (Fonseca et al. 2002). The parameters that classify the envelope response emerged from parameters fit to monotonic load-displacement curves (Foschi

1974; Dolan and Madsen 1992a). A complete nonlinear load-slip curve provides information about the ultimate load, initial stiffness, unloading stiffness, post-peak stiffness, ductility, and residual deformation after unloading (Foschi and Bonac 1977), as well as the degrading factors. Although the overall behaviors of a nailed specimen can be seen with the backbone curve, which encompasses all of the hysteresis loops (Foliente 1995) and functions as an envelope for the cyclic response, the backbone curve is not synonymous to a monotonic curve, but can be used as an approximation for monotonic results (Kalkert and Dolan 1997). The hysteretic response and essential parameters of a shearwall can be predicted using the hysteretic characteristics of individual sheathing-framing nailed joints with similar properties and boundary conditions (Foliente 1995).

2.2. Shearwall Design

The yield mode equations are the principal design method for dowel-like connections in timber engineering. However, monotonic and cyclic test data can be used to establish or assess connection capacity and other performance characteristics. Although cyclic test data are not used in design, they are used for wall models. When designing a shearwall, several factors are taken into account in addition to the typical specifications for sheathing thickness and grade, framing species, size and grade and fastener types and schedule (Rose 1998). The resistance capacity of the shearwall is given as a unit shear—the amount of shear the wall can resist per lineal foot. Allowable unit shears for various types of wood structural panel shearwalls are listed in design tables in the International Building Code (ICC 2003), National Design Specification® (NDS) (AF&PA 2001), NER-272 (National Evaluation Service Committee 1997) and NES 2002, and other building documents. The shearwall tables in these codes were developed from the results of static push-over tests as classified in E2126 (ASTM 2002). The tables list values for standard wall constructions with varying properties including the framing

species and size, the sheathing thickness and grade, the stud spacing, nail spacing and size, and the presence of blocking, gypsum, or plaster and lath. The design tables can be adjusted for duration of load, wet service, temperature, grade and construction factors (NDS). Footnotes allow for adjustments based on specific gravity (G) when Douglas Fir-Larch or Southern Pine is not the species of lumber selected. The tabular design values provide no modification factors for changing the quality or properties of the wood products or any of the other parts of the wall such as anchorage. Modification factors would be beneficial for new components being introduced into the market, or the presence of decay that has altered the condition and the performance of the materials.

The unit shear capacity of the wall must be larger than the unit shear produced by the load. The shear demand on the wall is calculated from the reaction from the forces of the horizontal diaphragm that are transferred from the collector and chord to the drag strut of the wall (Tissel 1993). The shear load is the total base shear divided by the length of the wall and a resistance factor. The base shear is determined using equation 16-56 from the IBC 2003:

$$V = \frac{1.2 S_{DS}}{R} W \qquad [1]$$

S_{DS} is the design response acceleration at short periods determined in section 1615.1.3, and R is the response modification factor from Table 1617.6.2. W is the effective seismic weight, which is the result of the dead load and other loads, such as permanent live loads and snow loads. The response modification factor is 2.5 for light-framed walls with wood shear structural panels.

The equation for deflection comes from the IBC equation 23-2 as a method to calculate the story drift. The equation accounts for bending and shear as well as nail deformation and anchorage slip, which represents each of the four main components of the shearwall (ICC 2003).

$$\Delta_s = \Delta_b + \Delta_s + \Delta_n + \Delta_a$$
$$\Delta_s = \frac{8vh^3}{EAb} + \frac{vh}{Gt} + \frac{3}{4}he_n + \frac{h}{b}d_a \qquad [2]$$

This equation is based on static force displacement, which only incorporates static elastic analysis. The IBC 1617.5.4 has a deflection equation for an inelastic response, which is more typical of real loads. Deflection is a key aspect of design because building codes place limitations on the amount of allowable wall drift. A typical drift limit set by the Federal Emergency management Agency (FEMA) is two percent of the wall height for Life Safety requirements and one percent for Immediate Occupancy, while the IBC limits drift to 1 to 1.5 percent. More stringent values may be imposed to protect important buildings or buildings with a brittle façade.

2.3. Shearwall Tests

In recent years, cyclic test protocols have been developed to improve the testing of shearwalls, advancing the art from standard static pushover tests like E 564 (ASTM 2000). The different protocols have been compared (He et al. 1998; Skaggs and Rose 1996; Gatto and Uang 2003). The CUREE loading protocol, which came out of the Caltech Woodframe Project, was developed based on a collection of several ground motions recoded in California (Krawinkler et al. 2000) and has been widely used in the last four years. It has been incorporated into ASTM E2126 as standard protocol. The loading history is scaled to a user defined reference displacement, which is useful in the development of analytical models (Fonseca et al. 2002). The reference displacement is defined as 60 percent of the displacement corresponding to 80 percent of the post-peak capacity as determined from monotonic tests. By altering the reference displacement, the test outcome may change, but the overall wall response will not be drastically affected (Langlois et al. 2002). The CUREE protocol produces failures that are consistent with those in seismic areas and is the first of its type to be created

for wood type components (Langlois et al. 2004). The CUREE loading protocol along with other cyclic test methods have been used to determine the capacity of cyclically loaded shearwalls.

Tests have been conducted with connections and walls to determine how the two are related (Dolan and Madsen 1992a, b). Experimental tests on connections have examined the influence of grain direction (Blass 1994a, b), the influence of moisture in the mechanical properties of the wood and the stiffness of the joint (Mohammad and Smith 1994, 1997), and the effect of the rate-of-load (Rosowsky and Reinhold 1999) among others. Tests of cyclically loaded shearwalls have examined the effect of overdriven nails (Jones and Fonseca 2002), the contribution of gypsum wallboard attached with different fasteners (Karacabeyli and Ceccotti 1996), the effect of oversized sheathing panels (Lam et al. 1997; He et al. 1999), tie-down and anchorage effects (Salenikovich and Dolan 2000; Heine and Dolan 2001), and the effect of aspect ratios (Salenikovich and Dolan 2003; Pryor et at. 2000). Although experimentation provides results, there remains a need for a more efficient way to predict and modify the behavior of cyclically loaded shearwalls, which means a deeper understanding of the relationships of the wood, the connection and their interaction. A first step in determining the relationships and developing models is to mathematically derive functions to fit the experimental data (McCutcheon 1985; Gupta and Kuo 1987; Gutkowski and Castillo 1988; Kalkert and Dolan 1997).

2.4. Shearwall Models

Finite-element analysis models have been developed for nailed joints (Chui et al. 1998; Ni and Chui 1996; Hunt and Bryant 1990). Hunt and Bryant experimentally found properties for the nail and wood and used them as input for their static model; although their finite-element results were in agreement with their test data, some experimentation was needed. Others used finite-elements to model each part of the wall; the nails were modeled as two

nonlinear three-node beams, while the wood embedment was a two-node spring element. When compared to actual test data the model had two major discrepancies: an underestimation of the load and an inconsistent shape of the curve at low displacements. The underestimation of the load was caused by the springs acting independently and having a low stiffness. Since the model was developed for pinched hysteresis loops the displacement loops at small displacements are only pinched to a slight degree, therefore a difference is expected. Other finite-element analyses developed complex stiffness analysis (Polensek 1976; Gupta and Kuo 1985; Cheung et al. 1988). Still other researchers created models that generated walls (Kasal and Leichti 1992) and simple three-dimensional structures with nonlinear load-displacement characteristics, using finite-elements and superimposed quasi-static elements (Kasal et al. 1994; Itani and Fridley 1999). Although finite-element analysis can be accurate and utilize nail behaviors, the size of finite-models is often computationally cumbersome. However, finite-element models in combination with numerical models are capable of the type of calculations necessary to predict the cyclic response of large systems (Itani and Cheung 1984; Gupta and Kuo 1985; Polensek and Schimel 1985; Dolan and Foschi 1991; White and Dolan 1995). These models use two springs with nonlinear characteristics to model the connection, beam elements for the frame, and plane-stress elements or plate-bending elements for the sheathing. Even though the finite-element numerical models do a fairly accurate job in predicting the load-displacement curves, the results are not any better than the simpler numerical models in determining the hysteretic response of connections (Foliente 1995) and walls (Filiatrault 1990; Folz and Filiatrault 2001).

Dolan and Foschi (1991) developed a program, SHWALL, utilizing the finite-element method and a static load to predict shearwall peak capacity and initial stiffness. The direct stiffness method and Newton-Raphson procedure were utilized to find the peak capacity; however, no post-peak behavior could

be simulated. This program identified the stiffness relationship between the connectors and the wall. White and Dolan (1995) developed a finite-element program called WALSEZ that performed a nonlinear analysis of a wood shearwall subjected to monotonic or dynamic loads. The advancement from SHWALL was the ability of WALSEZ to analyze dynamic loads and create hysteretic responses with post peak behaviors. The trend of these programs was to use finite-element models to identify global stiffness matrices for a nonlinear analysis. Filiatrault (1990) developed a model, Shear Wall Analysis Program (SWAP) that predicts the stiffness and the ultimate load capacity of shearwalls under static and dynamic loads. The program utilized the nonlinear load-slip characteristics of the fasteners and equilibrium equations for static and dynamic cases. Several kinematic assumptions required that four degrees of freedom were assigned to each panel plus one for the entire system, and a global stiffness matrix was developed and used in a displacement based energy formulation to approximate cyclic test data.

The most recent model Cyclic Analysis of SHEar Walls (CASHEW) (Folz and Filiatrault 2000; 2001), takes into account many aspects of the previous models and principles of nonlinear hysteretic nail responses without finite-element analysis. The goal of CASHEW was to create a simpler and more efficient way to find the load displacement response of a shearwall under a cyclic or monotonic load. The basis of this program is the hysteretic response of a single connection. This program uses the principle of virtual displacements and the same kinematic assumptions and global stiffness matrix as SWAP to sum individual nail slips based on the hysteretic response and locations of the nail in the local coordinate system on the panel, and in the global coordinate system. The nails furthest from the center have the highest contribution to the overall sum, which is the response of the wall. The nails that are furthest away from the mid height of the wall will experience fatigue first (He et al. 1998; Chai and Hutchinson 2003); therefore, the nails in the corners of the wall are the most critical. The peak load is recorded as soon as

the first nail in the tension corner tears through the edge (Salenikovich and Dolan 2000). The wall is assumed to distort into a parallelogram rather than experience rigid-body rotation, which results from boundary conditions that imply full anchorage and ignores uplift and overturning. These assumptions increase capacity and stiffness of the wall because the boundary conditions allow the wall to deform in a racking fashion, which allows the wall to better utilize the ductility of the fasteners at lower loads (Dolan and Madsen 1992b, Skaggs and Rose 1996).

CASHEW calculates the nail load-slip relationship from the input set of 10 hysteretic parameters for the typical sheathing-framing connection in the wall, along with the wall geometry, panel shear modulus, and locations of all of the fasteners. Previously defining the hysteretic parameters makes the analysis less cumbersome, and the solution follows a specific hysteresis model with a minimum number of path-following rules that can reproduce the response of a connector under general cyclic loading. The force-displacement response is then solved based on the CUREE loading protocol and the general equilibrium equation

$$K_s D = F \qquad [3]$$

where K_s is the global secant stiffness matrix, D is the displacement vector, and F is the global force vector. The equilibrium equation is solved using an incremental-iterative displacement control solution strategy. All of the discussed models, including CASHEW, have no methods to allow the incorporation of decay or other changes to either the components of the wall, the studs, the sheathing or the connections; similar to the limitations of the design tables.

2.5. Role of Moisture and Decay in Shearwall Performance

Moisture and decay are capable of changing the properties of the wood and wood-based composites (Wilcox 1978; Kent 2004). Historically, moisture moved freely through the building envelope until improved methods and

materials became available to seal buildings. With these improvements, water that once moved freely through the building can become trapped in the wall cavity and increase the moisture level of the wood. Smulski (1999; 2000) speculated that the wood structures built in the 1980's and 90's may be among the least durable structures ever built due to moisture related problems. Wood used in construction is typically below 20 percent moisture content, a level at which the structural properties are maximized (Nakajima 2000) and the wood is more resistant to decay (Zabel and Morrell 1992). As the moisture approaches the fiber saturation point (approximately 30 percent), the environment for abiotic and biological degradation of both the wood and the fasteners exists (Beall 1999).

Common locations of moisture are around windows (Nanami et al. 2000) places where walls encounter the ground (Scheffer 1971; Smulski 2000) and sole plates (Smulski 2000). Other studies have looked at the water pathways through the wall (Sherwood 1987; Sherwood and TenWold 1982) and physical measurements of moisture around homes have been evaluated (Scheffer and Moses 1993; Quarles 1989). Decay fungi and mold require adequate moisture, oxygen, proper temperature and nutrients. The nutrients include the cell wall material of wood. Therefore, when moisture increases in the wall cavity, decay can rapidly grow (Freyfield 1937; Griffin 1977; Humphrey 1923; Snell et al. 1925; Snell 1929). Only a limited number of fungi are common in buildings (Cowling 1957; Duncan and Lombar 1965) and it is estimated that 80 percent of decay in wood buildings can be attributed to brown rot decay (Green and Highley 1997).

Brown rot decay degrades the cellulose and hemicellulose, the main constituents of the wood cell wall. White rot on the other hand also degrades cellulose and hemicellulose, but after it degrades lignin (Zabel and Morrell 1992). The main carbohydrate constituents of wood cells are cellulose and hemicellulose. Cellulose, which is 40 to 50 percent of the cell by weight, is a long linear unbranched chain of glucose polymers which are organized into

slender stands of microfibrils, having crystalline and non-crystalline regions; longer chains have higher degrees of polymerization and greater strengths. Hemicellulose, which is 20 to 30 percent of the cell by weight is a branched chain comprised of multiple sugars that surround the cellulose fibers and serves to connect with the lignin. When the majority of the cell wall is removed, the mechanical properties, particularly the strength and stiffness, are affected even in the early stages of decay (Wilcox 1978), which in turn affects the embedment properties of the wood (Rammer 2001). This will inevitably alter the connection EYM lateral load by potentially making the connection more brittle, along with the hysteretic parameters of the connection. The failure mode can also change. Kent et al. (2004) reported that as the dominant mode of failure of a cyclically loaded connection changed from fatigue and withdrawal to crushing of the side member. Yield modes in decayed materials may exhibit no fastener yielding.

Ample research has been done with connections having ideal conditions and is not cited here. Some research has involved moisture (Mohammad and Smith 1994; 1997; Nakajima 2000; Rammer 2000; 2001; Leichti et al. 2002; Kent 2004). Weight loss had traditionally been a measure of decay progress (Wilcox 1978); however, Winandy et al. (2000) concluded that bending strength and stiffness were better indicators of the decay effect on the properties of wood. Even at very low levels of decay before dramatic weight loss has occurred, the mechanical properties are significantly affected (Wilcox 1978). Research has been aimed at establishing roles of strength and stiffness loss for sawn lumber as a function of decay (Morrell et al. 2000; Curling et al. 2000; Winandy et al. 2000). Other researchers have attempted to devise decay models based on specific locations and climate indexes (Scheffer 1971; Leicester et al. 2000; Kumaran et al. 2003). Some have looked at nail deterioration due to metal corrosion on the wood to determine the decay level wood (Imamura and Kiguchi 1999; Baker 1992; Falk and Baker 1993). However, the type of wood or sheathing (Quarrels and Flynn

2000), the location of the fastener (Kubler 1992), or the presence of CCA treated wood (Baker 1992; Ruddick 1988; Simm 1985) can change how the nail or fastener degrades or affects the wood material. A study by Leichti et al. (2002) looked at the effect of wetting and drying on the capacity of shearwalls similar to what could occur in a flood situation. Only Kent et al. (in press) and Kent et al. (2004) have reported the influence of decay on connections and the effect decay has on a shearwall was recently reported by (Kim et al. in press). As the connections change due to the decay, the response of the wall will also change and mimic the properties of the connection.

Effect of Nail Bending-Yield Stress on Cyclic Performance of Wood Shearwalls

Erin N. Anderson
Robert J. Leichti
Edward G. Sutt, Jr.
David V. Rosowsky

For Submission to Wood and Fiber Science
One Gifford Pinchot Drive
Madison, WI 53726-2398

3. Effect of Nail Bending-Yield Stress on Cyclic Performance on Wood Shearwalls

3.1. Abstract

This study investigates the effects of nail bending-yield stress on the cyclic behavior of laterally-loaded sheathing-framing connections and full-size 8 by 8 ft. engineered shearwalls under cyclic loading. The shearwalls are framed with Douglas-fir lumber and are sheathed with OSB. Four sets of nails were specially manufactured by Stanley Bostitch with bending yield stresses of 87, 115, 145 and 241 ksi. Tests were conducted to determine fastener bending-yield stress and to determine the hysteretic behavior of single-nail lateral connections. The parameters of the lateral nail tests were used as input for a numerical model used to predict the shearwall performance and its hysteretic parameters. Full-scale cyclic shearwall tests were conducted with the same materials as the connection tests to assess the competency of the numerical model. The parameters of the shearwall model were also used as input into another structural analysis program used to predict shearwall performance for a suite of seismic ground motions. In both single-nail lateral connection tests and shearwall tests, the probability of nonductile failure modes increased as nail bending-yield stress increased. Overall, the shearwall tests showed that the initial stiffness, displacement at peak capacity and energy dissipation were not significantly affected by changing the bending-yield stress of the nails. However, the peak capacity of the walls increased as bending-yield stress increased. In the end, nails having a bending-yield stress greater than 100 ksi did not enhance the overall cyclic behavior of wood shearwalls.

3.2. Introduction

Shearwalls are a main part of the lateral load resisting system in light-frame wood buildings, and the connections such as sheathing nails in the

shearwalls provide ductility, damping and energy dissipation through mechanisms such as internal friction, nonrecoverable damage, connection failure and yielding of the metal fasteners (Chui et al. 1998; Lam et al. 1997). The initial stiffness, resistance and energy dissipation capacity of a lateral load resisting system are important because altering any of these properties can affect the performance of a structure (Shenton et al. 1998). An extensive body of literature has developed since the 1950's describing the role of the nail spacing and other construction variables, such as exterior sheathing, framing, openings, and hold-downs, etc, on the performance of shearwalls.

A contemporary wood shearwall consists of four main parts, engineered structural panels such as plywood or oriented strandboard (OSB), a wood stud frame, nails connecting the panels to the stud frame, and the foundation including anchorage bolts and devices. The weakest link in a structure is often the connections (Kalkert and Dolan 1997); therefore, the key to numerically predicting the overall system response is successfully modeling the hysteretic behavior of the nails (Foliente 1995). From the load-displacement curves, the essential parameters including initial stiffness, and peak wall capacity and deflection at peak capacity can be extracted (Gupta and Kuo 1985; McCutcheon 1985; Filiatrault 1990; Dolan and Madsen 1992b).

Nails are one of the most common fasteners in structural timber construction, and wooden assemblies (Aune and Patton-Mallory 1986b). Yield limit theory (EYM) (Wilson 1917; Johansen 1949; Moller 1950; Larsen 1973; Aune and Patton-Mallory 1986 a, b) is the common method for design of laterally loaded dowel-type fasteners. The EYM analysis is based on the embedment strength of the wood, the bending-yield stress of the dowel, and the joint geometry (AF&PA 1999). The lateral connection yield modes involve nail bending, wood crushing, or a combination of the two. However, experience has shown that characteristically four post-yield failures can be described for sheathing-framing connections (Lattin 2002): withdrawal, fatigue, pull-through, and edge tear-out. These are observed mostly in post-peak

loading. Monotonically loaded nails show no signs of fatigue failure (Gatto and Uang 2003), and nail fatigue is not common in earthquake damage (He et al. 1998; Rose 1999; Langlois et al. 2004; Salenikovich and Dolan 2003).

Typically, to increase the performance of a shearwall the sheathing thickness is increased or the nail spacing is decreased; however, both have limitations; panels can only be manufactured to a certain thickness and nail spacing can only be decreased by a small amount. Therefore, to change the performance of the shearwall, the connections are evaluated. Studies by Langlois (2002) and Lattin (2002) have indicated that by altering the failure modes of the sheathing nails, the performance of the shearwall can improve. Both studies found that by using smooth shank nails, the dominate failure mode of a conventional sheathing-framing fastener was withdrawal, however, by using ring-shank nails, the dominate failure mode changed.

Langlois used 0.113-in. diameter annular ring-shank nails and found that the shearwall ultimate static strength could be increased by 40 percent using ring-shank nails, and the dominant failure modes switched to pull-through followed by fatigue. Lattin used a variety of nails including super sheather nails, which are partially annularly threaded and have a larger diameter head, and found that the ultimate capacity of a cyclically loaded shearwall with a sheathing nail diameter of 0.113 in. also increased. In Lattin's case, the dominate failure modes also changed to pull-through and fatigue; however, the percentage of pull-through failures remained approximately the same due to the larger nail head counteracting the additional pull-through forces created by the decrease in withdrawal failure, and the nail fatigue also increased to compensate for the decrease in withdrawal.

Although changing the bending-yield stress of a nail will change the properties of an individual connection, it is unknown what the effects will be on a shearwall. By changing the bending-yield stress of the nail, the expected yield mode of a fastener may change, but the withdrawal capacity of the nail will not change. Therefore, it can be speculated that since withdrawal is the

dominate failure mode of smooth shank nails in a shearwall, the overall performance of the shearwall will not be affected by increasing the bending-yield stress of the sheathing-framing nails.

Wood shearwalls have gained a reputation for being highly resistant to earthquakes due to the high strength-to-weight ratio of wood and the ductility of connections (Filiatrault 1990). However, damage to wood buildings in the Northridge and Loma Prieta earthquakes prompted further investigation of cyclic load effects in shearwalls and connections. The California Universities for Research in Earthquake Engineering Caltech Woodframe project (CUREE) was established to examine the performance of wood-frame buildings and their connections in earthquake prone regions; the investigation team developed the CUREE loading protocol (Krawinkler et al. 2000). The protocol was initially devised for shearwalls, but it also has been used to evaluate individual nail and staple connections (Jones and Fonseca 2002; Kent 2004).

When the wall or nail connection is subjected to a cyclic loading, the load-displacement curve is a series of pinched hysteresis loops where each successive loop has a degrading stiffness (Dolan and Madsen 1992b; Foliente 1995). At small displacements, a nail will behave elastically. However, at large displacements the nail behavior is inelastic and nonlinear without a distinct yield point (Filiatrault 1990), which makes hysteretic response of the connection is difficult to predict. Research has determined that the positive quadrant hysteretic behavior can be captured with ten extracted parameters to fully describe one connection (Foliente 1995). The first five parameters K_o (initial stiffness), r_1, F_o, r_2, Δ_u describe the envelope response of a connector (Foschi 1974, Dolan and Madsen 1992a), while the other five parameters r_3, r_4, F_l, α and β describe the hysteretic part of the response due to cyclic loading (Fonseca et al. 2002). The parameter for maximum force (F_u) is also used as a performance indicator. A complete nonlinear load-slip curve provides information about the ultimate load, initial stiffness, unloading stiffness, post-peak stiffness, ductility, and residual deformation after unloading (Foschi and

Bonac 1977), as well as the degrading factors. The hysteretic response and essential parameters of a shearwall can be predicted using the hysteretic characteristics of individual sheathing-framing nailed joints with similar properties and boundary conditions (Foliente 1995).

Several methods have been used to determine the capacity of cyclically loaded shearwalls, experimentation, finite-element analysis, and numerical methods. Finite-element analysis models have been developed for nailed joints (Chui et al. 1998; Ni and Chui 1996; Hunt and Bryant 1990). Other finite-element models for shearwalls analysis have been reported (Polensek 1976; Gupta and Kuo 1985; Cheung et al. 1988; Kasal and Leichti 1992; Kasal et al. 1994; Itani and Fridley 1999). Finite-element analysis can be accurate and can utilize nail behaviors, but finite-element models are often computationally cumbersome. Finite-element models used in conjunction with other numerical models are capable of the type of calculations necessary to predict cyclic responses of large systems (Itani and Cheung 1984; Gupta and Kuo 1985; Polensek and Schimel 1985; Dolan and Foschi 1991; White and Dolan 1995). A recent numerical model Cyclic Analysis of SHEar Walls (CASHEW) (Folz and Filiatrault 2000; 2001), takes into account many aspects of the previous models and principles of nonlinear hysteretic nail responses without finite-element analysis. CASHEW calculates the wall response based on the load-slip characteristics of the nail connections, which is described by the ten hysteretic parameters for the typical sheathing-to-framing connection in the wall, along with the wall geometry, shear modulus of the sheathing, and locations for the nails. Others have evaluated the effect of nail geometry, for example ring shank, annular shank, head shape, etc., on the performance of the connection, and presumably, the wall assembly could also be modified by changing the strength of the nail. After a thorough search of the literature, we could not identify engineering information that revealed the effect of nail bending-yield stress on the cyclic performance of laterally-loaded connections of wood frame shearwalls.

3.3. Objectives

The sheathing-framing connections govern the behavior of the shearwall, and altering the properties of the nail or the wood materials could modify the behavior of the shearwall. It is logical to hypothesize that increased bending-yield stress for sheathing nails will improve shearwall performance. Hence, the main objective of this study was to assess the effect of bending-yield stress (f_{yb}) of the sheathing nails on shearwall performance. Specific objectives included:

- Evaluate the laterally loaded single-nail connections with a range of nail f_{yb}.
- Experimentally evaluate shearwalls where the sheathing nail f_{yb} is the source of variation.
- Numerically evaluate probable shearwall performance for a suite of seismic ground motions where the subject shearwalls represent a range of nail f_{yb} values.

3.4. Materials and Methods

The nails were 0.113 in. diameter and 2-3/8 in. long with a full head and smooth shank. Stanley Bostitch manufactured nails with four different f_{yb} values that were: 87 ksi, 115 ksi, 145 ksi, and 241 ksi. Table 3.1 summarizes the test results to establish nail f_{yb} (Anderson 2005).

Table 3.1. Nail bending-yield stress from tests in compliance with F 1575 (ASTM 2002g), nail diameter 0.113 in., length 2-1/2 in., n=24.

f_{yb} Designation	f_{yb} Average	Std Dev	COV
87 ksi	85.0	6.34	0.06
115 ksi	115.4	3.62	0.03
145 ksi	144.6	5.75	0.04
241 ksi	240.9	4.46	0.02

The 87 ksi nail does not comply with ICC 2004 (National Evaluation Report), which requires nails with a diameter of less than 0.15 in. to have an average f_{yb} not less than 100 ksi.

The building materials were Stud grade Douglas Fir-Larch and 7/16-in. OSB sheathing (Exposure 1), with average moisture contents of 8.7 percent and 7.1 percent respectively. The moisture contents were measured in accordance with D 4444 (ASTM 2002b). The embedment values for the lumber and sheathing were found in conjunction with D 5764 (ASTM 2002c). The average embedment strengths were 912 psi and 267 psi for the lumber and sheathing, respectively.

The EYM equations given in the NDS (AF&PA 2001) were used to determine the expected design yield mode for the single-shear specimens built using these materials. The observed yield mode for each type of nail was found to be Mode III_s, a plastic hinge forming in the OSB along with some crushing of the OSB. The yield mode calculations (Table 3.2) also show that Mode III_s is the expected design yield mode for the nail connections regardless of nail f_{yb}.

Table 3.2. Yield mode calculations for laterally loaded single nail connections constructed with Douglas Fir-Larch and 7/16-in. OSB sheathing with four different f_{yb} nails.

Yield Mode	87 ksi	115 ksi	145 ksi	241 ksi
I_m	415	415	415	415
I_s	121	121	121	121
II	2455	2455	2455	2455
III_m	145	147	149	155
III_s	60	65	71	87
IV	73	83	94	121

3.4.1. Single-Fastener Connection Tests

The standard single-nail test configuration is an 8-in. piece of framing and a 4 by 6-in. piece of OSB sheathing nailed together with a single fastener while maintaining a minimum edge distance of 2 in. for all edges (Fig. 3.1a).

The test set up of the connection tests is shown in Fig. 3.1b. This apparatus kept the specimen straight and in-plane to reduce eccentricities caused when the nail withdraws. At first, two monotonic tests at a constant loading rate of 0.20 in./min were conducted for each nail type in order to determine a reference displacement used to scale the cyclic test protocol for each nail type (Fig. 3.2). Based on the results of the monotonic tests (Table 3.3), a reference displacement of 0.5 in was selected.

(a)

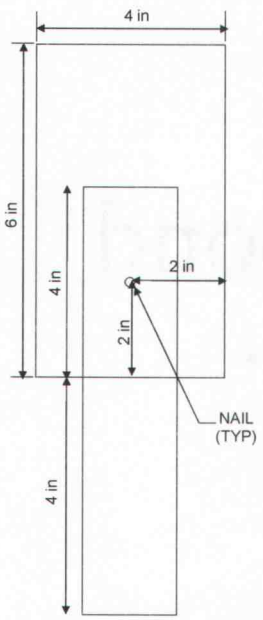

(b)

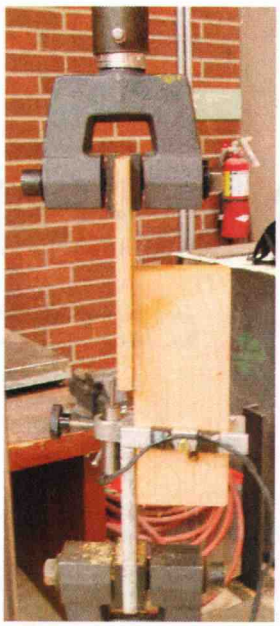

Fig. 3.1. Single nail lateral connection test specimen (a) dimensions and detail, (b) test apparatus.

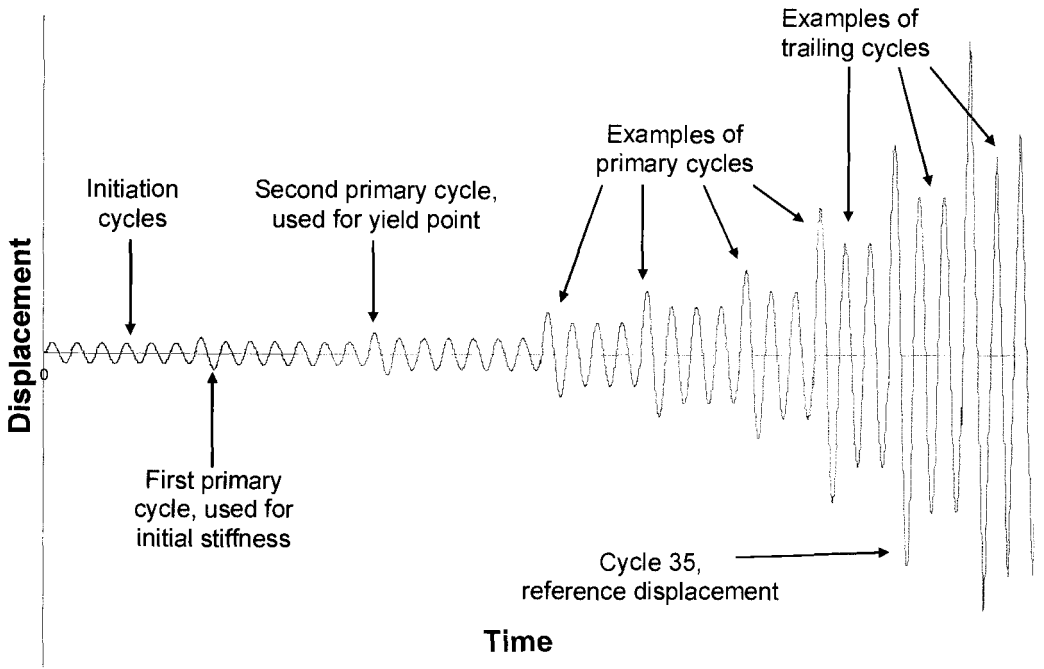

Fig. 3.2. CUREE loading protocol used for single nail and shearwall tests.

Table 3.3. Single fastener monotonic test results by nail f_{yb}.

Nail Test	Initial Stiffness (lb/in.)	P_{max} (lb)	Δ at P_{max} (in.)	P_{yield} (lb)	Ref Δ (in.)
1	3432	258	0.44	96.4	0.616
2	6555	296	0.47	127	0.766
Avg. 87 ksi	4994	277	0.45	112	0.691
3	8514	337	0.36	137	0.780
4	14218	370	0.37	185	0.740
Avg. 115 ksi	11366	353	0.36	161	0.760
5	7326	374	0.62	119	0.421
6	6784	367	0.60	128	0.398
Avg. 145 ksi	7055	371	0.61	124	0.410
7	9467	492	0.82	66.1	0.484
8	11129	379	1.04	112	0.420
Avg. 241 ksi	10298	436	0.93	88.8	0.452

A set of ten single nail specimens having the same configuration and set up as the monotonic tests were tested cyclically at 0.2 Hz. The hysteretic parameters of the cyclic lateral nail tests were determined using the software program SASHFIT (Elkins and Kim 2003b). This hysteretic data was later used in the shearwall models.

3.4.2. Shearwall Tests

Eight 8 by 8-ft shearwalls fully anchored with hold-downs were constructed with the framing for each wall spaced 16 in. o.c. (Fig. 3.3). The nails with different f_{yb} values were used only for the sheathing nails, the framing nails were typical construction nails. Two walls of each nail type were tested. The sheathing nails were spaced at 4-in. on the perimeters and 12 in. in the field of each panel. The minimum edge distance was 3/8 in. The plate-to-stud connection was end nailed using two 16d common nails; the double top plates were connected with one 16d common nail every 6 in. The double end studs were connected using two 10d common nails every 8.5 in. except in the areas where hold-downs were located (the bottom 13 in. of the end studs).

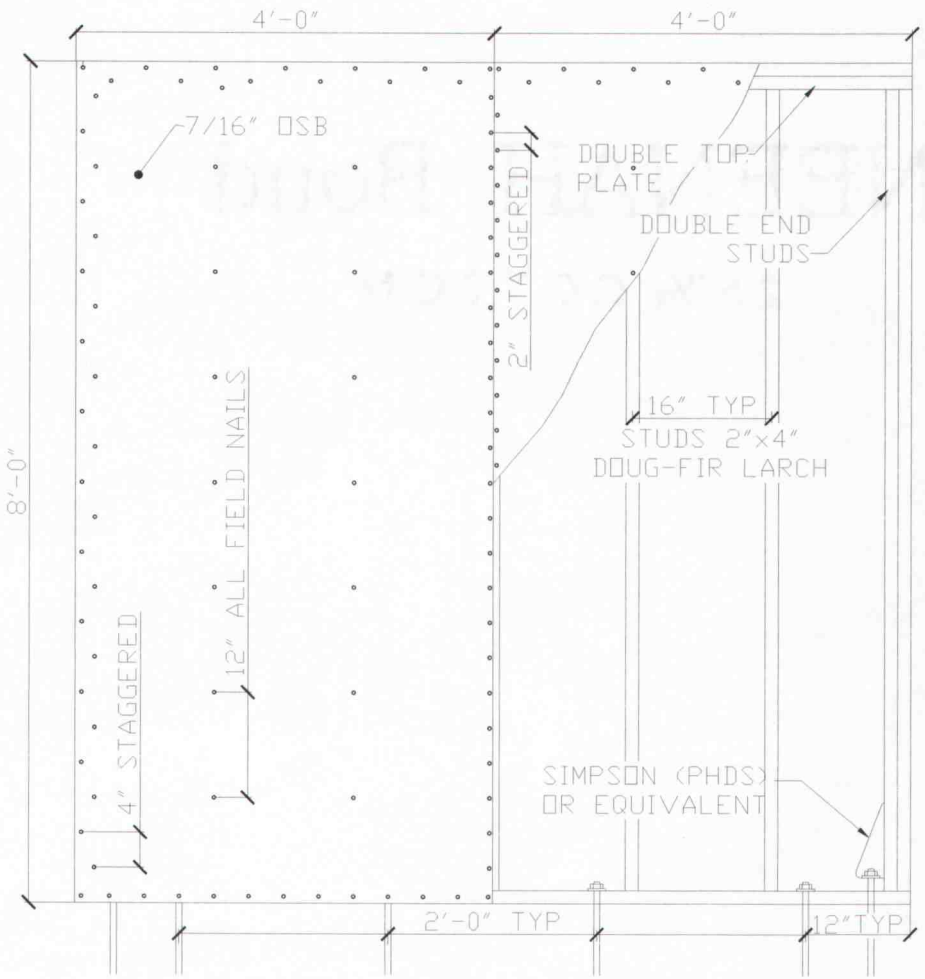

Fig. 3.3. Shearwall configuration for cyclic tests and numerical models.

The walls were tested in accordance with E 2126 (ASTM 2002f) following the same loading protocol that was used for the individual connections. Rather than testing a wall monotonically to determine the reference displacement, the selection of the reference displacement was based on previous studies conducted at Oregon State University as well as the limits of the testing equipment. To maximize the possibility of causing post-yield behavior, a reference displacement of 3 in. was used. The quantitative wall performance parameters were initial stiffness, maximum capacity (P_{max}), displacement at maximum capacity (ΔP_{max}), energy dissipation (Energy), and ductility.

3.4.3. Analysis Programs

The average nail hysteretic parameters were used as input for CASHEW, a program that uses the geometry of a shearwall along with the connection hysteresis parameters to predict the load-displacement response and energy dissipation of the shearwall under a user defined loading. CASHEW governs global hysteretic parameters for the cyclic response of the entire wall as output. The wall hysteretic parameters are then used as input to the program SASH1 (Elkins and Kim 2003c). This program performs dynamic time history analysis of a wood shearwall, modeling the wall as a nonlinear single-degree-of-freedom system. The SASH1 analysis uses an input earthquake ground motion record. The records considered in this study included 20 earthquakes from the Los Angeles area that characterize non-near fault ground motions. Each record was scaled such that its mean 5-percent damped spectral value between periods of approximately 0.1 and 0.6 seconds matched the design spectral value for the same period range. The spectral value was matched to 1.1 g for the life safety (LS) limit state, also defined as a 10-percent in 50 years (10/50) hazard level by the Federal Emergency Management Administration (FEMA 2000). The spectral design value is matched to 0.633 g for the immediate occupancy (IO) hazard level, also defined as a 50-percent chance in 50 years (50/50) by FEMA. Seismic

zone 4 and soil type D were assumed for both hazard levels. Rosowsky and Kim (2003) give further information on the procedure for characterizing seismic hazard.

3.5. Results and Discussion

3.5.1. Single-Fastener Connection Tests

Ten hysteretic parameters were extracted for every single-fastener test, and they are summarized by nail f_{yb} in Table 3.4. Analysis of variance (AVOVA) was conducted and for tests of significance at an alpha level of 0.05 there is a significant difference in the initial stiffness (K_o) (p-value 0.0022) and the ultimate capacity (F_u) (p-value<<0.001). Further inspection of the data shows that the K_o is not changed by increasing the nail from f_{yb} from 115 ksi to 241 ksi (p-value 0.147). However, connection capacity F_u was increased by approximately 20 percent from f_{yb} 115 ksi to f_{yb} 241 ksi. The displacement at peak capacity was statistically similar for each nail f_{yb} (p-value=0.952). The other hysteretic parameters were not evaluated by ANOVA.

Table 3.4. Average hysteretic nail parameters for single lateral nail specimens from SASHFIT, Std & Btr, Douglas Fir-Larch and 7/16-in. OSB.

Nail (f_{yb})		n	Initial Stiffness (lb/in.)	r_1	r_2	r_3	r_4	F_0 (lb)	F_I (lb)	Δ_u (in.)	α	β	P_{max} (lb)
87	Avg	24	2574	0.050	-0.066	4.36	0.012	237	31.1	0.424	0.244	1.18	296
	COV		0.19	0.72	0.65	0.18	0.22	0.22	0.05	0.15	0.40	0.09	0.19
115	Avg	24	2851	0.037	-0.069	3.91	0.028	249	32.4	0.425	0.265	1.15	287
	COV		0.12	0.50	0.61	0.14	0.36	0.14	0.09	0.22	0.31	0.09	0.11
145	Avg	24	2866	0.051	-0.075	4.43	0.041	261	29.2	0.402	0.244	1.13	314
	COV		0.11	0.38	0.69	0.17	0.45	0.17	0.15	0.10	0.44	0.06	0.14
241	Avg	21	3099	0.057	-0.051	4.77	0.064	305	28.7	0.401	0.158	1.08	358
	COV		0.12	0.53	0.41	0.13	0.72	0.14	0.12	0.30	0.47	0.23	0.12

The connection failure characteristics are summarized by nail f_{yb} in Table 3.5. Withdrawal is the dominate failure feature (more than 50 percent of failures) for all four nail types. However, the percentage of fatigue failures increased as nail f_{yb} increased.

Table 3.5. Percentage of nail failures for single lateral connections and shearwalls by nail f_{yb} value.

Nail f_{yb}	Test	Nail Failure (%)			
		Withdrawal	Pull-through	Fatigue	Tear-out
87	lateral nail	75	8	17	0
	shearwall[a]	80	12	7	1
115	lateral nail	71	8	21	0
	shearwall[a]	65	28	7	0
145	lateral nail	67	8	25	0
	shearwall[a]	49	39	10	2
241	lateral nail	55	0	45	0
	shearwall[a]	42	32	24	2

[a] Perimeter nails only, field nails not considered

3.5.2. Shearwall Tests

To characterize the behavior of the walls constructed with a given nail type, the results from the two shearwalls having the same nail f_{yb} values were averaged to define the backbone curves (Fig. 3.4). The maximum load (P_{max}) (Table 3.5) increases as nail f_{yb} increases. However, the values of P_{max} for the 241-ksi shearwalls are close to the 145-ksi shearwalls; in fact, the P_{max} values are statistically similar based on significance tests at an alpha level of 0.01. Though the P_{max} values for the 87-ksi and 115-ksi walls are significantly lower than the 145-ksi and 241-ksi walls, the 95-percent confidence intervals for the two groups overlap. The range of the displacement at P_{max} (Table 3.6) indicates that nail f_{yb} is not a factor with respect to this parameter. Also, no significant differences (p-value=0.104, alpha level=0.05) were found in the cumulative energy dissipated by the different walls (Fig. 3.5). At primary cycle 7, which is the cycle of peak displacement, the 87-ksi wall has the lowest cumulative energy dissipated with 94,400 lb·in while the 145 ksi wall has the highest with 102,000 lb·in; the difference is 8.6 percent.

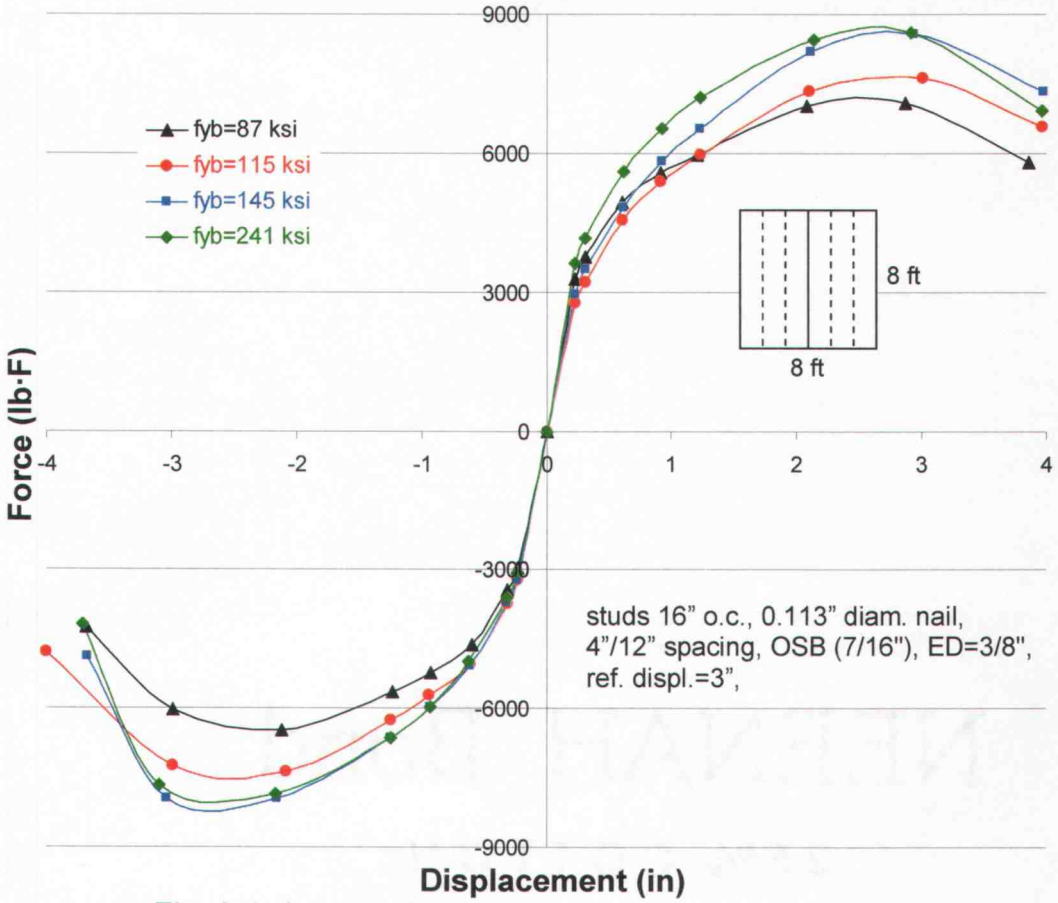

Fig. 3.4. Average backbone curves for the two walls at each bending-yield stress value.

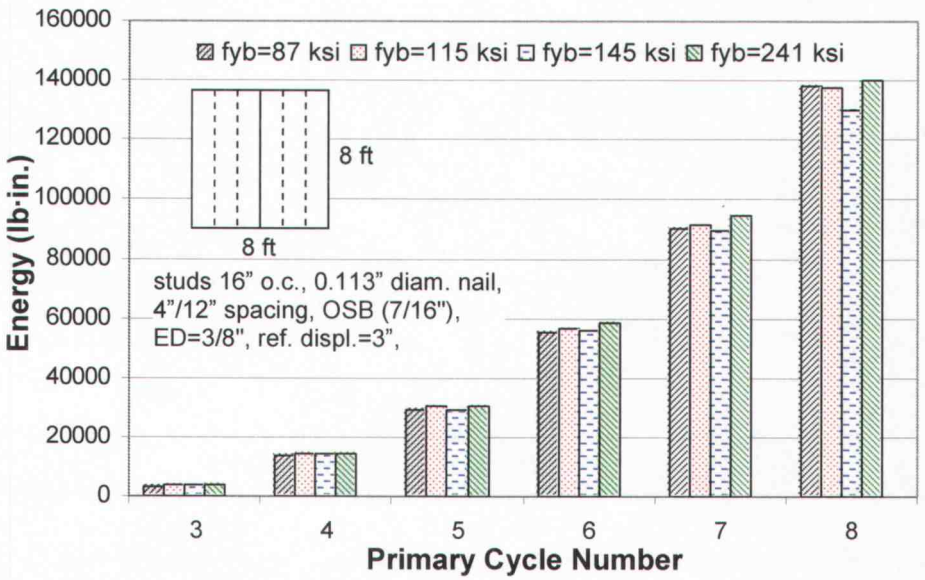

Fig. 3.5. Average cumulative energy dissipated at the primary cycles for the two walls at each f_{yb} value.

The initial stiffness values (K_o), which are based on the ascending branch of the first primary cycle between 10 percent and 40 percent of the maximum load, are statistically similar based on an alpha–level of 0.05 for the shearwalls (Table 3.6). The single nail tests (Table 3.3) and the CASHEW analysis (Table 3.6) both suggest that as the sheathing nail f_{yb} increases, the initial stiffness will as well. However, the shearwall results contradicted this expectation; the sheathing nail f_{yb} does not affect the initial stiffness of the shearwall assembly.

Table 3.6. Summary of cyclically tested 8 by 8-ft. shearwall results for each nail bending-yield stress.

Wall Test	Initial Stiffness (lb/in.)	P_{max} (lb)	Δ at P_{max} (in.)	Energy (kip·in.)	Ductility
1	11211	6999	2.84	131	9.18
2	12320	7155	2.11	124	9.43
Mean 87 ksi	11760	7077	2.48	128	9.30
3	9856	7393	2.95	131	9.71
4	11774	7846	2.99	142	9.75
Mean 115 ksi	10815	7619	2.97	136	9.73
5	12478	8656	2.87	147	9.34
6	9753	8501	2.91	147	9.68
Mean 145 ksi	11115	8578	2.89	147	9.56
7	11190	8871	3.05	143	9.77
8	12256	8345	2.94	135	9.08
Mean 241 ksi	11723	8608	3.00	139	9.42

In the wall tests, the dominant assembly failure characteristic was the sheathing pulling away from the framing at the center stud and elsewhere at the perimeters. Another post-peak behavior was the studs pulling away from the top of the bottom plate. Typically the end studs separated from the top plate.

When looking at the perimeter nails in each of the walls, different types of failures were characteristic of each sheathing nail f_{yb}. In fact, four different observed modes of failure were observed for the sheathing nails: withdrawal, pull-through, fatigue, and tear-out. Similar to the single-nail connection tests,

the dominant failure mode in the walls was withdrawal for all nail types. As the nail f_{yb} increases, the percentage of nails failing from pull-through also increases, along with the percentage of nails failing from fatigue (Table 3.5). The higher f_{yb} nails were more likely to have nonductile failures in the shearwall tests, and the pattern is also evident in the single fastener tests (Table 3.5). Tear-out was not a common mode of failure since the minimum edge distance was at least 3/8 in., but the locations where tear-out occurred were the corners of the sheathing and along the center stud. These failure results parallel those reported by Lattin (2002).

The overall ductility of the walls (displacement at P_{max} divided by the yield displacement) was not affected by the nail f_{yb} even though the higher f_{yb} nails had more nonductile failures. The walls with the highest ductility were the 115-ksi walls with an average ductility of 9.7. The average ductility of the other walls ranged from 9.3 to 9.6 with the 87 ksi walls being the lowest, and the 145-ksi walls being the highest. Thus, no correlation was observed between fastener bending-yield stress and wall ductility.

3.5.3. CASHEW Models and Seismic Analyses

Comparisons between the CASHEW results (Table 3.7) and the actual shearwall tests (Table 3.6) for initial stiffness and capacity show that the models represent the shearwall tests with a few exceptions. The general shapes of the backbone curves are similar, but CASHEW predicted a higher peak load (6 to 22 percent higher) at a lower displacement (15 to 30 percent lower) than seen in the shearwall tests (Fig. 3.6).

Table 3.7. Hysteretic parameters (n=1) from CASHEW for modeled shearwalls.

Wall f_{by}	K_o (lb/in.)	r_1	r_2	r_3	r_4	F_0 (lb)	F_1 (lb)	Δ_u (in.)	α	β	F_u+ (lb)
87	11330	0.033	-0.077	2.89	0.181	7950	962	2.10	0.307	1.164	8311
115	12565	0.017	-0.084	2.62	0.416	8392	1042	2.08	0.336	1.130	8444
145	12420	0.028	0.089	2.83	0.058	8974	981	2.02	0.327	1.110	9088
241	12690	0.022	-0.578	2.93	0.077	1098	989	2.05	0.374	1.070	10482

The initial stiffness comparisons for the CASHEW results and the test shearwalls showed the differences in values between the experimental and calculated initial stiffness range from -4 percent for the 87-ksi walls, to 14 percent for the 115-ksi walls, with intermediate deviations of 11 percent and 8 percent for the 145-ksi walls and 241-ksi walls, respectively. The differences in initial stiffness estimates are not correlated with the differences in the peak capacity.

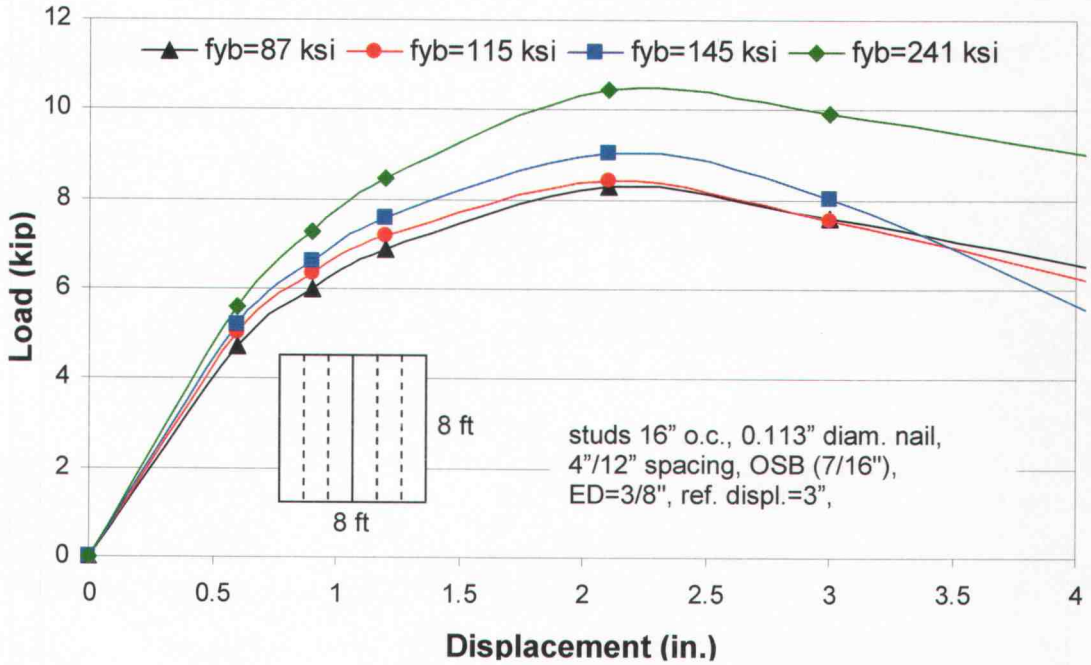

Fig. 3.6. Summary of CASHEW backbone curves for each sheathing nail bending-yield stress.

CASHEW predicted that the walls would exhibit nearly the same cumulative energy dissipation (Fig. 3.7) as the tested shearwalls (Fig. 3.5). The cumulative energy of the test shearwalls is between 128,000 lb·in and 149,000 lb·in, while the CASHEW-predicted values, ranged from just under 130,000 lb·in to about 140,000 lb·in. The CASHEW predicted energy for the 145-ksi wall is substantially lower than the tested wall average with a 13-percent difference. The 87-ksi walls have and 8-percent difference while the 115-ksi and 241-ksi walls have 1-percent difference.

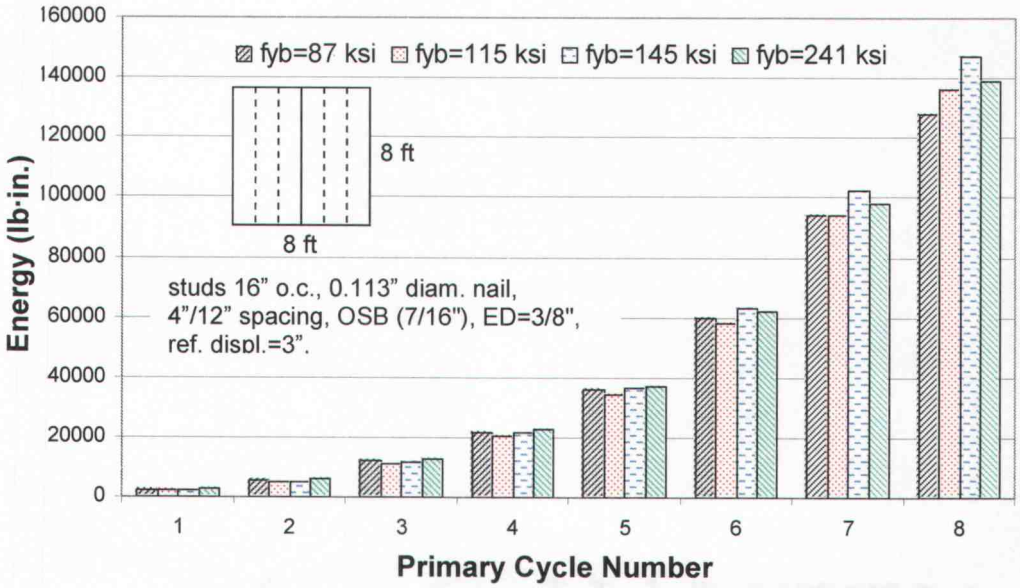

Fig. 3.7. Cumulative energy dissipated at the primary cycles from the shearwalls evaluated with CASHEW at each nail bending-yield stress value.

The peak displacement values (one for each wall) from SASH1 for the seismic ground motions are rank-ordered and plotted as cumulative distribution functions. For the life-safety (Fig. 3.8) and immediate-occupancy (Fig. 3.9) limit states. These types of figures can be used to evaluate the relative failure probabilities (probability of exceeding specified drift limits) for the different walls considering different performance requirements. The FEMA drift limits (2-percent and 1-percent for life-safety and immediate-occupancy, respectively) are shown on these figures for reference. The sheathing nail f_{yb} appears to have no influence on the shearwall performance with respect to the immediate-occupancy limit state. At the life-safety limit state, wall performance may be marginally improved by increasing the sheathing nail f_{yb} from 145 ksi to 241 ksi, but there appears to be no real advantage in the range 87 ksi to 145 ksi for sheathing nail f_{yb}.

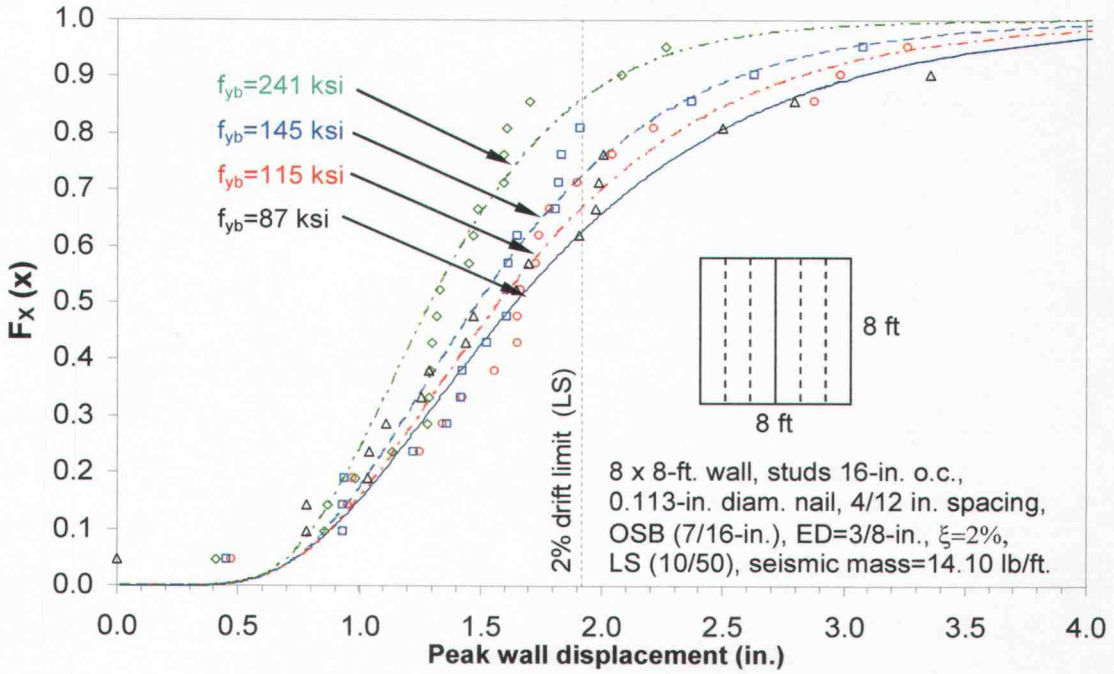

Fig. 3.8. Comparison of predicted peak wall displacements for the life-safety limit state.

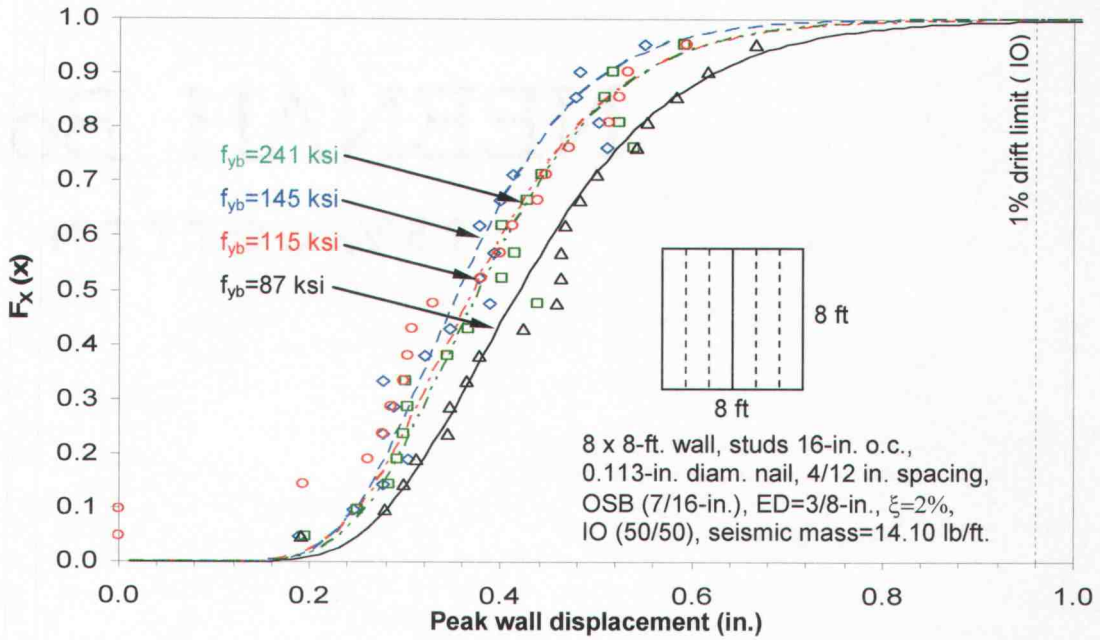

Fig. 3.9. Comparison of predicted peak wall displacements for the immediate-occupancy limit state.

3.6. Conclusions

This study examined the effect of sheathing nail f_{yb} on connection properties and shearwall performance. Four sheathing nail types were manufactured with f_{yb}=87, 115, 145, and 241 ksi, but were similar in all other geometric and surface characteristics. Shearwalls built with four different sheathing nail types had similar energy dissipation characteristics. Although the shearwalls built with 115-ksi nail had the highest ductility, none of the other walls had a substantially lower ductility. The peak capacity of the walls increased with higher f_{yb} nails, however beyond 145-ksi, no significant increase was seen. Unlike the peak capacity, the displacement at peak capacity, the initial stiffness and the energy dissipation were not statistically affected by the nail f_{yb}. The dominant failure mode for the sheathing nails was withdrawal; however, the 241-ksi nail exhibited more fatigue failure than the other nails. Wall models were used to assess probable performance with respect to life-safety and immediate-occupancy limit states for a suite of seismic ground motions. The models showed that increased sheathing nail f_{yb} did little to enhance the seismic performance of the shearwalls. Based on the tests completed in this study, the sheathing nail f_{yb} does not appear to enhance the overall behavior of cyclically loaded shearwalls.

3.7. References

AF&PA. 2001. National Design Specifications® for Wood Construction. American Forest and Paper Association, Washington, D.C.

AF&PA. 1999. General dowel equations for calculating lateral connection values. Tech. Rept 12. American Forest and Paper Association, Washington DC. 174 pp.

American Society for Testing and Materials (ASTM). 2002b. Standard test methods for use and calibration of hand-held moisture meters. Annual book of ASTM standards. D4444-92. ASTM, West Conshohocken, PA.

American Society for Testing and Materials (ASTM). 2002c. Standard test method for evaluating dowel-bearing strength of wood and wood-base products. Annual book of ASTM standards. D5764-97a. ASTM, West Conshohocken, PA.

American Society for Testing and Materials (ASTM). 2002f. Standard methods for cyclic (reversed) load test for shear resistance of framed walls for buildings. Annual book of ASTM standards. E2126-01. ASTM, West Conshohocken, PA.

American Society for Testing and Materials (ASTM). 2002g. Standard test method for determining bending yield moment of nails. Annual book of ASTM standards. F1575. ASTM, West Conshohocken, PA..

Anderson, E.N. 2005. The Effects of Nail Bending-Yield Stress and Biological Deterioration on the Cyclic Performance of Shearwalls. M.S. thesis, Oregon State University, Corvallis, OR.

Aune,P., and M. Patton-Mallory. 1986a. Lateral load-bearing capacity of nailed joints based on the yield theory: Experimental Verification. Res. Pap. FPL-RP-470. Madison, WI:U.S. Department of Agriculture, Forest Service, Forest Products Laboratory, Madison, WI.

Aune,P., and M. Patton-Mallory. 1986a. Lateral load-bearing capacity of nailed joints based on the yield theory: Theoretical Development. Res. Pap. FPL-RP-471. Madison, WI:U.S. Department of Agriculture, Forest Service, Forest Products Laboratory, Madison, WI.

Cheung, K.C.K., R.Y. Itani, and A. Polensek. 1988. Characteristics of wood diaphragms: experimental and parametric studies. Wood and Fiber Science 20(4):438-456.

Chui, Y.H., C. Ni, and L. Jaing. 1998. Finite-element model for nailed wood joints under reversed cyclic load. J. Struct. Engrg. 124(1): 96-103.

Dolan, J.D., and R.O. Foschi. 1991. Structural analysis model for static loads on timber shear walls. J. Struct. Engrg. 117(3): 851-861.

Dolan, J.D., and B. Madsen. 1992a. Monotonic and cyclic nail connection tests. Can J. of Civ. Engrg. 19(1): 97-104.

Dolan, J.D., and B. Madsen. 1992b. Monotonic and cyclic tests of timber shear walls. Can J. of Civ. Engrg. 19(4): 415-422.

Elkins, L. and J.H Kim. 2003b. Introduction to SASHFIT. User's manual, Oregon State University, Corvallis, OR.

Elkins, L. and J.H Kim. 2003c. Introduction to SASH1. User's manual, Oregon State University, Corvallis, OR.

Federal Emergency Management Agency (FEMA). 2000. *NEHRP guidelines for the seismic rehabilitation of buildings*, FEMA-273, Federal Emergency Management Agency, Washington, DC.

Filiatrault, A. 1990. Static and dynamic analysis of timber shear walls. Can J. Civ. Engrg. 17(4): 643-651.

Foliente G.C. 1995. Hysteresis modeling of wood joints and structural systems. J. Struct. Engrg. 121(6): 1013-1022.

Folz, B., and A. Filiatrault. 2001. Cyclic analysis of wood shear walls. J. Struct. Engrg. 127(4): 433-441.

Folz, B., and A. Filiatrault. 2000. CASHEW—Version1.0: A computer program for cyclic analysis of wood shear walls. CUREE Publication No. W-08, Consortium of Universities for Research in Earthquake Engineering, Richmond CA.

Fonseca, F. S., R. Sterling, and S. Campbell. 2002. CUREE-caltech Woodframe Project, Task 1.4.8.1-Nail, wood, screw and staple fastnener connections. Brigham Young University, Provo, UT.

Foschi, R.O. 1974. Load-slip characteristics of nails. Wood Sci. 7(1): 69-74.

Foschi, R.O., and T. Bonac. 1977. Load-slip characteristics for connections with common nails. Wood Sci. 9(3): 118-123.

Gatto, K., and C.M. Uang. 2003. Effects of loading protocol on the cyclic response of woodframe shearwalls. J. Struct. Engrg. 129(10): 1384-1393.

Gupta, A.K., and G.P. Kuo. 1985. Behavior of wood-framed shear walls. J. Struct. Engrg. 111(8): 1722-1733.

He, M., F. Lam, and H.G.L. Prion. 1998. Influence of cyclic test protocols on performance of wood-based shear walls. Can. J. of Civ. Engrg. 25(3): 539-550.

Hunt, R.D., and A.H. Bryant. 1990. Laterally loaded nail joints in wood. J.Struct. Engrg. 116(1): 111-123.

ICC Evaluation Service. 2004. National Evaluation Report, NER-272. ICC-ES, Whittier, CA. 32pp.

Itani, R.Y., and C.K. Cheung. 1984. Nonlinear analysis of sheathed wood diaphragms. J. Struct. Engrg. 110(9): 2137-2147.

Itani, R.Y., and K. J. Fridley. 1999. Seismic response of light-frame wood buildings. In: Proceedings of the Invitational Workshop on Seismic Testing, Analysis and Design of Woodframe Construction, Los Angeles, CA. 111-116.

Johansen, K.W. 1949. Theory of timber connections. Publ. 9. Bern: International Association of Bridge and Structural Engineering. Zurich, Switzerland.

Jones, S.N., and F.S. Fonseca. 2002. Capacity of oriented stand board shear walls with overdriven sheathing nails. J. Struct. Engrg.28(7): 898-907

Kalkert, R.E., and J.D. Dolan. (1997). Behavior of 8-D nailed stud-to-sheathing connections. For. Prod. J. 47(6): 95-102.

Krawinkler, H., F. Parisi, L. Ibarra, A. Ayoub, and R. Medina. 2000. Development of a testing protocol for wood frame structures. CUREE Publication No. W-02, Richmond, CA.

Kasal, B., and R.J. Leichti. 1992. Nonlinear finite-element model for light-frame stud walls. J. Struct. Engrg. 118(11): 3122-3135.

Kasal, B., R.J. Leichti, and R.Y. Itani. 1994. Nonlinear finite-element model of complete light-frame wood structures. J. Struct. Engrg. 120(1):100-119.

Kent, S.M. 2004. The effect of biological deterioration on the performance of nailed oriented strand board sheathing to Douglas-fir framing member connections. Ph.D. dissertation. Oregon State University, Corvallis, OR.

Kim, J.H. 2003. Performance-based seismic design of light-frame shearwalls. Ph.D. dissertation, Department of Civil, Construction, and Environmental Engineering, Oregon State University, Corvallis, OR.

Lam, F., H.G.L. Prion, and M. He. 1997. Lateral resistance of wood shear walls with large sheathing panels. J. Struct. Engrg. 123(12): 1666-1673.

Langlois, J.D. 2002. Effects of Reference displacement and damage accumulation in wood shear walls subjected to the CUREE protocol. MS thesis, Oregon State University. Corvallis, OR.

Langlois, J.D., R. Gupta, and T.H. Miller. 2004. Effects of reference displacement and damage accumulation in wood shear walls. J. Struct. Engrg. 130(3): 470-479.

Larsen, H.J. 1973. The yield load of bolted and nailed joints. Proceedings, International Union on Forestry Research Organizations working group on structural utilization; September/ October. Pretoria, Republic of South Africa; [n.d.].

Lattin, P.D. 2002. Fully reversed cyclic loading of wood shearwalls fastened with super sheather nails. M.S. thesis, Brigham Young University. Provo, UT.

Moller, T. 1950. En ny method for berakning av spikforband: New method of estimating the bearing strength of nailed wood connections (in Swedish, with English translation). No. 117. Gothenburg. Sweden: Chalmers Tekniska Hogskolas Handlingar.

McCutcheon, W.J. 1985. Racking deformations in wood shear walls. J. Struct. Engrg. 111(2): 257-269.

National Evaluation Service Committee. 1997. Power-driven staples and nails for use in all types of building construction. *Rep. No. NER-272*, Council of American Building Officials.

Ni, C., and Y.H. Chui. 1996. Predicting the response of timber joints under reversed cyclic load. Proc: Int. Wood Engrg. Conf. Vol. 2, pp. 98-105, New Orleans, LA.

Polensek, A., and B. D. Schimel. 1985. Analysis of nonlinear connection systems in wood dwellings. J. Computing in Civil Engrg. 2(4): 365-379.

Polensek, A. 1976. Finite-element analysis of wood stud walls. J. of the Struct. Div. 102(7):1317-1335.

Rose, J. 1999. Seismic testing needs for wood shearwalls and diaphragms. Proc. Invitational Workshop Construction, Pub. No. W-01, California Universities for Research in Earthquake Engineering, Richmond, California. 103-109.

Rosowsky D.V., and J. H. Kim. 2002. Reliability studies, CUREE Publication no. W-10, Consortium of Universities for Research in earthquake Engineering, Richmond, CA.

Salenikovich, A.J., and J.D. Dolan. 2003. The racking performance of shear walls with various aspect ratios. Part 2. Cyclic tests of fully anchored walls. For. Prod. J. 53(11/12): 37-45.

Shenton, H.W., D.W. Dinehart, and T.E. Elliott. 1998. Stiffness and energy degradation of wood frame shear walls. Can. J. of Civ. Engrg. 25(3): 412-423.

White, M.W., and J.D. Dolan. 1995. Non-linear shear-wall analysis. J. Struct. Engrg. 121(11): 1629-1635.

Wilson, T.R.C. 1917. Tests made to determine lateral resistance of wire nails. Engineering Records. 75: 303-304.

Cyclic Performance of Wood Shearwalls as Affected by Decay

Erin N. Anderson
Robert J. Leichti

For Submission to Wood and Fiber Science
One Gifford Pinchot Drive
Madison, WI 53726-2398

4. Cyclic Performance of Wood Shearwalls as Affected by Decay

4.1. Abstract

Biological deterioration is known to have detrimental effects on wood assemblies. Some studies have shown that decay fungi degrades nail connection performance in light-frame structures, however, the effect of decay on the overall wall performance has received little attention. This study investigates the effect of biological deterioration on the cyclic performance of a light-frame shearwall of typical construction. The evaluation is based on the hysteretic parameters of laterally loaded single fastener tests and structural analysis using a numerical model Cyclic Analysis of SHEar Walls (CASHEW). The effect of decay is introduced by using the connection hysteretic parameters from cyclic test data of sheathing nail connections that were incubated to different levels of decay. The analysis presumes that a window is permitting water ingress at a corner of the window sill and that moisture ingress proceeds down a stud and along the sill plate of the adjacent shearwall. The condition creates a plume of moisture and decay that are represented by the hysteretic parameters from nail test data. First, the side of the wall is wet and the bottom of the wall is dry, then as moisture spreads, decay follows until the side and entire bottom of the wall are decayed to an extreme level. The nail parameters were randomly generated and assigned to appropriate nail locations on a shearwall. The CASHEW model output provides hysteretic parameters for the wall system, which were used to assess the impact of decay as a temporal and spatial variable on the performance of the shearwall. Based on the results for the shearwall assembly, the initial stiffness is more sensitive than peak capacity when the wall is exposed to decay while the displacement at peak capacity is unaffected. However, shearwall performance is not seriously affected until a large proportion of the perimeter nail connections are severely decayed.

4.2. Introduction

Light-frame wood buildings have earned a reputation as being highly resistant to earthquakes and wind primarily due to their lateral-force resisting systems. It is the sheathing connections in these assemblies that are the source of strength, stiffness, energy dissipation (Chui et al. 1998), and ductility (Filiatrault 1990). At the same time, Smulski (1999; 2000) has speculated that the wood structures built in the 1980's and 90's are among the least durable structures ever built due to moisture related problems. His speculations are derived from experiences that show new construction practices sometimes cause water to become trapped in wall cavities increasing the moisture level of the wood up to the fiber saturation point. The high moisture content makes the wood more prone to decay (Zabel and Morrell 1992).

Decay, even in the early stages, is capable of significantly reducing the mechanical properties of wood and wood-based materials and altering the yield mode of wood connections (Kent et al. 2004) with little observable change or weight loss (Wilcox 1978). Since considerable damage can occur before significant weight loss, bending strength and stiffness are better indicators of the decay effect (Winandy et al. 2000). Even though biological agents have been identified as a significant problem in light-frame wood construction and structural remediation, the topic has received little attention in the literature and design. Only Kent et al. (in press) and Kent (2004) have reported on the influence of decay on the cyclic performance of nail connections and the influence of decay on the connection yield modes. Recently, the effect of decay on shearwall performance was reported by Kim et al. (in press) in a fragility analysis for shearwalls with deterministic decay conditions subjected to a suite of ground motions. Numerical models developed to evaluate shearwalls have not provided methods to allow the incorporation of decay or other changes into the components of the wall, the studs, the sheathing or the connections. This is a limitation similar to those in the design tables.

This paper reports a numerical evaluation of a wood–frame shearwall that experiences changes in the wood condition at the connection level because of moisture and decay conditions. The performance criterion includes initial stiffness, peak capacity, displacement at peak capacity and energy dissipated. This study also provides the information necessary for subsequent conditional probability analysis using fragility methods.

4.3. Analysis and Design Scenario

This analysis was organized to assess the performance of shearwalls at increasing levels of decay. One shearwall configuration was considered. The spatial effect of the decay levels is simulated by applying the decay conditions in a stepwise fashion to the three treatment zones: edge of wall, bottom of left panel, and bottom of right panel.

The shearwall configuration for this study is the 8 by 8-ft. wall next to the window (Fig. 4.1). The shearwall is framed with Douglas Fir-Larch lumber. The rated sheathing is 4 by 8-ft oriented strandboard (OSB) 15/32-in. thick, vertically oriented, and nailed using 4-in. edge and 12-in. field nail schedules (Fig. 4.1). The wall was assumed to have a double top plate, double end studs and a single sole plate, and the wall was fully anchored with hold downs. The nailing on the end studs and top plates alternated studs. The nailing on the center stud was offset by 2 in. This is a typical shearwall for seismically designed wood frame structures. The design capacity for this configuration is 295 lb/ft or 2360 lb for the 8-ft shearwall (ICC Evaluation Service 2004).

The structural model scenario involves a window next to a shearwall segment, and the window is leaking at the bottom corner. The water drips down the side of the wall and across the bottom of the sill plate (Fig. 4.1). The presence of water initiates the temporal decay (indicated by "decay condition"). This study investigates seven decay conditions (Table 4.1); decay condition 1 is the best case scenario where the wall is new and dry and meets all design conditions, while decay condition 7 is the worst case scenario where

severe decay is widely distributed along the wall side and base and is so severe that the affected sheathing nails make no contribution to the strength or stiffness of the wall.

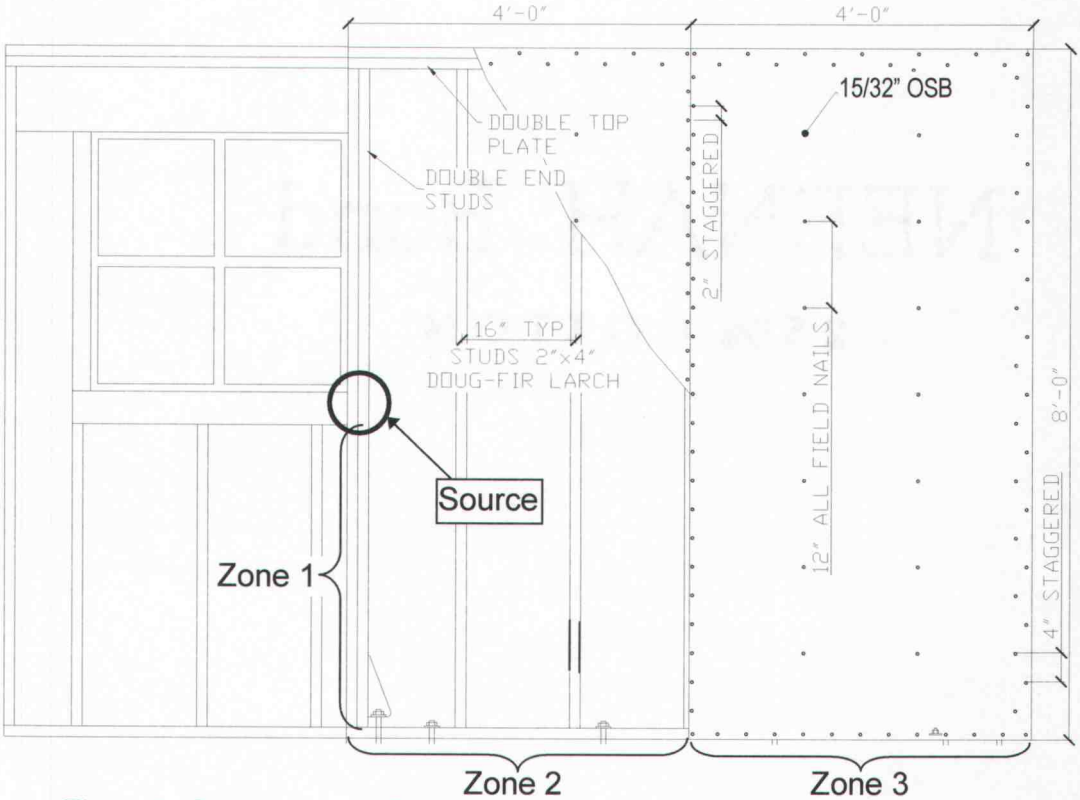

Fig. 4.1. Structural configuration: shearwall with window where water enters at the window sill and runs down the stud (Zone 1) and along the sill plate (Zone 2 and 3).

Table 4.1. Decay conditions for the shearwall where decay condition is described by Kent (2004).

	Decay Zone		
Decay Condition	Zone 1	Zone 2	Zone 3
1	Dry	Dry	Dry
2	Wet	Dry	Dry
3	Mild	Wet	Dry
4	Moderate	Mild	Wet
5	Severe	Moderate	Mild
6	Severe	Severe	Moderate
7	Severe	Severe	Severe

4.4. Methods and Materials

The basis for fastener properties in this study is nail connections between the wood framing members and the sheathing. The nail is an 8d common (0.113 in. diameter and 2.5 in. length). The connections were moisture conditioned, inoculated with *Postia placenta* (a common brown rot fungus), and incubated to four decay levels. The incubation periods described by Kent (2004) were (0, 10, 20, and 30 weeks) and a dry control group. The control, 0, 10, 20, and 30 decay conditions are referred to as dry, wet, mild decay, moderate decay, and severe decay, respectively, in this paper.

The conditioned connections were tested as single fastener lateral nail tests using the Consortium of Universities for Research in Earthquake Engineering (CUREE) protocol (Krawinkler et al. 2000). The CUREE protocol (Fig. 4.2) is scaled to a reference displacement found from the load-displacement curve of a monotonic test of replicate specimens. The reference displacement (Δ_{ref}) is $0.6\Delta_m$, where Δ_m is defined as the displacement at which the applied load drops for the first time below 0.8 of the maximum load. Ten connections were tested at each decay level. The complete experimental details and results for tests with decayed nail connections can be found in Kent et al. (2004), Kent et al. (in press) and (Kent 2004).

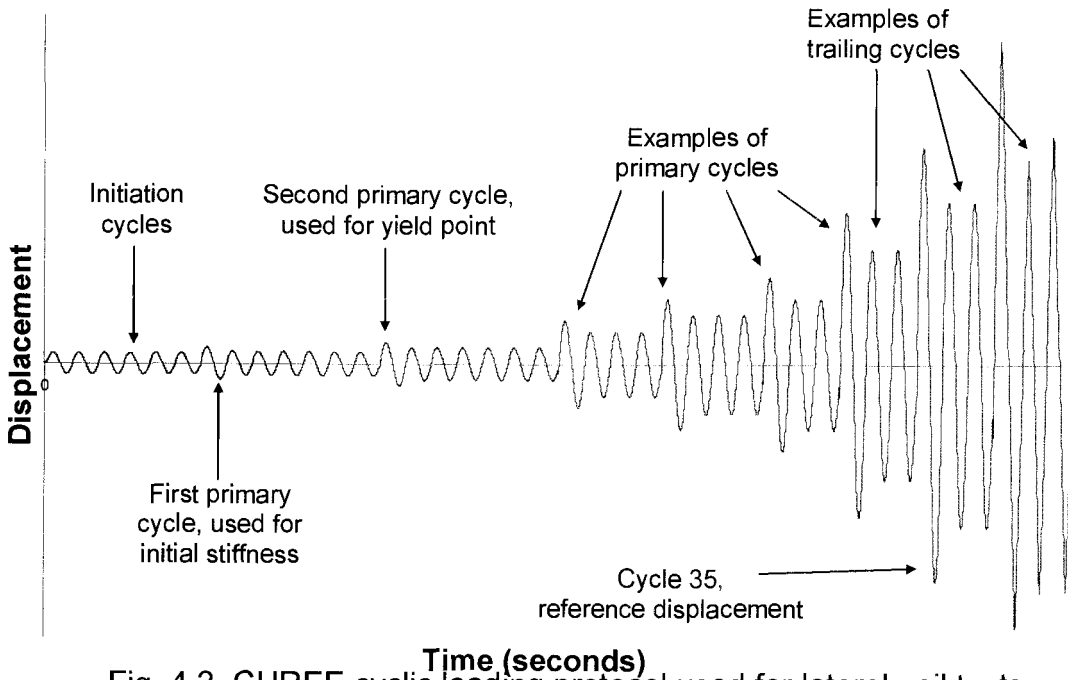

Fig. 4.2. CUREE cyclic loading protocol used for lateral nail tests by Kent (2004).

Each connection specimen produces a load-displacement response consisting of a set of hysteresis loops. Idealized hysteretic test data are shown in Fig. 4.3, and the hysteretic parameters are defined in Table 4.2. A program, SASHFIT (Elkins and Kim 2003b), was used to fit each real set of hysteresis loops from the connection tests with a theoretical set of hysteresis loops. The theoretical hysteretic loops are generated by adjusting ten hysteretic parameters, and the parameters for each sample have unique numerical values. The parameters F_o, F_I, K_o, r_1 and r_2 define the backbone curve that encompasses all of the hysteretic loops, while r_3, r_4, Δ_u, alpha (α) and beta (β) define the hysteretic nature of the curves. All of the hysteretic parameters except α and β are extracted directly from the load-displacement curves. The degradation parameters α and β are calculated as shown in Fig. 4.3. Parameter K_p is a function of the previous loading history through the last unloading displacement δ_{un} (point A, Fig. 4.3) with a corresponding force F_{un}. If the connector reaches δ_{un} in an additional cycle, then the corresponding load

will be less then F_{un} (point G, Fig. 4.3) due to the strength and stiffness degradations α and β. The initial stiffness, K_o, is defined as the slope of the ascending branch of the hysteresis curve corresponding to the first primary cycle of the CUREE protocol between two and forty percent of the maximum load. Ultimate load, F_u, is not a hysteretic parameter, but it is important in the description of the overall hysteretic behavior. For the purpose of this study, we assumed that each of the SASHFIT parameters is normally distributed.

Table 4.2. Description of hysteretic parameters extracted from cyclic data by SASHFIT.

Parameter	Description
K_o	Initial stiffness
δ_u	Deflection at ultimate load
F_o	y-intercept for secondary stiffness
F_I	y-intercept for Pinching Stiffness
r_1K_o	Secondary (asymtotic) stiffness
r_2K_o	Post-peak stiffness
r_3K_o	Unloading stiffness
r_4K_o	Pinching stiffness
α	Stiffness degradation
β	Strength degradation
F_u	Ultimate load

The set of ten parameters can be used to define the hysteretic behavior of nails or shearwalls that are tested by a cyclic loading protocol. Additional information about the hysteresis of nail connections is given elsewhere (Folz and Filiatrault 2000, 2001; Filiatrault 1990; Dolan and Madsen 1992a; Foschi 1974). Typical hysteretic nail test data are shown in Fig. 4.4 with the SASHFIT hysteretic data overlaid to illustrate data fit. The ten parameters provided (Table 4.3) are subsequently used as input for structural analysis of the shearwall in each decay condition using CASHEW (Cyclic Analysis of SHEar Walls).

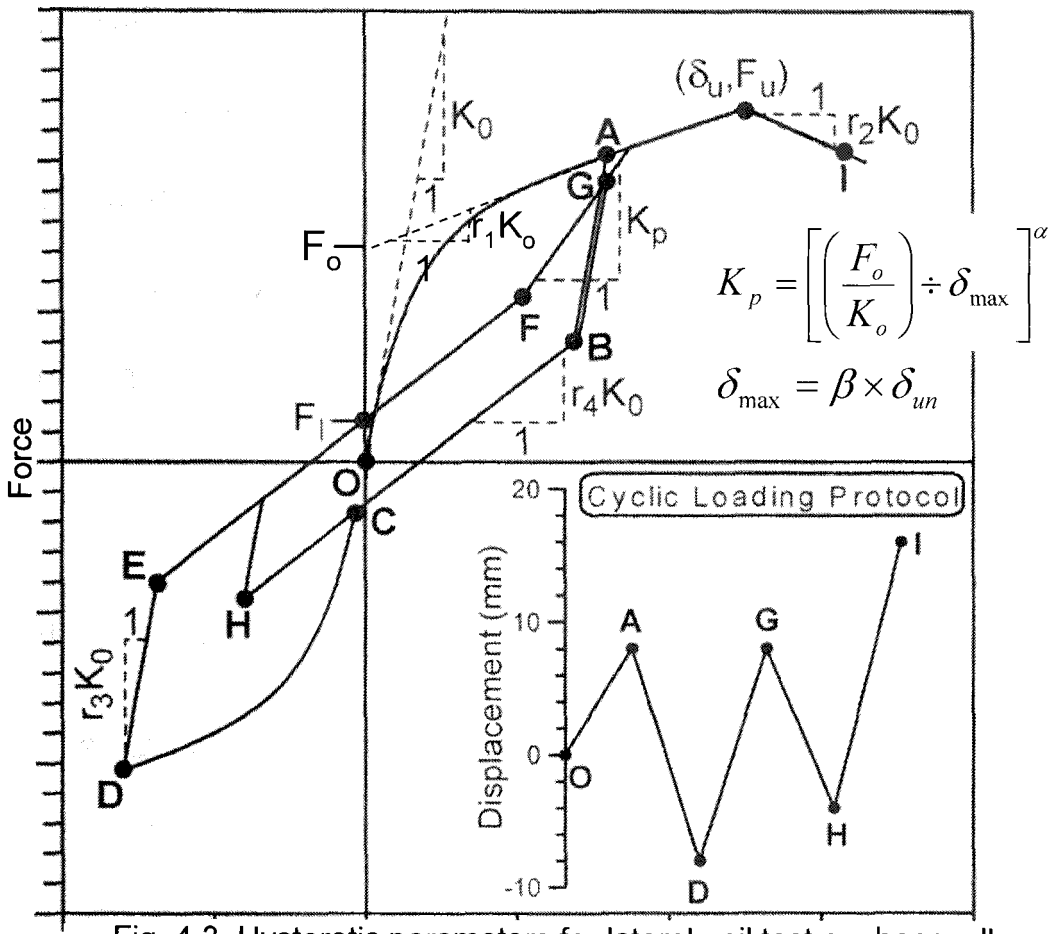

Fig. 4.3. Hysteretic parameters for lateral nail test or shearwall tests under cyclic loading (Folz and Filiatrault 2000).

Table 4.3. Hysteretic parameters for nailed connections, where parenthetical values are coefficients of variation.

Decay Condition	K_o lb/in.	r_1	r_2	r_3	r_4	F_0 lb	F_1 lb	Δ_u in.	α	β	F_u+ lb
Dry	3833	0.049	-0.103	1.55	0.0218	177	29.1	0.507	0.464	1.08	256
	0.19	0.53	1.53	0.21	0.30	0.10	0.14	0.39	0.15	0.04	0.11
Wet	2657	0.091	-0.071	1.27	0.0195	140	24.9	0.751	0.429	1.07	310
	0.17	0.24	0.54	0.37	0.27	0.27	0.12	0.29	0.15	0.05	0.17
Mild	2844	0.128	-0.053	1.78	0.0306	96	26.0	0.480	0.372	1.09	265
	0.14	0.52	0.49	0.24	0.29	0.32	0.14	0.33	0.46	0.03	0.31
Moderate	2480	0.088	-0.052	1.75	0.0310	134	21.2	0.581	0.496	1.10	251
	0.24	0.37	0.56	0.24	0.52	0.45	0.24	0.33	0.22	0.07	0.37
Severe	1915	0.071	-0.059	1.37	0.0228	68	9.32	0.351	0.559	1.17	105
	0.36	0.61	0.28	0.30	0.74	0.21	0.76	0.43	0.21	0.06	0.41

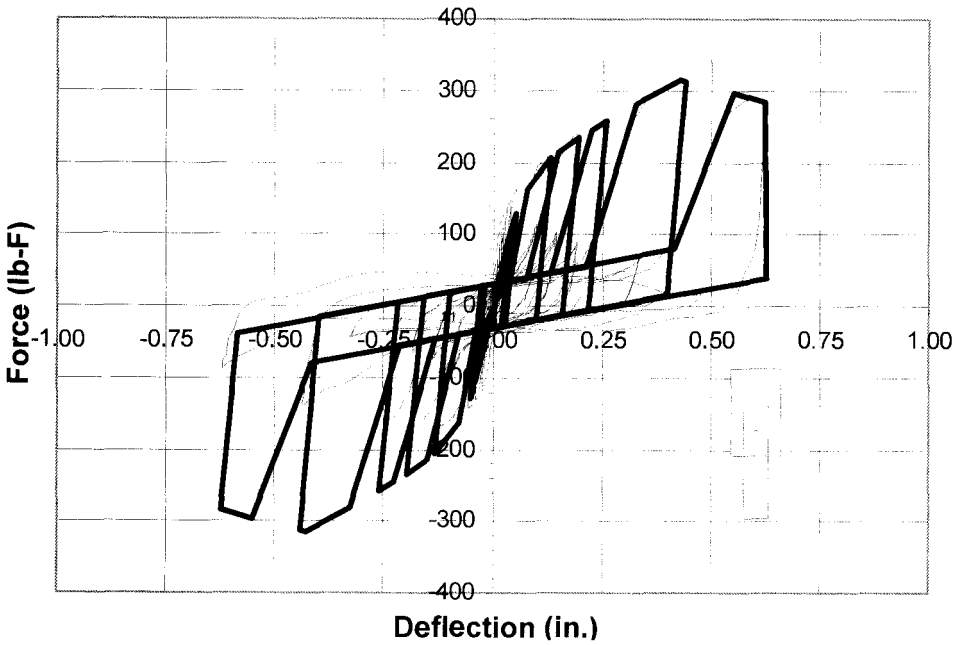

Fig. 4.4. Force-displacement response of a single lateral connection under CUREE loading protocol fit with SASHFIT estimated response.

CASHEW is a numerical model capable of predicting the load displacement response of a light-frame shearwall under a quasi-static cyclic loading (Folz and Filiatrault 2000, 2001). With information on shearwall geometry, nailing schedule, material properties and hysteretic behavior of the individual fasteners, CASHEW can be used to calculate the parameters of a single-degree of freedom (SDOF) model. The SDOF hysteretic model is used to predict the global cyclic response of a shearwall assembly under quasi-static or cyclic loading (Sutt et al. 2004). The CASHEW output is the hysteretic response of a fully anchored full-scale shearwall, and other output includes backbone curves, energy dissipation, and ten hysteresis parameters.

The original version of CASHEW had two modifications for this study. The original CASHEW allows only one set of hysteretic connector properties to be assigned to all of the sheathing nails in the wall, and there were some restrictions on the output. We modified CASHEW to allow multiple sets of hysteretic connector properties for the sheathing nails so that each row of nails

in the wall can have different properties (Anderson 2005). We also modified the original CASHEW so that all of the hysteretic parameters could be extracted when a user defined loading was used. A user-defined loading is sometimes needed to reduce the step-size so that the numerical convergence can be reached.

For each decay condition, thirty geometrically identical walls were simulated where the OSB sheathing and lumber framing were assigned deterministic material properties. The sheathing-nail properties were generated from SASHFIT hysteretic parameters of Table 4.3 . These data were applied to appropriate positions in the shearwall. For example in wall 1 at decay condition 4, the top row of sheathing nails on the right panel of the wall was assigned the hysteretic parameters from nail test 4 at the control condition, the bottom row of sheathing nails along the sole plate of the right panel were given hysteretic parameters corresponding to nail test 9 at the moderate decay level, the vertical line of sheathing nails on the center stud of the right panel were assigned hysteretic parameters from nail test 2 at the control condition, etc. The wall-by-wall assignment of nail connection data for the 210 simulated shearwalls (7 decay conditions × 30 shearwalls) is given in Anderson (2005). The shearwall properties where the decay conditions are the source of variation are analyzed by analysis of variance (ANOVA). The alpha level for significance is 0.05 unless specified otherwise.

4.5. Results

The backbone curve for cyclic tests data is created by drawing straight line segments between the peak load-displacement data points at each primary cycle. The cyclic backbone summary for the CASHEW hysteretic curves (Fig. 4.5a) for quadrant I depicts the overall behavior of the walls in each decay condition. The summary curves are the averages of the thirty simulations. The shapes of the decay condition backbone curves are similar. It can be seen that as the decay condition becomes more severe, the initial

stiffness and peak capacity decline. At the maximum load, the top four backbone curves are close to one another, and the average displacement at maximum load is typically around 2 in. of displacement (Fig. 4.5c). This indicates that the peak capacities at these decay levels are similar until later decay levels. At 0.4 in. of displacement, the displacement corresponding to the first primary cycle in the CUREE protocol, the points are ordered and progressively decline with each decay condition (Fig. 4.5b) indicating the initial stiffness of the walls are not similar and degrade with each increasing decay condition.

The hysteretic parameters and the energy dissipated from the thirty CASHEW simulations at each level of decay are summarized in Table 4.4, and some of the results are presented using box plots. A box plot provides a visual comparison of data that can be used to identify potential outliers, check for skewness, and identify differences between group medians. Box plots are drawn based on the median and displacement quartiles; the box represents the middle fifty percentile of data with the median marked in the box, the height of the box is defined as the interquartile range. Outlier data are marked as dots outside the whiskers, which are 1.5 times the interquartile range in length.

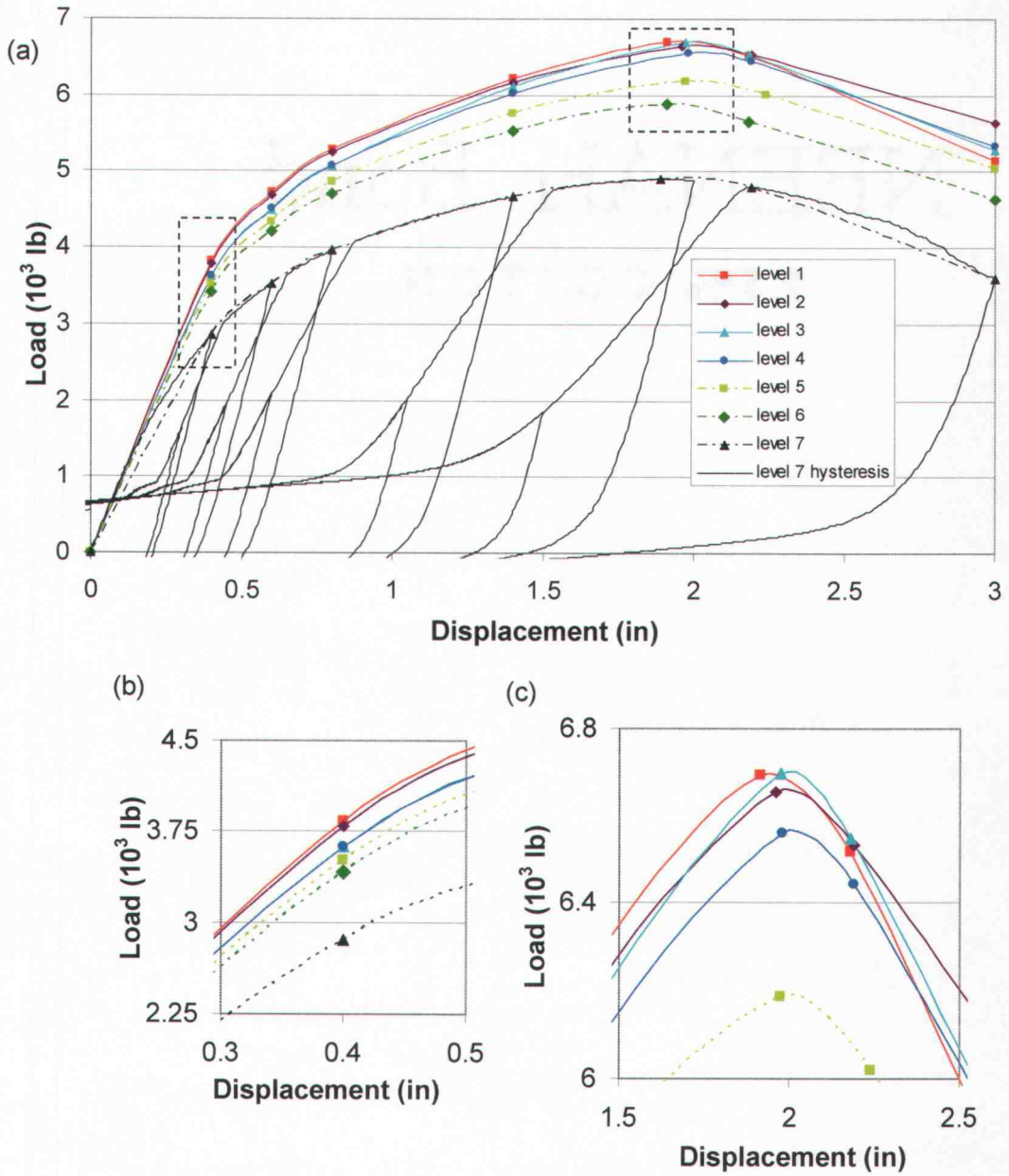

Fig. 4.5. Average backbone curves at each decay condition, (a) complete backbone curves in quadrant I; (b) backbone curves from 0.3 to 0.5 in. of displacement; (c) backbone curves for decay conditions 1 to 5 at maximum load.

Table 4.4. Hysteretic shearwall parameters from CASHEW (n=30), where parenthetical values are coefficients of variation.

Decay Condition	K_o 10^3lb/in.	Δ_u in.	r_1	r_2	r_3	r_4	F_o 10^3lb	F_l 10^3lb	F_u^+ 10^3lb
1	15.4 (0.058)	1.98 (0.14)	0.052 (0.218)	-0.072 (0.416)	0.871 (0.056)	0.035 (0.111)	5.22 (0.043)	0.836 (0.058)	6.71 (0.048)
2	15.2 (0.047)	2.05 (0.14)	0.052 (0.204)	-0.070 (0.615)	0.862 (0.053)	0.033 (0.09)	5.19 (0.037)	0.845 (0.049)	6.69 (0.04)
3	14.9 (0.047)	2.05 (0.147)	0.063 (0.172)	-0.066 (0.51)	0.901 (0.042)	0.036 (0.078)	4.97 (0.053)	0.840 (0.052)	6.73 (0.035)
4	14.5 (0.064)	2.04 (0.072)	0.059 (0.134)	-0.076 (0.497)	0.872 (0.049)	0.034 (0.112)	4.97 (0.069)	0.800 (0.05)	6.61 (0.047)
5	14.3 (0.06)	2.00 (0.062)	0.052 (0.241)	-0.072 (0.431)	0.897 (0.055)	0.036 (0.102)	4.86 (0.048)	0.763 (0.066)	6.22 (0.059)
6	14.0 (0.047)	2.00 (0.086)	0.044 (0.301)	-0.078 (0.508)	0.875 (0.049)	0.034 (0.113)	4.79 (0.057)	0.727 (0.06)	5.91 (0.05)
7	11.8 (0.054)	2.00 (0.13)	0.039 (0.295)	-0.082 (0.491)	0.888 (0.063)	0.037 (0.097)	4.16 (0.05)	0.648 (0.053)	4.95 (0.044)

An analysis of variance (ANOVA) for the initial stiffness (Fig. 4.6) of all decay conditions yielded a p-value of zero, that is, the mean initial stiffness at all decay conditions are not equal. The initial stiffness at each decay conditions was compared to the control condition (decay condition 1) using a paired t-test; starting at decay level 3, there is a significant loss of initial stiffness.

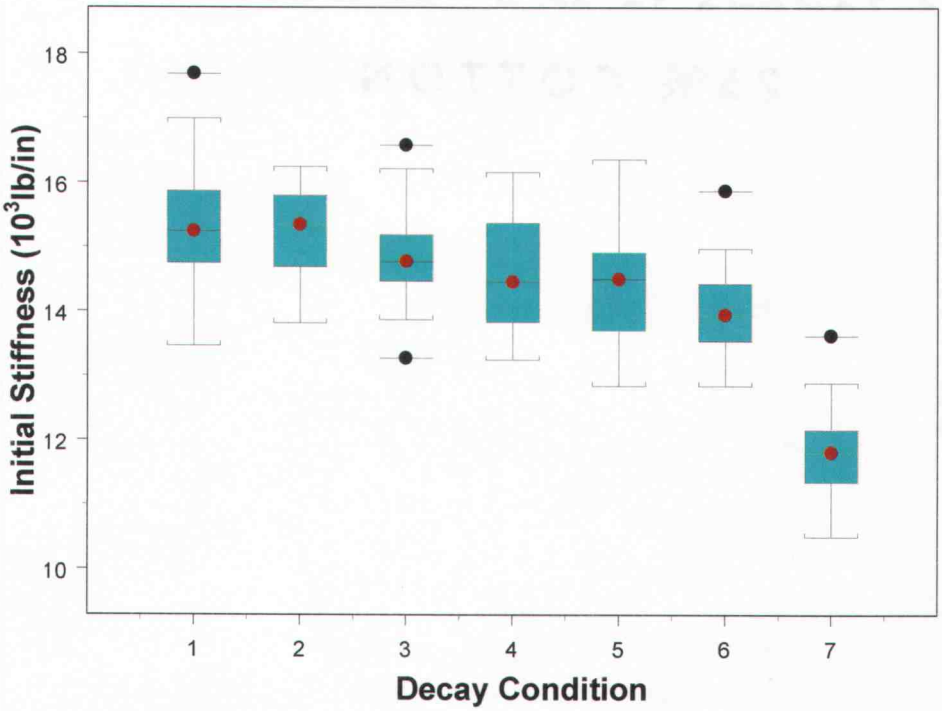

Fig. 4.6. Box plots for initial stiffness values from CASHEW.

The mean displacement at peak capacity (Fig. 4.7), is approximately 2 in. for each decay condition and is therefore unaffected by decay. The ANOVA produced a p-value of 0.885, so we inferred that even though the displacement at peak capacity is not affected by decay level, the load required to produce a 2-in. displacement is reduced by approximately 25 percent.

The peak capacity (Fig. 4.8) was affected by the decay condition (p-value<<0.001), but is more robust with respect to decay severity than the initial stiffness. Comparing peak capacity at each decay condition to the peak capacity at the control decay level showed that the peak capacity is not significantly different from that of the control until decay condition 5. At decay condition 5, each of the three zones has some decay exposure–zone 1, severe decay; zone 2, moderate decay; zone 3, 10 mild decay.

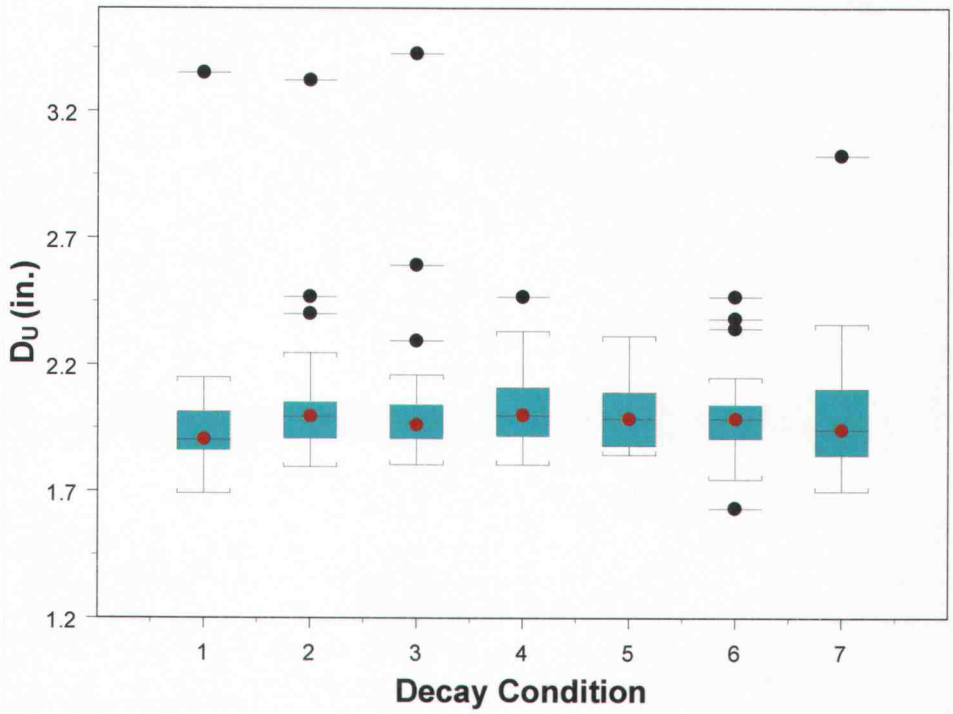

Fig. 4.7. Box plots for displacement at peak capacity from CASHEW.

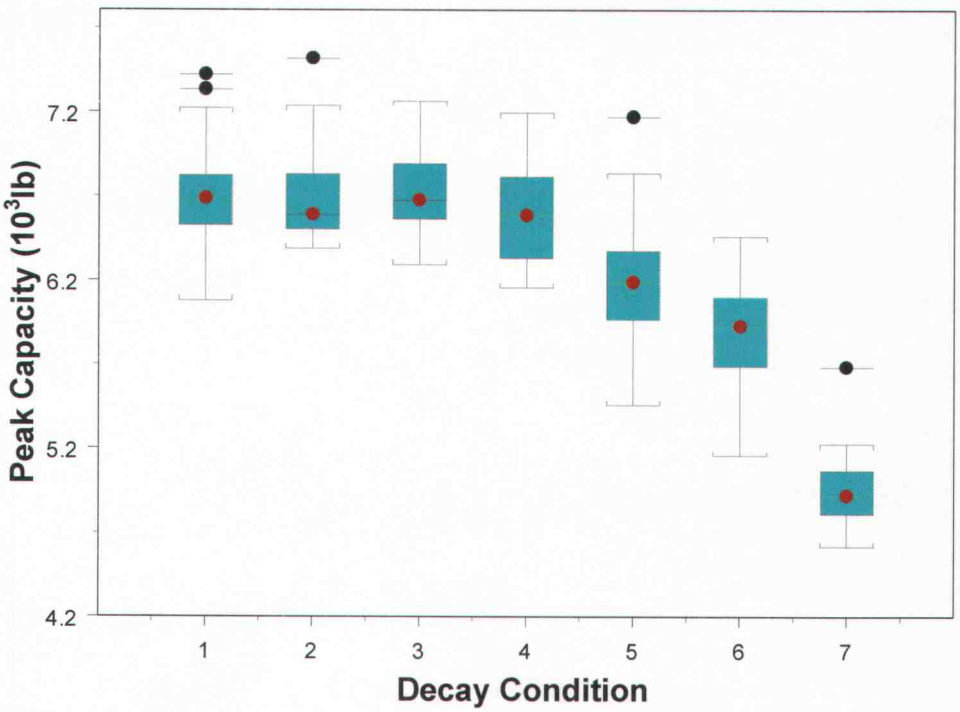

Fig. 4.8. Box plots for peak capacity values from CASHEW.

The model shearwall has 172 nails-144 perimeter nails and 28 field nails. A statical analysis of the shearwall shows that the perimeter nails have more influence than the field nails on wall system performance. In decay condition 7, 38 perimeter nails are ineffective (essentially missing) due to the severe decay condition, which is 22 percent of the total number of nails and 26 percent of the perimeter nails. Decay condition 7 causes a 23 percent reduction in average initial stiffness relative to the control, while the average peak capacity is reduced 26 percent relative to the control. This loss changes the estimated ratio of capacity to design from 2.8 to 2.1. When the peak capacity becomes significantly different from the control at decay condition 5, 7.6 percent of the nails, or 9 percent of the perimeter nails are affected by mild to severe decay, and the average of the CASHEW values for initial stiffness and peak capacity where reduced by approximately 7 percent.

In the single-nail lateral connection tests, decay level did not have a significant effect on initial stiffness and peak capacity (p-value=0.138 and p-value=0.506 respectively), but the yield load decreased significantly at the severe decay level (p-value=0.001 tensile yield load, and >0.001 for the compressive yield load) (Kent et al. in press). However, the shearwall initial stiffness is significantly affected at decay condition 3, even though the single-nail connection properties were not significantly affected at this point. Connection properties were considered to be significantly different from the control conditions at the severe decay level (Kent et al. in press).

The cumulative energy dissipated by the shearwalls increases exponentially though the primary cycles (Fig. 4.9). The total amount of energy dissipated by the walls (cycle 18) at each decay condition is statistically similar to the control level until decay condition 5 (p-value<0.001); which follows the peak capacity results. However, at each primary cycle leading up to the end, the energy dissipated is significantly different from the control level at decay condition 4. Unlike decay condition 5 when each zone of the wall is exposed to decay, decay condition 4 is the decay condition when each zone is no

longer in the control condition-zone 1, moderate decay; zone 2, mild decay; zone 3, wet.

The boundary condition for CASHEW models is full anchorage, and if the anchorage was removed or also lost due to decay, the loss of initial stiffness and peak capacity would increase by an additional unknown amount. However, Kent (2004) showed that the OSB sheathing side member of the nailed connection always deteriorated at a faster rate than the wood main member of the connection. Thus, the decay condition in the OSB sheathing controls the changes, if any, in the structural performance. For this reason, anchorage deterioration is not included in the model.

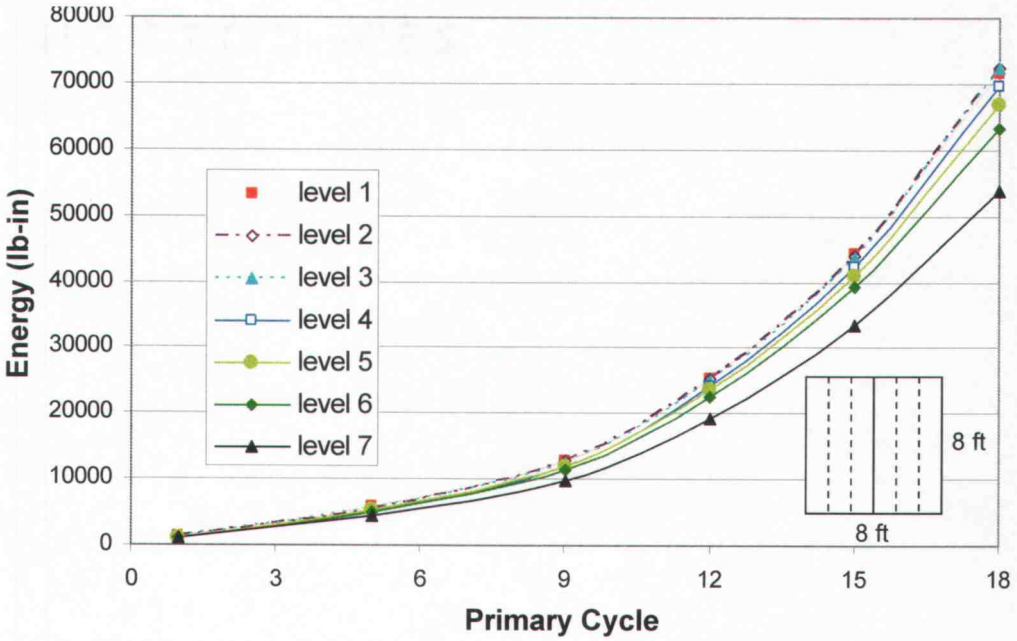

Fig. 4.9. Average cumulative energy dissipated at the primary cycle of the CUREE loading protocol for shearwalls at each decay condition.

An ANOVA was conducted for each of the hysteretic parameters. The results suggest that r_2 is not affected by decay (p-value=0.524). However, the other mean hysteretic characteristics r_3 and r_4 are significantly affected. The evidence of differences for the r_3 parameter is moderate (p-value=0.01),

however, r_4 is strongly affected by decay level (p-value<0.001). The remaining parameters F_o, F_l, Δ_u and r_1, which are characteristic of the ascending portion of the backbone are strongly affected by decay (p-values<<0.001). This data indicates that the overall behavior of the wall classified by the backbone is more sensitive to decay than the parameters that describe the hysteric nature of the curves (r_3 and r_4).

The distributions for initial stiffness and peak capacity at each decay level were evaluated for normality using the Kolmogrov-Smirnov test. The analysis showed that initial stiffness and peak capacity can be described by the normal distribution over a broad range of conditions. Probability distributions needed for reliability-based design were created for initial stiffness (Fig. 4.10) and peak capacity (Fig. 4.11). If a minimum initial stiffness or peak capacity was required, these plots could provide a convenient method to estimate the probability of failure for this particular wall configuration. For example, the effect of decay and moisture on peak capacity can be seen in Fig 4.11. If a minimum peak capacity of 6 kips is required, the shearwalls at the first four decay conditions at least a 95 percent chance of achieving this value; however, at decay condition 6, there is a 35 percent chance that the peak capacity will not be achieved.

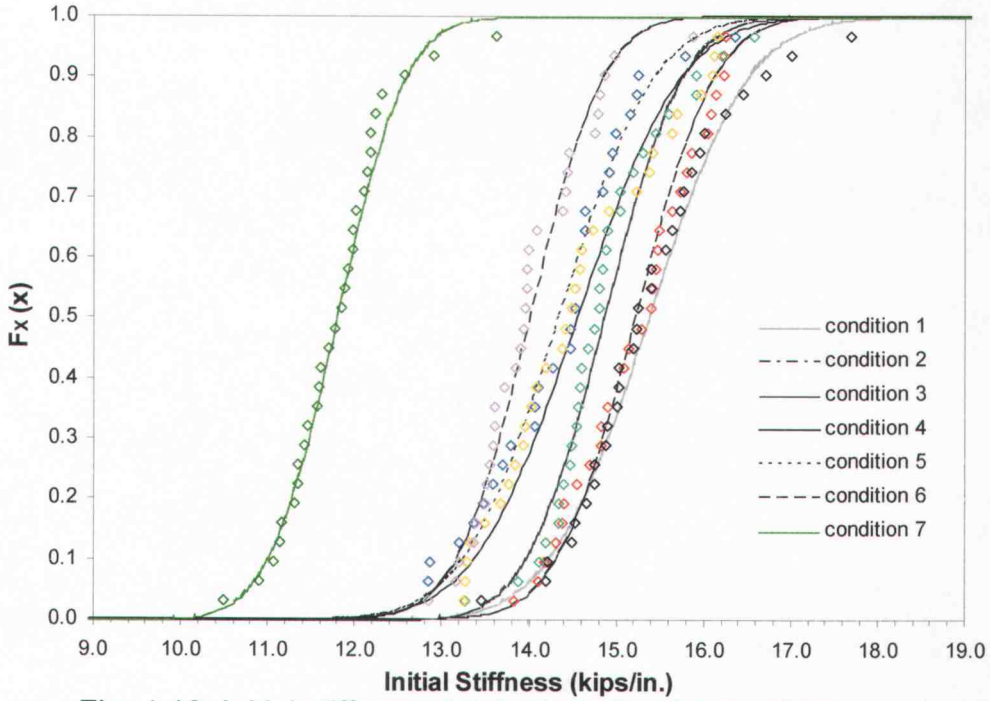

Fig. 4.10. Initial stiffness distributions for shearwalls shown by decay condition.

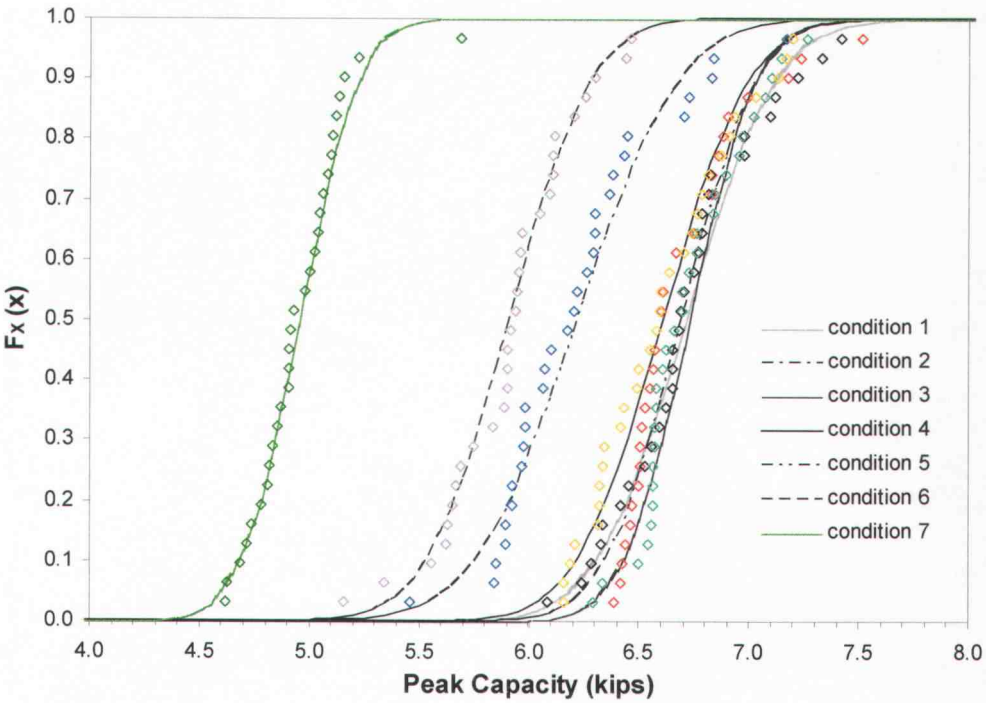

Fig. 4.11. Peak capacity distributions for shearwalls shown by decay condition.

4.6. Conclusions

This paper described a study that investigated the cyclic performance of shearwalls as affected by combined moisture and decay conditions. The investigation used a numerical model that relied on the properties of sheathing-nail connections. The high moisture and decay conditions were applied only to the perimeter nails in a manner that reflected a probable moisture-decay situation in light-frame structures. The inferences are based only on the numerical results because no shearwalls were actually conditioned and tested.

The initial stiffness was affected at a relatively low level of decay damage while the energy dissipation and peak capacity were more robust with respect to the effects of decay. Energy dissipation and peak capacity were affected once a large percentage of the perimeter nails were included in the plume of moisture and decay. However, even when the severe decay condition affected 26 percent of the perimeter nails, the ratio of capacity to design was still approximately 2.1. Decay and moisture plumes occurring at field nails would have a lesser effect on performance than the case considered in this study. The peak capacity and initial stiffness parameters appear to be normally distributed over a broad range of physical conditions. Displacement at peak capacity was not affected by decay and moisture, however, if dynamic ground motions been considered, displacement at peak capacity may have been more variable.

This is not a comprehensive study on the evaluation of biological deterioration and shearwalls, because it addresses one wall configuration and one fungal agent. However, the process used here could be applied to other configurations, building materials and fungal deterioration at varying levels.

4.7. References

Anderson, E.N. 2005. The Effects of Nail Bending-Yield Stress and Biological Deterioration on the Cyclic Performance of Shearwalls. M.S. thesis, Oregon State University, Corvallis, OR.

Chui, Y.H., C. Ni, and L. Jaing. 1998. Finite-element model for nailed wood joints under reversed cyclic load. J. Struct. Engrg. 124(1): 96-103.

Dolan, J.D., and B. Madsen. 1992a. Monotonic and cyclic nail connection tests. Can J. of Civ. Engrg. 19(1): 97-104.

Elkins, L. and J.H. Kim. 2003b. Introduction to SASHFIT. User's manual, Oregon State University, Corvallis, OR.

Filiatrault, A. 1990. Static and dynamic analysis of timber shear walls. Can J. Civ. Engrg. 17(4): 643-651.

Foschi, R.O. 1974. Load-slip characteristics of nails. Wood Science. 7(1): 69-74.

Folz, B. and A. Filiatrault. 2001. Cyclic analysis of wood shear walls. J. Struct. Engrg. 127(4): 433-441.

Folz, B. and A. Filiatrault. 2000. CASHEW—Version1.0: A computer program for cyclic analysis of wood shear walls. CUREE Publication No. W-08, Consortium of Universities for Research in Earthquake Engineering, Richmond CA.

ICC Evaluation Service. 2004. National Evaluation Report, NER-272. ICC-ES, Whittier, CA. 32 pp.

Kent, S.M. 2004. The effect of biological deterioration on the performance of nailed oriented strand board sheathing to Douglas-fir framing member connections. Ph.D. dissertation. Oregon State University, Corvallis, OR.

Kent, S.M., R.J. Leichti, D.V. Rosowsky, and J.J. Morrell. 2004. Effects of wood decay by *postia placenta* on the lateral capacity of nailed oriented strandboard sheathing and douglas-fir framing members. Wood and Fiber Sci. 36(4): 560-572.

Kent, S.M., R.J. Leichti, D.V. Rosowsky, and J.J. Morrell. In Press. Effects of decay on the cyclic properties of nailed connections. J. Mater. in Civ. Engrg.

Kim, J.H., S.M. Kent, and D.V. Rosowsky. In Press. The effect of biological deterioration on the dynamic performance of woodframe shearwalls. Computer-Aided Civil and Infrastructure Engineering.

Krawinkler, H., F. Parisi, L. Ibarra, A. Ayoub, and R. Medina. 2000. Development of a testing protocol for wood frame structures. CUREE Publication No. W-02, Richmond, CA.

Smulski, S. 1999. Durability of energy efficient wood-frame houses. For. Prod. J. 49(5): 8-15.

Smulski, S. 2000. Ensuring the durability of energy-efficient houses. Fine Homebuilding 132: 72-77.

Sutt, E., Rosowsky, D., and Anderson, E. 2004. Effect of fastener bend-yield stress on cyclic performance of lateral wood connection. Proc. World Conference on Timber Engineering. Lahti, Finland. Association of Finnish Civil Engineers RIL. pp 119-124.

Wilcox, W.W. 1978. Review of literature on the effects of early stages of decay on wood strength. Wood and Fiber Sci. 9(4): 252-257.

Winandy, J.E., and J.A. Micales, C.A. Clausen, and S.F. Curling. 2000. Predicting the effects of decay on wood properties and modeling residual service life. Poster presentation, Disaster Mitigation in Wood Frame Structures. Madison, WI.

Zabel, R.A. and J.J. Morrell. 1992. Wood Microbiology — Decay and its Prevention. Academic Press, New York, NY.

5. Conclusions

The combined studies presented here considered the properties used to evaluate the accepted yield mode equations and the effects on not only the single lateral connections, as well as shearwalls constructed with similar materials under cyclic loading, when selected properties are changed. The effects of varying f_{yb} using specially manufactured nails and the effects of degrading the embedment strength of the wood by exposing the materials to a brown rot fungus *Postia placenta* are both individually assessed. The preprocessor SASHFIT determines the hysteretic parameters of the connections and the numerical model CASHEW is used in conjunction with the connections to predict shearwall behavior based on initial stiffness, peak capacity, displacement at peak capacity and energy dissipation.

5.1. Bending-Yield Stress Analysis

Overall, the performance of the shearwall is not affected by varying the f_{yb} of the sheathing nail. As the bending-yield stress of the sheathing nail increased, the peak capacity of the wall also increased but the amount of increase was not significant after 145 ksi. Although the dominant failure mode for all nails types was withdrawal, as the f_{yb} increased, so did the probability of the nail experiencing fatigue and other nonductile failures such as pull-through. Interestingly, even though the nails became more brittle with the increasing f_{yb}, the ductility of the walls was not affected. This finding suggests that shearwall ductility is a function of the wood materials. Unlike peak capacity, the initial stiffness, displacement at peak capacity and energy dissipated by each wall were not significantly affected by the nail f_{yb}. The nail f_{yb} also did little to enhance the displacement performance of the shearwalls under seismic loads at the immediate occupancy and life safety limit states. The results of these tests and analyses show that mechanisms other than nail

strength should be examined when seeking to improve the lateral force resistance of wood shearwalls.

5.2. Decayed Shearwall Analysis

The presence of decay influences the performance of cyclically loaded shearwalls. The performance of the shearwalls is affected by the area affected by decay as well as the severity of the decay. Decay conditions at the perimeter nails have a greater potential to affect the wall performance than decay conditions in the field of the sheathing panel. The initial stiffness and peak capacity parameters appear to be normally distributed over a broad range of physical conditions. The initial stiffness of the shearwall is affected even when the decay condition at the perimeter nails is only mildly severe. The peak capacity and energy dissipation are more resistant to the effects of decay and show no significant signs of losse until 13.3 percent of the shearwall perimeter nails are exposed to moderate levels of decay. The displacement at peak capacity is unaffected by the decay, but if dynamic ground motions had been considered, that may not have been the case. All properties besides the displacement continue to decline as the severity of the decay in the perimeter wall zones increases. The hysteretic parameters that describe the behavior of the shearwall are also affected by decay with the exception of r_2.

5.3. Combined Assessment

In both studies, it has been shown that the performance of a cyclically loaded shearwall can be predicted by the hysteretic parameters of connections tested using the same load protocol, the same materials, and similar boundary conditions in conjunction with CASHEW. Also, it is possible to incorporate changing material properties into numerical models to better understand situations with non-ideal conditions. This study, particularly the decay

analysis, has opened the door to evaluating other shearwall scenarios where full-scale testing is not possible.

Bibliography

AF&PA. 1999. General dowel equations for calculating lateral connection values. Tech. Rept 12. American Forest and Paper Association, Washington DC. 174 pp.

AF&PA. 2001. National Design Specifications® for Wood Construction. American Forest and Paper Association, Washington, D.C.

American Society for Testing and Materials (ASTM). 2002a. Standard test methods for specific gravity of wood and wood-based materials. Annual book of ASTM standards. D2395-02. ASTM, West Conshohocken, PA.

American Society for Testing and Materials (ASTM). 2002b. Standard test methods for use and calibration of hand-held moisture meters. Annual book of ASTM standards. D4444-92. ASTM, West Conshohocken, PA.

American Society for Testing and Materials (ASTM). 2002c. Standard test method for evaluating dowel-bearing strength of wood and wood-base products. Annual book of ASTM standards. D5764-97a. ASTM, West Conshohocken, PA.

American Society for Testing and Materials (ASTM). 2002d. Standard Test Method of Optimal Emission Vacuum Spectrometric Analysis of Carbon and Low-Alloy Steel. Annual book of ASTM standards. E 415-99a. ASTM, West Conshohocken, PA.

American Society for Testing and Materials (ASTM). 2002e. Standard practice for static load test for shear resistance. Annual book of ASTM standards. E 564-00. ASTM, West Conshohocken, PA.

American Society for Testing and Materials (ASTM). 2002f. Standard methods for cyclic (reversed) load test for shear resistance of framed walls for buildings. Annual book of ASTM standards. E2126-02. ASTM, West Conshohocken, PA.

American Society for Testing and Materials (ASTM). 2002g. Standard test method for determining bending yield moment of nails. Annual book of ASTM standards. F1575. ASTM, West Conshohocken, PA.

American Society for Testing and Materials (ASTM). 2003. Standard Test methods for determination of Carbon, Sulfur, Nitrogen, and Oxygen in Steel and in Iron, Nickel, and Cobalt Alloys. Annual book of ASTM standards. E 1019-03. ASTM, West Conshohocken, PA.

Anderson, E.N. 2005. The Effects of Nail Bending-Yield Stress and Biological Deterioration on the Cyclic Performance of Shearwalls. M.S. thesis, Oregon State University, Corvallis, OR.

Aune,P., and M. Patton-Mallory. 1986a. Lateral load-bearing capacity of nailed joints based on the yield theory: Experimental Verification. Res. Pap. FPL-RP-470. Madison, WI:U.S. Department of Agriculture, Forest Service, Forest Products Laboratory, Madison, WI.

Aune,P., and M. Patton-Mallory. 1986b. Lateral load-bearing capacity of nailed joints based on the yield theory: Theoretical Development. Res. Pap. FPL-RP-471. Madison, WI:U.S. Department of Agriculture, Forest Service, Forest Products Laboratory, Madison, WI.

Baker, A.J. 1992. Corrosion of metal fasteners in CCA- and ACA-preservative treated wood in two environments. For. Prod. J. 42(9): 39-41.

Beall, F. 1999. Comments from workshop participants. Proceedings of the Invitational Workshop on Seismic Testing, Analysis and Design of Woodframe Construction. Los Angeles, CA. California Universities for Research in Earthquake Engineering, Richmond, CA.

Blass, H.J. 1994a. Variation of load-slip behavior in nailed joints: variation parallel to the grain. For. Prod. J. 44(1):15-20.

Blass, H.J. 1994b. Variation of load-slip behavior in nailed joints: variation perpendicular to the grain. For. Prod. J. 44(2):30-34.

Breyer, D.E., K. J. Fridley, D. G. Pollock, and K. Cobeen. 2003. Design of Wood Structures—ASD, McGraw Hill, New York, NY.

Chai, Y.H., and T.C. Hutchinson. 2003. Seismic damage characteristics of cripple walls. Earthquake Spectra. 19(4): 753-778.

Cheung, K.C.K., R.Y. Itani, and A. Polensek. 1988. Characteristics of wood diaphragms: experimental and parametric studies. Wood and Fiber Science 20(4):438-456.

Chui, Y.H., C. Ni, and L. Jaing. 1998. Finite-element model for nailed wood joints under reversed cyclic load. J. Struct. Engrg.124(1): 96-103.

Cowling, C.B. 1957. A partial list of fungi associate with decay of wood products in the United States. Plant Disease Reporter 41: 894-898.

Curling, S., J. E. Winandy, and C.A. Clausen. 2000. An experimental method to simulate incipient decay of wood by basidiomycete fungi. International Working Group on Wood Preservation, IRG/WP 00-20200. Stockholm, Sweden.

Dinehart, D.W., and H.W. Shenton. 1998. Comparison of static and dynamic response of shear walls. J. of Struct. Engrg.124(6): 686-695.

Dolan, J.D. 1989. The dynamic response of timber shear walls. Ph. D thesis, University of British Columbia, Vancouver, B.C.

Dolan, J.D., and R.O. Foschi. 1991. Structural analysis model for static loads on timber shear walls. J. Struct. Engrg.117(3): 851-861.

Dolan, J.D., and B. Madsen. 1992a. Monotonic and cyclic nail connection tests. Can J. of Civ. Engrg. 19(1): 97-104.

Dolan, J.D., and B. Madsen. 1992b. Monotonic and cyclic tests of timber shear walls. Can J. of Civ. Engrg. 19(4): 415-422.

Duncan, C.G., and F.F. Lombard. 1965. Fungi associated with principal decays in wood products in the United States. U.S. Forest Service Research Paper WO-4, U.S. Department of Agriculture, Washington, D.C.

Elkins, L., and J.H. Kim. 2003a. Introduction to CASHEW. User's manual, Oregon State University, Corvallis, OR.

Elkins, L., and J.H. Kim. 2003b. Introduction to SASHFIT. User's manual, Oregon State University, Corvallis, OR.

Elkins, L., and J.H. Kim. 2003c. Introduction to SASH1. User's manual, Oregon State University, Corvallis, OR.

Falk, R.H., and A.J. Baker. 1993. Fasteners for exposed wood structures. Wood Design Focus. 4(3): 14-17.

Federal Emergency Management Agency (FEMA). 2000. NEHRP guidelines for the seismic rehabilitation of buildings, FEMA-273, Federal Emergency Management Agency, Washington, DC.

Filiatrault, A., and B. Folz. 2002. Performance-based seismic design of wood framed buildings. J. Struct. Engrg. ASCE, 128(1): 39-47.

Filiatrault, A. 1990. Static and dynamic analysis of timber shear walls. Can J. Civ. Engrg. 17(4): 643-651.

Foliente G.C. 1995. Hysteresis modeling of wood joints and structural systems. J. Struct. Engrg.121(6): 1013-1022.

Foliente, G.C. 1994. Hysteresis characterization and modeling of timber joints and structures. Proc: Pacific Timber Engineering Conference. Gold Coast, Australia. 2(6):9-18.

Folz, B., and A. Filiatrault. 2004a. Seismic analysis of wood frame structures. I: Model formulation. J. of Struct. Engrg.130(9): 1353-1370.

Folz, B., and A. Filiatrault. 2004b. Seismic analysis of woodframe structures. II: Model implementation and verification. J. Struct. Engrg.130(9):1361-1370.

Folz, B., and A. Fillatrault. 2001. Cyclic analysis of wood shear walls. J. Struct. Engrg.127(4): 433-441.

Folz, B., and A. Filiatrault. 2000. CASHEW—Version1.0: A computer program for cyclic analysis of wood shear walls. CUREE Publication No. W-08, Consortium of Universities for Research in Earthquake Engineering, Richmond CA.

Fonseca, F.S., S.K. Rose, and S.H. Campbell. 2002. CUREE-Caltech Woodframe Project, Task 1.4.8.1-Nail, wood, screw and staple fastener connections. Brigham Young University. Provo, UT.

Foschi, R.O. 1974. Load-slip characteristics of nails. Wood Science. 7(1): 69-74.

Foschi, R.O., and T. Bonac. 1977. Load-slip characteristics for connections with common nails. Wood Science. 9(3): 118-123.

Freyfield, E.E. 1939. The effect of humidity on the growth of wood destroying fungi in timber (abstract, in Russian). Review of Applied Mycology. 18: 644.

Gatto, K., and C.M. Uang. 2003. Effects of loading protocol on the cyclic response of woodframe shearwalls. J. Struct. Engrg.129(10): 1384-1393.

Green, F., and T.L. Highley. 1997. Brown-rot wood decay—In sights gained from a low-decay isolate to determine the effects of fungi on strength. Tappi. 47(8): 449-451.

Griffin, D.M. 1977. Water potential and wood decay fungi. Annual Review of Phytopathology.15: 319-329.

Gupta, A.K., and G.P. Kuo. 1987. Wood-framed shear walls with uplifting. J. Struct. Engrg.113(2): 241-259.

Gupta, A.K., and G.P. Kuo. 1985. Behavior of wood-framed shear walls. J. Struct. Engrg.111(8): 1722-1733.

Gutkowski, R.M. and A.L. Castillo. 1988. Single- and double-sheathed wood shear walls study. J. Struct. Engrg.114(6): 1268-1284.

He, M., F. Lam, and H.G.L. Prion. 1998. Influence of cyclic test protocols on performance of wood-based shear walls. Can. J. of Civ. Engrg. 25(3): 539-550.

He, M., H. Magnusson, F. Lam, and H.G.L. Prion. 1999. Cyclic performance of perforated wood shear walls with over sized panels. J. Struct. Engrg.125(1): 10-18.

Heine, C.P. and J.D. Dolan. 2001. Dynamic performance of perforated light-frame shear walls with various end restraints. For. Prod. J. 51(7/8): 65-72.

Humphrey, C.J. 1923. Nature and cause of decay in building timbers. Paper R28, U.S. Department of Agriculture, Forest Service, Forest Products Laboratory. Madison, WI.

Hunt, R.D., and A.H. Bryant. 1990. Laterally loaded nail joints in wood. J. Struct. Engrg.116(1): 111-123.

ICC Evaluation Service. 2004. National Evaluation Report, NER-272. ICC-ES, Whittier, CA. 32pp.

Imamura, H., and M. Kiguchi. 1999. Prediction of wood decay in the exterior wall of wooden houses by the deterioration of nails. Proc. Eighth international conference on durability of building materials and components, Vancouver, Canada. Vol.2, pp. 746-755. NRC Reseach Press, Ottawa.

International Code Council. 2003. International Building Code (IBC). International Code Council, Inc. Falls Church, VA.

Itani, R.Y., and C.K. Cheung. 1984. Nonlinear analysis of sheathed wood diaphragms. J. Struct. Engrg.110(9): 2137-2147.

Itani, R.Y., and K. J. Fridley. 1999. Seismic response of light-frame wood buildings. In: Proceedings of the Invitational Workshop on Seismic Testing, Analysis and Design of Woodframe Construction, Los Angeles, CA. 111-116.

Johansen, K.W. 1949. Theory of timber connections. Publ. 9. Bern: International Association of Bridge and Structural Engineering. Zurich, Switzerland.

Jones, S.N., and F.S. Fonseca. 2002. Capacity of oriented stand board shear walls with overdriven sheathing nails. J. Struct. Engrg.28(7): 898-907.

Kalkert, R.E., and J.D. Dolan. (1997). Behavior of 8-D nailed stud-to-sheathing connections. For. Prod. J. 47(6): 95-102.

Karacabeyli, E., and A. Ceccotti. 1996. Test results on the lateral resistance of nailed shear walls. Proc: Intl. Wood Engrg Conf. Vol. 2. pp. 179-186. 1996 International Wood Engineering Conference, New Orleans, LA.

Kasal, B., and R.J. Leichti. 1992. Nonlinear finite-element model for light-frame stud walls. J. Struct. Engrg.118(11): 3122-3135.

Kasal, B., R.J. Leichti, and R.Y. Itani. 1994. Nonlinear finite-element model of complete light-frame wood structures. J. Struct. Engrg.120(1):100-119.

Kent, S.M. 2004. The effect of biological deterioration on the performance of nailed oriented strand board sheathing to Douglas-fir framing member connections. Ph.D. dissertation. Oregon State University, Corvallis, OR.

Kent, S.M., R.J. Leichti, D.V. Rosowsky. and J.J. Morrell. 2004. Effects of wood decay by *postia placenta* on the lateral capacity of nailed oriented strandboard sheathing and douglas-fir framing members. Wood and Fiber Sci. 36(4): 560-572.

Kent, S.M., R.J. Leichti, D.V. Rosowsky, and J.J. Morrell. (in press). Effects of decay on the cyclic properties of nailed connections. J. Mater. in Civ. Engrg.

Kim, J.H. 2003. Performance-based seismic design of light-frame shearwalls. Ph.D. dissertation, Department of Civil, Construction, and Environmental Engineering, Oregon State University, Corvallis, OR.

Kim, J.H., S.M. Kent, and D.V. Rosowsky. (in press). The effect of biological deterioration on the dynamic performance of woodframe shearwalls. Computer-Aided Civil and Infrastructure Engineering.

Krawinkler, H., F. Parisi, L. Ibarra, A. Ayoub, and R. Medina. 2000. Development of a testing protocol for wood frame structures. CUREE Publication No. W-02, Richmond, CA.

Kubler, H. 1992. Corrosion of nails in wood construction interfaces. For. Prod. J. 42(1): 47-49.

Kumaran, M.K., P. Mukhopadhyaya, S.M. Cornick, M.A. Lacasse, M. Rousseau, W. Maref, M. Nofal, J.D. Quirt and W.A. Dalgliesh. 2003. An intergrated methodology to develop moisture management strategies for exterior wall systems. Proc. 9th Canadian conference on building science and technology, Vancouver, B.C. pp. 45-62. Institute for research in construction, Canada.

Lam, F., H.G.L. Prion, and M. He. 1997. Lateral resistance of wood shear walls with large sheathing panels. J. Struct. Engrg.123(12): 1666-1673.

Langlois, J.D., R. Gupta, and T.H. Miller. 2004. Effects of reference displacement and damage accumulation in wood shear walls. J. Struct. Engrg.130(3): 470-479.

Langlois, J.D. 2002. Effects of Reference displacement and damage accumulation in wood shear walls subjected to the CUREE protocol. MS thesis, Oregon State University. Corvallis, OR.

Langlois, J.D., R. Gupta, and T.H. Miller. 2002. Reference displacement effects in wood shear walls subjected to the CUREE protocol. Proc: 7th World Conf. on Timber Engineering. Shah Alam, Malaysia. 2: 447-454.

Larsen, H.J. 1973. The yield load of bolted and nailed joints. Proc: International Union on Forestry Research Organizations Working Group on Structural Utilization; Pretoria, Republic of South Africa; [n.d]

Lattin, P.D. 2002. Fully reversed cyclic loading of wood shearwalls fastened with super sheather nails. M.S. thesis, Brigham Young University. Provo, UT.

Leicester, R.H., C.H. Wang, G.C. Foliente, J.D. Thornton, G.C. Johnson, M. Cause, and C. MacKenzie. 2000. Engineering models for decay of timber. Proc: World Conf. on Timber Engrg. Paper 6.5.1. Vancouver, B.C. University of British Columbia. Paper 6.5.1.

Leichti, R.J., J.J. Morrell, D.V. Rosowsky. 2005. Effect of decay on wall system behavior. Wood Design Focus. 16(1): 3-7.

Leichti, R.J., R. Stable, and D.V. Rosowsky. 2002. A performance assessment of flood-damaged shearwalls. Proc: 9th International conference on durability of building materials. Australian Corrosion Association, New Bedford, NSW. Paper 50.

McCutcheon, W.J. 1985. Racking deformations in wood shear walls. J. Struct. Engrg.111(2): 257-269.

Mohammad, M.A.H., and I. Smith. 1997. Nail embedment responses of lumber and OSB: Influences of moisture conditioning. J. Inst. of Wood Sci. 14(3):131-139.

Mohammad, M.A.H., and I. Smith. 1994. Stiffness of nailed OSB-to-lumber connections. For. Prod. J. 44(11/12): 37-44.

Moller, T. 1950. En ny method for berakning av spikforband: New method of estimating the bearing strength of nailed wood connections (in Swedish, with English translation). No. 117. Gothenburg. Sweden: Chalmers Tekniska Hogskolas Handlingar.

Morrell, J.J., C.S. Love, R.J. Leichti, and R.J. Scott. 2000. Predicting decay rates in structures: The effects of wood moisture content. International Working Group on Wood Preservation, IRG/WP 00-20200. Stockholm, Sweden.

Nakajima, S. 2000. The effect of the moisture contents on the strength and stiffness properties of nailed joints and shear walls. Proc: World Conf. on Timber Engrg. Paper 1.1.3. University of British Columbia, Vancouver, B.C.

Nanami, N., T. Shibusawa, M. Sato, T. Arima, and M. Kawai. 2000. Durability assessment of wood-framed walls and mechanical properties of plywood in use. Proc: World Conference on Timber Engrg. Paper 6.5.3. University of British Columbia, Vancouver, B.C.

National Evaluation Service Committee. 1997. Power-driven staples and nails for use in all types of building construction. *Rep. No. NER-272*, Council of American Building Officials, La Grange, IL.

NES. 2002. Protocol for durability assessment of building products and systems. National Evaluation Service Inc., Lessburg, VA.

Ni, C., and Y.H. Chui. 1996. Predicting the response of timber joints under reversed cyclic load. Int. Wood Engrg. Conf. Paper. Vol. 3, pp.98-105. 1996 International Wood Engineering Conference, New Orleans, LA.

Ni, C., and Y. Chui. 1994. Response of nailed wood joints to dynamic loads. Pacific Timber Engrg. Conf., Gold Coast, Australia. 2(6):26-32.

Polensek, A. 1976. Finite-element analysis of wood stud walls. J. Engrg. Struct. Div. 102(7):1317-1335.

Polensek, A., and B. D. Schimel. 1985. Analysis of nonlinear connection systems in wood dwellings. J. Computing in Civil Engrg. 2(4): 365-379.

Pryor, S., G.W. Taylor, and C.E. Ventura. 2000. Seismic testing and analysis program on high aspect ratio wood shear walls. Proc: World Conf. on Timber Engineering, British Columbia. Paper 1.1.4. University of British Columbia, Vancouver, B.C.

Quarles, S.L. 1989. Factors influencing the moisture conditions in crawl spaces. For. Prod. J. 39(10): 71-75.

Quarles, S.L., and K.A. Flynn. 2000. Performance o wood and wood-based materials in multi-family housing: issues from a California perspective. Proc: 2nd annual conference on durability and disaster mitigation in wood-frame housing. Forest Products Society, Madison, WI. pp. 3-9.

Rammer, D.R. 2001. Effect of moisture content on nail bearing strength. Res. Pap. FPL-RP-591. Madison, WI:U.S. Department of Agriculture, Forest Service, Forest Products Laboratory, Madison, WI.

Rammer, D.R., and S.G. Winistorfer. 2001. Effect of moisture content on dowel-bearing strength. Wood and Fiber Sci. 33(1): 126-139.

Rose, J.D. 1998. Preliminary testing of wood structural panels shear walls under cyclic (reversed) loading. APA Research Rep. No. 158. American Plywood Association, Tacoma, WA.

Rose, J. 1999. Seismic testing needs for wood shearwalls and diaphragms. Proc. Invitational Workshop Construction, Pub. No. W-01, California Universities for Research in Earthquake Engineering, Richmond, California. 103-109.

Rosowsky D.V., and J. H. Kim. 2002. Reliability studies, CUREE Publication no. W-10, Consortium of Universities for Research in Earthquake Engineering, Richmond, CA.

Rosowsky D.V. and T.A. Reinhold. Rate-of-load and duration-of-load effects for wood fasteners. J. Struct. Engrg. 125(7): 719-724.

Ruddick, J.N.R. 1988. Corrosion of metal fasteners in contact with preservative treated wood. Proc: of the American Wood Preservers' Association, AWPA. Woodstock, MD. 84: 216-224.

Salenikovich, A.J., and J.D. Dolan. 2003. The racking performance of shear walls with various aspect ratios. Part 2. Cyclic tests of fully anchored walls. For. Prod. J. 53(11/12): 37-45.

Salenikovich, A. J., and J.D. Dolan. 2000. The racking performance of light-frame shear walls with various tie-down restraints. Proc: World Conf. on Timber Engineering, British Columbia. Paper 2.1.3. University of British Columbia, Vancouber, B.C.

Scheffer, T.C. 1971. A climate index for estimating potential for decay in wood structures above ground. For. Prod. J. 21(10): 25-32.

Scheffer, T.C., and C.S. Moses. 1993. Survey of moisture content in houses for evidence of decay susceptibility. For. Prod. J. 43(11/12): 45-51.

Shenton, H.W., D.W. Dinehart, and T.E. Elliott. 1998. Stiffness and energy degradation of wood frame shear walls. Can. J. of Civ. Engrg. 25(3): 412-423.

Sherwood, G.E. 1987. Condensation potential in wood-frame walls. In: Thermal Insulations: Materials and Systems (F.J. Powell and S.L. Mathews, eds.). ASTM STP 922. American Society for Testing and Materials, Philadelphia, PA. 405-417.

Sherwood, G.E., and A. TenWolde. 1982. Moisture movement and control in light-frame structures. For. Prod. J. 32(10): 69-73.

Simm, D.W. 1985. Corrosion behavior of certain metals in CCA-treated timber, environmental tests at 100% relative humidity. Corrosion Prevention & Control. 32(2): 25-35.

Skaggs, T.D., and J.D. Rose. 1996. Cyclic load testing of wood structural panel shear walls. Proc: Intl. Wood Engrg. Conf., New Orleans, Vol 2, 195-200. 1996 International Wood Engineering Conference, New Orleans, LA.

Smith, I., S.T. Craft, and P. Quenneville. 2001. Design capacities of joints with laterally loaded nails. Can. J. of Civ. Engrg. 28(4): 282-290.

Smulski, S. 1999. Durability of energy efficient wood-frame houses. For. Prod. J. 49(5): 8-15.

Smulski, S. 2000. Ensuring the durability of energy-efficient houses. Fine Homebuilding 132: 72-77.

Snell, W.H. 1929. The relationship of moisture contents of wood to its decay. American Journal of Botany 16: 543-546.

Snell, W.H., N.O. Howard, and M.V. Lamb. 1925. The relation between moisture contents of wood and decay. Science 62: 377-379.

Sutt, E., Rosowsky, D., and Anderson, E. 2004. Effect of fastener bend-yield stress on cyclic performance of lateral wood connection. Proc. World Conference on Timber Engineering, Lahti, Finland. Pp119-124. Finnish Association of Civil Engineers, Helsinki.

Tissel, J.R. 1993. Wood Structural Panel Shear Walls. APA Research Rep. No. 154. American Plywood Association, Tacoma, WA.

White, M.W., and J.D. Dolan. 1995. Non-linear shear-wall analysis. J. Struct. Engrg.121(11): 1629-1635.

Wilcox, W.W. 1978. Review of literature on the effects of early stages of decay on wood strength. Wood and Fiber Sci. 9(4): 252-257.

Wilkinson, T.L. 1991. Dowel bearing strength. Res. Pap. FPL-RP-505. Madison, WI:U.S. Department of Agriculture. Forest Service. Forest Products Laboratory. Madison, WI.

Wilson, T.R.C. 1917. Tests made to determine lateral resistance of wire nails. Engineering Records. 75: 303-304.

Winandy, J.E., and J.A. Micales, C.A. Clausen, and S.F. Curling. 2000. Predicting the effects of decay on wood properties and modeling residual service life. Poster presentation, Disaster Mitigation in Wood Frame Structures. Madison, WI.

Zabel, R.A., and J.J. Morrell. 1992. Wood Microbiology — Decay and its Prevention. Academic Press, New York, NY.

Appendices

Appendix A –Nail Bending-Yield Stress Data

Data colleted by Tim Davis at Oregon State University during the Spring 2003.

Nail Dimensions: 0.113 in. × 2.5 in.
Chemical designation determined by methods E 415 (ASTM 2002d) and E 1019 (ASTM 2003)

Nail Type

1. (C1005): meets the chemical requirements at the midpoint shank hardness of UNS-G-10050 for AISI 1005 Carbon Steel
2. (C1018): meets the chemical requirements at the midpoint shank hardness of UNS-G-10180 for AISI 1018 Carbon Steel
3. (C1035): meets the chemical requirements at the midpoint shank hardness of UNS-G-10350 for AISI 1035 Carbon Steel
4. (C1035 HT) meets the chemical requirements at the midpoint shank hardness of UNS-G-10350 for AISI 1035 Carbon Steel an is heat treated

Table A1. Summary of nail properties, n=24 per box, determined in accordance with F 1575 (ASTM 2002g).

Nail Type	Box	Label	Stat	Pmax lb	Slope lb-in	Pyield lb	f_{yb} ksi
1	6	1005B	Mean	76.54	3262	61.25	85.0
			Std. Dev.	5.01	134	4.57	6.34
			COV	0.065	0.041	0.075	0.075
	7	1005B	Mean	76.68	3297	62.89	87.3
			Std. Dev.	4.19	162	4.04	5.61
			COV	0.055	0.049	0.064	0.064
2	2	1018	Mean	113.3	3246	83.16	115.4
			Std. Dev.	1.77	199	2.61	3.62
			COV	0.016	0.061	0.031	0.031
	5	1018	Mean	113.7	3269	84.04	116.6
			Std. Dev.	1.15	147	2.05	2.85
			COV	0.010	0.045	0.024	0.024
3	3	1035	Mean	141.5	2946	104.2	144.6
			Std. Dev.	2.91	135	4.64	6.44
			COV	0.021	0.046	0.045	0.045
	4	1035	Mean	142.8	2862	104.2	144.6
			Std. Dev.	2.40	136	4.14	5.75
			COV	0.017	0.047	0.040	0.040
4	1	1035 HT	Mean	248.8	3837	169.7	235.6
			Std. Dev.	2.77	50.7	3.79	5.26
			COV	0.011	0.013	0.022	0.022
	8	1035 HT	Mean	249.3	3822	173.5	240.9
			Std. Dev.	3.81	61.4	3.21	4.46
			COV	0.015	0.016	0.019	0.019

Appendix B – Lateral Nail Connection Tests

This appendix discusses the experimentation of the connection tests used to evaluate the differences lateral nail connection characteristics resulting from bending-yield stress of the nails.

The connection geometry is similar to that of a field nail in a typical light-framed wood shearwall. The nail was centered in the thickness of the framing members 2 in. from the end, and centered on the width of the 4 in. dimension of the sheathing side member, 2 in. from the end. A piece of ultra high molecular weight polyethylene was placed between the framing and the sheathing in every connection to minimize the effect of side member-main member friction. The connections were built using 2×4 Douglas fir-Larch framing for the main member and various types of sheathing (exposure 1) side members including 15/32-in. OSB, 7/16-in. OSB, sheathing rated, and ½-in. plywood CD.

The framing for the preliminary connection tests with 15/32-in. OSB was Select Structural (kiln-dried) and conditioned to 12-percent moisture content. The embedment property for the lumber was done later when the lumber had equilibrated with the lab condition. This framing was also used as the top and bottom plates of the wall test specimens. The wall studs used in the remainder of the connection tests, including those with 7/16-in. OSB and the plywood, were Stud grade and No. 2 & Better, surfaced green. When the lumber was received, the moisture content was above the fiber saturation point. The lumber was placed in a conditioning room at 37.5 °C and a beginning relative humidity of 9 percent for 15 days. The moisture content was reduced to approximately 12 percent, and then reduced to approximately 8 percent, which matched the moisture content of the OSB. After the fabrication of the single lateral connections, the specimens were conditioned for a week to allow the wood fibers around the nail to relax.

The test set-up held the framing main member by screws to a fixed aluminum plate, which was in plane with the OSB side member. The OSB was clamped at the end of the sheathing, the fixture in the hydraulic actuator. For subsequent connection tests (7/16-in. OSB and1/2 in. plywood sheathing), the fixture was modified to provide more stability and prevent even more of the inherent eccentricities. The fixture modification removed the aluminum plate and replaced it with an L-shaped steel angle (Fig. B1). This set-up also decreased the amount of time needed to set up the connection test specimens.

Fig. B1. Modified lateral connection test set-up.

The preliminary connection tests were monotonic tests with 15/32-in. OSB. The results of the monotonic tests were run at a constant rate of 0.2 in. per minute by a computer controlled hydraulic testing machine. A linear variable differential transducer (LVDT) attached to the specimen measured the slip up to 0.748 in. The LVDT integrated to the hydraulic actuator was used to

measure the slip beyond 0.748 in. The data was collected at 5 points/sec. A reference displacement of 0.5 in. was calculated from the results of the monotonic tests.

The CUREE loading protocol (a quasi-static protocol) was used to test additional connections with 15/32-in. OSB. The cyclic connection test specimens were fabricated and tested using the same set up as the monotonic tests. The CUREE protocol is displacement controlled and the protocol was run at 0.2 Hz. The load-slip data were record by the data acquisition system at a rate of 20 Hz, which provided 100 data points per cycle. Initially, five connections at each type of nail (defined by bending-yield stress) were tested; later five more connections were tested for a total of ten. The results were plotted and then fit using SASHFIT (Elkins and Kim 2003a). The results for each nail type are given in Tables B1-B4.

To assess the effect of test frequency, ten more cyclic tests following the same procedure were conducted for the f_{yb}=87-ksi and 241-ksi nail types at a reduced rate of load, 0.1 Hz, which provided 200 data points per cycle. The SASHFIT results for these tests are found in Tables B5 and B6. Based on paired t-tests of the samples at each f_{yb}, at an alpha level of 0.01, the 87 ksi initial stiffness and peak capacity values were statistically similar (p-values=0.119 and 0.212, respectively) between the different rates of load. Similarly, the 241-ksi tests at each rate were statistically similar for initial stiffness and peak capacity (p-values of 0.555 and 0.748, respectively). It was concluded that the rate of load did not affect the hysteretic properties of the nails. Therefore, the average hysteretic parameters based on the 0.2 Hz frequency were used as input for CASHEW with 4/12 in. and 6/12 in. nailing schedules. The CASHEW results were processed with SASH1.

The results of these tests were used to select a nailing schedule and configuration to be used for the construction of the shearwall tests (Appendix C).

Table B1. f_{yb}=87 ksi nail hysteretic parameters for 15/32-in. OSB at 0.2 Hz

Sample	K_o lb/in	r_1	r_2	r_3	r_4	F_0 lb	F_l lb	Δ_u in	α	β	F_u+ lb
87-5	1742	0.021	-0.05	4.0	0.010	200	28.1	0.322	0.30	1.0	199
87-7	2956	0.020	-0.05	2.2	0.008	247	33.7	0.514	0.45	1.1	277
87-11	2242	0.006	0.00	3.4	0.009	281	27.0	0.604	0.06	1.3	378
87-12	2670	0.012	-0.05	2.8	0.010	270	28.1	0.562	0.50	1.3	285
87-13	2777	0.015	-0.05	3.6	0.009	326	33.7	0.576	0.50	1.3	347
87-30	5465	0.024	-0.09	2.6	0.010	259	27.0	0.475	0.60	1.5	319
87-31	3735	0.013	-0.10	1.5	0.006	247	29.2	0.454	0.45	1.0	269
87-32	4433	0.013	-0.05	1.4	0.009	225	27.0	0.493	0.60	1.3	250
86-33	3599	0.065	-0.05	1.8	0.008	225	30.3	0.496	0.50	1.2	339
87-34	3589	0.007	0.00	2.6	0.010	270	28.1	0.719	0.55	0.9	288
Avg	3321	0.020	-0.061	2.59	0.009	255	29.2	0.522	0.451	1.19	295
Std Dev	1089	0.017	0.021	0.888	0.001	35.2	2.60	0.104	0.162	0.185	52.1
COV	0.328	0.870	-0.343	0.343	0.151	0.14	0.089	0.200	0.360	0.156	0.177

Table B2. fyb=115 ksi nail hysteretic parameters for 15/32-in. OSB at 0.2 Hz.

Sample	K_o lb/in	r_1	r_2	r_3	r_4	F_0 lb	F_l lb	Δ_u in	α	β	F_u+ lb
115-5	2227	0.057	-0.05	1.5	0.009	180	27.0	0.544	0.30	1.1	248
115-6	3141	0.076	-0.14	2.8	0.013	270	45.0	0.469	0.20	1.3	380
115-8	3309	0.027	-0.05	2.2	0.012	253	45.0	0.557	0.60	1.0	319
115-11	4568	0.025	-0.04	1.6	0.009	315	62.9	0.552	0.50	1.3	379
115-12	3370	0.017	-0.06	2.0	0.009	253	29.2	1.136	0.50	1.1	314
115-13	3340	0.029	-0.03	2.6	0.009	202	29.2	0.460	0.40	1.2	247
115-14	3233	0.057	-0.05	3.4	0.009	247	27.0	0.476	0.30	1.1	331
115-15	3529	0.009	-0.06	2.0	0.010	259	28.1	0.708	0.50	1.3	281
115-16	3088	0.043	-0.06	2.0	0.008	225	31.5	0.696	0.40	1.2	317
115-17	3069	0.014	-0.09	1.8	0.012	303	30.3	0.696	0.60	1.3	333
115-18	3370	0.029	-0.07	1.7	0.009	281	27.0	0.448	0.30	1.2	324
115-19	4234	0.021	-0.05	1.5	0.013	281	34.8	0.544	0.50	1.0	320
115-20	3353	0.045	-0.06	1.5	0.009	225	29.2	0.452	0.35	1.1	294
Avg	3372	0.035	-0.06	2.05	0.010	253	34.3	0.595	0.419	1.17	314
Std Dev	559.7	0.020	0.027	0.578	0.002	38.5	10.6	0.188	0.125	0.111	40.4
COV	0.166	0.571	-0.440	0.283	0.174	0.152	0.309	0.316	0.298	0.095	0.128

Table B3. fyb=145 ksi nail hysteretic parameters for 15/32-in. OSB at 0.2 Hz

Sample	K_o lb/in	r_1	r_2	r_3	r_4	F_0 lb	F_l lb	Δ_u in	α	β	F_u+ lb
145-4	2701	0.011	-0.13	2.2	0.023	427	45.0	0.543	0.19	1.5	427
145-6	3530	0.016	-0.06	1.8	0.010	259	33.7	0.509	0.45	1.5	288
145-7	3113	0.031	-0.05	2.4	0.010	360	33.7	0.543	0.30	1.2	409
145-8	2968	0.050	-0.05	3.2	0.020	303	33.7	0.567	0.10	1.5	386
145-10	2181	0.103	-0.07	6.8	0.020	225	33.7	0.490	0.08	1.5	332
145-11	3730	0.029	-0.12	2.0	0.017	405	33.7	0.385	0.30	1.1	433
145-12	3569	0.047	-0.05	1.8	0.015	214	27.0	0.472	0.35	1.1	291
145-13	3041	0.140	-0.09	2.6	0.009	214	31.5	0.523	0.10	1.0	435
145-14	4652	0.070	-0.04	1.8	0.009	202	27.0	0.513	0.50	1.2	371
145-15	3709	0.027	-0.06	2.4	0.008	337	33.7	0.684	0.40	1.2	404
Avg	3319	0.042	-0.072	3.28	0.017	315	36.0	0.523	0.224	1.44	378
Std Dev	677.1	0.041	0.031	1.51	0.006	84.1	4.95	0.076	0.153	0.1989	56.1
COV	0.204	0.974	-0.434	0.459	0.337	0.267	0.1376	0.145	0.682	0.1381	0.149

Table B4. fyb=241 ksi nail hysteretic parameters for 15/32-in. OSB at 0.2 Hz

Sample	K_o lb/in	r_1	r_2	r_3	r_4	F_0 lb	F_1 lb	Δ_u in	α	β	F_u+ lb
241-4	2892	0.063	-0.14	2.6	0.022	309	45.0	0.584	0.23	1.3	414
241-5	2630	0.064	-0.09	2.7	0.020	303	45.0	0.475	0.11	1.3	377
241-7	2829	0.040	-0.09	2.4	0.020	348	45.0	0.577	0.13	1.3	410
241-9	3292	0.005	-0.06	2.5	0.015	371	45.0	0.446	0.10	1.5	370
241-10	3205	0.027	-0.09	2.6	0.015	360	45.0	0.525	0.26	1.3	402
241-30	2875	0.040	0.00	2.7	0.009	303	29.2	1.087	0.30	1.0	427
241-31	2950	0.069	-0.07	2.0	0.009	247	22.5	0.530	0.30	1.0	354
241-32	2607	0.021	0.00	3.0	0.050	348	13.5	0.562	0.30	1.1	386
241-33	4211	0.063	-0.06	2.0	0.030	303	28.1	0.562	0.43	1.1	496
241-34	4985	0.022	-0.09	1.9	0.020	303	27.0	0.470	0.40	1.2	351
Avg	3248	0.041	-0.086	2.44	0.021	320	34.5	0.582	0.256	1.21	399
Std Dev	765.4	0.022	0.043	0.363	0.012	36.9	11.8	0.184	0.114	0.160	42.5
COV	0.236	0.543	-0.502	0.149	0.569	0.116	0.343	0.316	0.447	0.132	0.107

Table B5. fyb=87 ksi nail hysteretic parameters for 15/32-in. OSB at 0.1 Hz

Sample	K_o lb/in	r_1	r_2	r_3	r_4	F_0 lb	F_1 lb	Δ_u in	α	β	F_u+ lb
87-16	2423	0.045	-0.03	3.6	0.007	191	28.1	0.228	0.60	1.1	203
87-17	1216	0.289	-0.20	6.0	0.006	180	33.7	0.574	0.05	1.1	374
87-19	2353	0.035	-0.07	4.2	0.013	270	33.7	0.469	0.40	1.1	303
87-20	2415	0.018	-0.07	4.6	0.009	247	28.1	0.469	0.38	1.3	262
87-21	2333	0.034	-0.10	3.8	0.014	247	28.1	0.543	0.52	1.1	289
87-22	2423	0.048	-0.04	4.4	0.007	191	28.1	0.228	0.40	1.1	211
87-23	3254	0.019	-0.10	4.0	0.015	247	28.1	0.566	0.80	1.1	282
87-24	2456	0.072	-0.30	3.0	0.030	202	33.7	0.338	0.02	1.3	258
87-25	1927	0.024	-0.04	4.3	0.030	191	28.1	0.254	0.60	0.9	186
87-26	2777	0.059	-0.14	2.5	0.008	202	31.5	0.544	0.31	1.1	283
Avg	2358	0.064	-0.109	4.04	0.014	217	30.1	0.421	0.408	1.12	265
Std Dev	525.9	0.081	0.085	0.948	0.009	32.3	2.69	0.145	0.243	0.114	55.3
COV	0.223	1.26	-0.779	0.235	0.651	0.149	0.0893	0.344	0.595	0.1014	0.209

Table B6. fyb=241 ksi nail hysteretic parameters for 15/32-in. OSB at 0.1 Hz

Sample	K_o lb/In	r_1	r_2	r_3	r_4	F_0 lb	F_1 lb	Δ_u in	α	β	F_u+ lb
241-11	2066	0.095	-0.20	4.0	0.009	225	11.2	0.446	0.03	0.2	291
241-12	3611	0.003	-0.12	3.0	0.030	382	39.3	0.573	0.25	1.5	386
241-15	3178	0.057	-0.05	3.3	0.006	315	28.1	0.443	0.30	1.2	390
241-16	3045	0.025	-0.15	2.8	0.009	427	28.1	0.828	0.32	1.0	489
241-17	1273	0.102	-0.25	11	0.020	360	33.7	0.574	0.50	0.5	374
241-18	2423	0.167	-0.06	5.0	0.010	337	22.5	0.256	0.03	1.3	371
241-19	3842	0.041	-0.02	3.4	0.020	315	39.3	0.493	0.30	1.0	392
241-21	3006	0.008	-0.10	4.4	0.030	495	56.2	0.493	0.19	1.5	481
241-22	3778	0.090	-0.03	1.8	0.007	247	28.1	0.608	0.25	1.3	413
241-23	4568	0.065	-0.05	1.6	0.012	337	45.0	0.522	0.21	1.3	491
Avg	3079	0.065	-0.103	4.03	0.015	344	33.2	0.524	0.238	1.08	408
Std Dev	960.6	0.050	0.077	2.67	0.009	79.3	12.6	0.145	0.139	0.4264	63.4
COV	0.312	0.767	-0.747	0.66	0.597	0.231	0.3786	0.278	0.587	0.3948	0.155

A 4/12 in. nailing pattern and 7/16-in. OSB was selected to be used in the construction of two walls with each nail type. A total of eight walls were built and tested. After the completion of the shearwall tests, the walls were dismantled and undamaged sections of framing and sheathing materials were removed. Framing and sheathing materials were randomly selected form each wall and used to fabricate 12 lateral nail test specimens that matched the previous cyclic tests. These were tested using a 0.5-in. reference displacement and the second lateral nail test set-up.

The lateral nail tests were plotted and fit by SASHFIT (Tables B7-B14). There are only 21 specimens from walls 7 and 8 because three tests in these groups were thrown out due to malfunctions with the testing equipment. The average hysteretic parameters of each nail type (Table B15) are used as input for CASHEW. The results of the CASHEW analysis can then be compared to the wall tests.

Sample	K_o lb/in	r_1	r_2	r_3	r_4	F_0 lb	F_1 lb	Δ_u in	α	β	F_u+ lb
1-1	2064	0.017	-0.030	4.3	0.016	225	30.3	0.409	0.26	1.3	234
1-2	2950	0.112	-0.030	4.5	0.009	236	36.0	0.408	0.14	1.1	369
1-3	1956	0.155	-0.045	3.8	0.015	101	30.3	0.468	0.16	1.1	244
1-4	2752	0.037	-0.090	3.8	0.010	259	32.6	0.346	0.33	1.3	286
1-5	2283	0.046	-0.030	4.6	0.015	202	30.3	0.443	0.26	1.1	247
1-6	2304	0.035	-0.060	4.8	0.015	292	30.3	0.442	0.07	1.0	315
1-7	2210	0.082	-0.150	4.6	0.015	202	30.3	0.467	0.26	1.3	285
1-8	2071	0.020	-0.050	3.5	0.014	180	29.2	0.445	0.36	1.3	196
1-9	2847	0.055	-0.045	3.5	0.010	247	31.5	0.368	0.28	1.2	301
1-10	2262	0.117	-0.020	6.3	0.015	202	31.5	0.425	0.08	1.1	311
1-11	2331	0.024	-0.070	4.4	0.010	270	31.5	0.428	0.24	1.0	286
1-12	3319	0.042	-0.028	4.0	0.009	348	30.3	0.389	0.26	1.2	393
Avg	2446	0.062	-0.054	4.34	0.013	230	31.2	0.420	0.225	1.2	289
Std Dev	420.7	0.045	0.036	0.76	0.003	61.8	1.74	0.038	0.092	0.115	55.6
COV	0.172	0.720	-0.673	0.175	0.222	0.268	0.06	0.090	0.411	0.099	0.192

Table B8. Wall 2, fyb=87 ksi nail hysteretic parameters

Sample	K_o lb/in	r_1	r_2	r_3	r_4	F_0 lb	F_1 lb	Δ_u in	α	β	F_u+ lb
2-1	2333	0.014	-0.040	3.5	0.014	236	33.7	0.387	0.10	1.1	243
2-2	3396	0.051	-0.060	3.4	0.008	247	30.3	0.406	0.32	1.1	316
2-3	3373	0.053	-0.100	4.0	0.009	259	31.5	0.425	0.24	1.3	333
2-4	2253	0.035	-0.095	4.6	0.014	202	29.2	0.366	0.21	1.2	227
2-5	3781	0.031	-0.030	5.0	0.008	360	31.5	0.405	0.20	1.1	401
2-6	2289	0.046	-0.100	4.6	0.012	202	31.5	0.407	0.24	1.2	243
2-7	2589	0.015	-0.085	4.0	0.012	225	29.2	0.407	0.54	1.1	238
2-8	2891	0.063	-0.050	3.8	0.014	230	30.3	0.426	0.22	1.2	306
2-9	2228	0.015	-0.080	4.6	0.010	202	29.2	0.389	0.28	1.3	212
2-10	2489	0.014	-0.200	4.6	0.013	292	33.7	0.681	0.30	1.1	315
2-11	2394	0.058	-0.055	3.8	0.010	236	30.3	0.425	0.24	1.4	291
2-12	2411	0.052	-0.030	6.6	0.013	225	31.5	0.407	0.26	1.3	273
Avg	2702	0.037	-0.077	4.38	0.011	243	31.0	0.428	0.26	1.2	283
Std Dev	531.1	0.019	0.047	0.86	0.002	44.9	1.55	0.082	0.104	0.104	54.5
COV	0.197	0.509	-0.604	0.197	0.203	0.185	0.05	0.191	0.395	0.087	0.192

Table B9. Wall 3, fyb=115 ksi nail hysteretic parameters

Sample	K_o lb/in	r_1	r_2	r_3	r_4	F_0 lb	F_1 lb	Δ_u in	α	β	F_u+ lb
3-1	2993	0.016	-0.075	3.4	0.018	236	29.2	0.345	0.31	1.2	249
3-2	3049	0.051	-0.070	4.6	0.047	274	34.8	0.387	0.22	1.2	330
3-3	2999	0.024	-0.030	4.2	0.026	337	38.2	0.453	0.30	1.1	364
3-4	3352	0.018	-0.070	3.5	0.018	282	34.8	0.466	0.31	1.1	308
3-5	2776	0.048	-0.060	2.5	0.036	214	25.9	0.406	0.28	1.2	266
3-6	2308	0.025	-0.085	4.4	0.038	247	31.5	0.407	0.13	1.1	265
3-7	3206	0.022	-0.050	3.8	0.021	232	33.7	0.424	0.36	1.3	261
3-8	3197	0.028	-0.055	3.2	0.025	292	37.1	0.388	0.21	1.3	323
3-9	3106	0.060	-0.050	3.2	0.023	236	36.0	0.345	0.28	1.2	297
3-10	3055	0.022	-0.050	4.2	0.061	225	33.7	0.703	0.39	1.3	273
3-11	2387	0.027	-0.200	4.5	0.034	303	33.7	0.453	0.12	1.1	323
3-12	2613	0.096	-0.065	3.8	0.022	202	32.6	0.366	0.10	1.1	291
Avg	2920	0.036	-0.072	3.78	0.031	257	33.4	0.429	0.250	1.18	296
Std Dev	330.3	0.024	0.043	0.637	0.013	40.8	3.39	0.095	0.096	0.083	34.6
COV	0.113	0.646	-0.599	0.169	0.425	0.159	0.10	0.222	0.382	0.071	0.117

Table B10. Wall 4, fyb=115 ksi nail hysteretic parameters

Sample	K_o lb/in	r_1	r_2	r_3	r_4	F_0 lb	F_1 lb	Δ_u in	α	β	F_u+ lb
4-1	2632	0.049	-0.065	3.5	0.025	214	29.2	0.401	0.31	1.0	263
4-2	3066	0.029	-0.070	4.3	0.032	281	30.3	0.421	0.27	1.0	314
4-3	2890	0.025	-0.050	3.9	0.022	247	31.5	0.345	0.27	1.1	267
4-4	2559	0.030	-0.040	3.5	0.030	214	29.2	0.423	0.36	1.1	244
4-5	3240	0.041	-0.070	3.4	0.018	264	31.5	0.344	0.26	1.2	306
4-6	2760	0.019	-0.040	4.5	0.021	236	33.7	0.386	0.25	1.0	253
4-7	2421	0.050	-0.050	4.7	0.020	214	31.5	0.425	0.35	1.0	263
4-8	2415	0.057	-0.060	4.2	0.027	247	31.5	0.424	0.19	1.0	300
4-9	2160	0.030	-0.200	4.3	0.030	191	27.0	0.692	0.34	1.3	235
4-10	2688	0.036	-0.050	4.3	0.028	270	31.5	0.388	0.19	1.2	301
4-11	3297	0.052	-0.060	4.0	0.021	270	34.8	0.345	0.19	1.1	324
4-12	3247	0.029	-0.050	4.0	0.022	236	34.8	0.453	0.38	1.3	277
Avg	2781	0.037	-0.067	4.05	0.025	240	31.4	0.421	0.280	1.11	279
Std Dev	371.5	0.012	0.04	0.41	0.005	28.1	2.32	0.093	0.068	0.116	29.3
COV	0.134	0.334	-0.642	0.102	0.187	0.117	0.074	0.221	0.245	0.105	0.105

Table B11. Wall 5, fyb=145 ksi nail hysteretic parameters

Sample	K_o lb/in	r_1	r_2	r_3	r_4	F_0 lb	F_1 lb	Δ_u in	α	β	F_u+ lb
5-1	2782	0.060	-0.030	4.7	0.017	270	31.5	0.387	0.26	1.2	328
5-2	2610	0.059	-0.050	3.3	0.034	247	28.1	0.388	0.18	1.1	301
5-3	3062	0.035	-0.080	5.1	0.029	230	31.5	0.389	0.30	1.1	271
5-4	3191	0.055	-0.070	4.4	0.033	332	36.0	0.366	0.19	1.2	384
5-5	2682	0.020	-0.080	4.7	0.040	242	31.5	0.439	0.50	1.3	264
5-6	3228	0.025	-0.030	4.0	0.080	270	22.5	0.407	0.34	1.2	300
5-7	3562	0.051	-0.070	4.3	0.030	348	32.6	0.440	0.29	1.1	424
5-8	2593	0.048	-0.060	3.8	0.039	214	29.2	0.346	0.21	1.1	252
5-9	3075	0.053	-0.043	4.0	0.023	281	32.6	0.410	0.21	1.2	344
5-10	2859	0.044	-0.075	4.9	0.039	298	32.6	0.387	0.18	1.1	337
5-11	2357	0.042	-0.300	3.3	0.077	242	22.5	0.484	0.32	1.1	285
5-12	2294	0.029	-0.080	4.8	0.050	202	18.0	0.442	0.56	1.2	230
Avg	2858	0.043	-0.081	4.28	0.041	265	29.0	0.407	0.295	1.16	310
Std Dev	377.8	0.013	0.072	0.603	0.020	44.7	5.33	0.038	0.124	0.067	56.2
COV	0.132	0.309	-0.888	0.141	0.477	0.169	0.184	0.094	0.419	0.058	0.181

Table B12. Wall 6, fyb=145 ksi nail hysteretic parameters

Sample	K_o lb/in	r_1	r_2	r_3	r_4	F_0 lb	F_1 lb	Δ_u in	α	β	F_u+ lb
6-1	2917	0.023	-0.090	3.2	0.034	275	30.3	0.416	0.24	1.1	299
6-2	2936	0.035	-0.080	4.0	0.025	298	29.2	0.449	0.25	1.1	340
6-3	3011	0.068	-0.110	3.3	0.034	242	31.5	0.341	0.26	1.2	307
6-4	3151	0.067	-0.070	5.0	0.028	247	30.3	0.436	0.25	1.1	338
6-5	2865	0.060	-0.075	4.3	0.038	270	34.8	0.362	0.12	1.2	325
6-6	2840	0.061	-0.050	5.5	0.033	236	30.3	0.359	0.09	1.0	294
6-7	2946	0.060	-0.065	5.7	0.035	281	30.3	0.379	0.15	1.1	341
6-8	3287	0.022	-0.070	4.8	0.079	348	27.0	0.366	0.22	1.1	362
6-9	2572	0.096	-0.040	5.3	0.076	169	24.7	0.479	0.20	1.1	287
6-10	3010	0.072	-0.050	3.8	0.032	242	31.5	0.366	0.24	1.1	317
6-11	2547	0.062	-0.050	4.8	0.031	236	23.6	0.425	0.15	1.1	300
6-12	2405	0.073	-0.075	5.4	0.043	236	29.2	0.387	0.14	1.0	298
Avg	2874	0.058	-0.069	4.59	0.041	257	29.4	0.397	0.193	1.10	317
Std Dev	255.0	0.022	0.020	0.860	0.018	43.5	3.06	0.043	0.059	0.060	23.7
COV	0.089	0.374	-0.286	0.187	0.438	0.169	0.10	0.108	0.308	0.055	0.075

Table B13. Wall 7, fyb=241 ksi nail hysteretic parameters

Sample	K_o lb/in	r_1	r_2	r_3	r_4	F_0 lb	F_1 lb	Δ_u in	α	β	F_u+ lb
7-1	3507	0.021	-0.050	4.2	0.035	315	27.0	0.544	0.24	1.2	354
7-2	2860	0.060	-0.035	4.8	0.061	303	34.8	0.382	0.05	1.0	360
7-3	2829	0.065	-0.025	5.6	0.056	292	27.0	0.400	0.14	1.3	358
7-4	2838	0.043	-0.045	5.8	0.042	315	24.7	0.449	0.11	1.1	362
7-5	2629	0.064	-0.015	4.7	0.083	259	27.0	0.400	0.22	1.1	320
7-6	3405	0.016	-0.055	4.8	0.039	377	30.3	0.383	0.19	1.2	384
7-7	3087	0.070	-0.040	5.5	0.053	315	28.1	0.472	0.26	1.2	384
7-8	3503	0.034	-0.035	4.2	0.044	393	33.7	0.360	0.22	1.2	419
7-9	2627	0.065	-0.080	5.2	0.050	315	25.9	0.360	0.05	1.0	357
7-10	2874	0.132	-0.060	4.5	0.047	247	27.0	0.254	0.19	1.3	326
7-11	3267	0.048	-0.045	4.2	0.055	292	33.7	0.317	0.21	1.2	332
Avg	3039	0.056	-0.044	4.86	0.051	311	29.0	0.393	0.170	1.16	360
Std Dev	332.1	0.031	0.018	0.585	0.013	43.3	3.55	0.077	0.073	0.103	28.7
COV	0.109	0.558	-0.399	0.120	0.255	0.139	0.12	0.197	0.429	0.088	0.080

Table B14. Wall 8, fyb=241 ksi nail hysteretic parameters

Sample	K_o lb/in	r_1	r_2	r_3	r_4	F_0 lb	F_1 lb	Δ_u In	α	β	F_u+ lb
8-1	2670	0.108	-0.070	5.0	0.250	281	24.7	0.206	0.02	0.1	292
8-2	3296	0.061	-0.065	5.0	0.048	337	30.3	0.376	0.11	1.0	401
8-3	3288	0.034	-0.040	4.4	0.058	303	33.7	0.381	0.16	1.1	340
8-5	3488	0.047	-0.020	3.5	0.043	264	27.0	0.383	0.21	1.2	324
8-6	3591	0.091	-0.075	5.5	0.110	292	22.5	0.253	0.14	1.0	358
8-7	3526	0.056	-0.050	4.4	0.070	326	32.6	0.672	0.23	1.2	459
8-8	2311	0.078	-0.075	5.4	0.063	225	29.2	0.358	0.10	1.1	282
8-9	3406	0.009	-0.030	4.2	0.037	309	24.7	0.433	0.24	1.1	320
8-10	2791	0.027	-0.090	5.4	0.061	382	27.0	0.695	0.04	1.0	432
8-11	3281	0.075	-0.075	3.8	0.039	264	31.5	0.340	0.19	1.1	342
Avg	3220	0.053	-0.058	4.62	0.059	300	28.7	0.432	0.158	1.09	362
Std Dev	426.1	0.031	0.023	0.704	0.064	44.1	3.74	0.159	0.076	0.324	58.4
COV	0.132	0.575	-0.395	0.152	1.090	0.147	0.13	0.367	0.485	0.298	0.161

f_{yb}			K_o	r_1	r_2	r_3	r_4	F_0	F_l	Δ_u	α	β	F_u+
			lb/in					lb	lb	in			lb
87	Avg	24	2574	0.050	-0.066	4.36	0.012	237	31.1	0.424	0.244	1.18	
	COV		0.189	0.723	0.649	0.182	0.217	0.225	0.052	0.147	0.402	0.092	0.188
115	Avg	24	2851	0.037	-0.069	3.91	0.028	249	32.4	0.425	0.265	1.15	
	COV		0.123	0.500	0.607	0.139	0.364	0.142	0.094	0.217	0.312	0.093	0.113
145	Avg	24	2866	0.051	-0.075	4.43	0.041	261	29.2	0.402	0.244	1.13	314
	COV		0.110	0.379	0.692	0.168	0.448	0.166	0.146	0.100	0.444	0.061	
241	Avg	21	3099	0.057	-0.051	4.77	0.064	305	28.7	0.401	0.158	1.08	358
	COV		0.121	0.527	0.413	0.134	0.719	0.141	0.124	0.300	0.469	0.228	

The remaining pieces of framing from the walls were used in lateral nails tests with ½-in. plywood side members. These were also tested with the second lateral nail test set-up and fit with the hysteretic parameters as determined by SASHFIT. These results (Tables B16-B19) were not used in this study, but could be used in shearwall simulations for walls sheathed with plywood.

Table B16. fyb=87 ksi nail hysteretic parameters for 1/2 in. plywood

Sample	K_o	r_1	r_2	r_3	r_4	F_0	F_l	Δ_u	α	β	F_u+
	lb/in					lb	lb	in			lb
1-1	3011	0.017	-0.030	4.3	0.016	214	31.5	0.464	0.26	1.3	276
1-2	2053	0.112	-0.030	4.5	0.009	247	31.5	0.463	0.14	1.1	276
1-3	2465	0.155	-0.045	3.8	0.015	270	29.2	0.365	0.16	1.1	326
1-4	2202	0.037	-0.090	3.8	0.010	270	29.2	0.419	0.33	1.3	338
2-1	2734	0.046	-0.030	4.6	0.015	180	37.1	0.440	0.26	1.1	263
2-2	2465	0.035	-0.060	4.8	0.015	281	31.5	0.365	0.07	1.0	326
2-3	2767	0.082	-0.150	4.6	0.015	259	31.5	0.422	0.26	1.3	313
Std Dev	368.8	0.049	0.041	0.475	0.003	40.9	2.94	0.097	0.099	0.125	37.8
COV	0.142	0.780	-0.684	0.112	0.192	0.172	0.09	0.250	0.429	0.105	0.129

Table B17. fyb=115 ksi nail hysteretic parameters for 1/2 in. plywood

Sample	K_o	r_1	r_2	r_3	r_4	F_0	F_l	Δ_u	α	β	F_u+
	lb/in					lb	lb	in			lb
3-1	2843	0.087	-0.150	3.1	0.015	202	29.2	0.385	0.10	1.0	297
3-2	3205	0.009	-0.030	2.6	0.026	236	29.2	0.342	0.24	1.1	243
3-3	3028	0.036	-0.070	4.0	0.018	303	33.7	0.383	0.25	1.2	336
3-4	2863	0.032	-0.075	5.0	0.021	303	36.0	0.625	0.04	1.1	325
3-5	2943	0.028	-0.040	3.5	0.027	259	29.2	0.404	0.04	1.1	288
3-6	3714	0.018	-0.055	2.4	0.024	259	37.1	0.384	0.34	1.1	282
3-7	2715	0.035	-0.050	3.7	0.009	247	11.2	0.548	0.20	1.1	298
3-9	3235	0.027	-0.045	3.4	0.030	287	39.3	0.405	0.32	1.1	318
Avg	3068	0.034	-0.064	3.46	0.021	262	30.6	0.434	0.191	1.100	298
Std Dev	315.8	0.023	0.038	0.828	0.007	34.9	8.76	0.098	0.118	0.053	29.2
COV	0.103	0.690	-0.585	0.239	0.328	0.133	0.29	0.225	0.617	0.049	0.098

Table B18. fyb=145 ksi nail hysteretic parameters for 1/2 in. plywood

Sample	K_o lb/in	r_1	r_2	r_3	r_4	F_0 lb	F_1 lb	Δ_u in	α	β	F_u+ lb
6-1	3370	0.023	-0.090	3.2	0.034	315	39.3	0.321	0.24	1.1	360
6-2	2414	0.035	-0.080	4.0	0.025	253	29.2	0.405	0.25	1.1	275
6-3	2465	0.068	-0.110	3.3	0.034	337	29.2	0.365	0.26	1.2	340
6-4	3116	0.067	-0.070	5.0	0.028	292	29.2	0.404	0.25	1.1	332
6-5	2704	0.060	-0.075	4.3	0.038	236	27.0	0.365	0.12	1.2	269
6-6	2832	0.061	-0.050	5.5	0.033	214	27.0	0.404	0.09	1.0	232
6-7	2929	0.060	-0.065	5.7	0.035	236	33.7	0.322	0.15	1.1	294
6-8	3381	0.022	-0.070	4.8	0.079	315	30.3	0.438	0.22	1.1	334
6-9	3403	0.096	-0.040	5.3	0.076	450	40.5	0.386	0.20	1.1	500
Avg	2957	0.055	-0.072	4.57	0.042	294	31.7	0.379	0.198	1.11	326
Std Dev	386.0	0.024	0.021	0.922	0.020	72.3	5.05	0.039	0.063	0.060	77.1
COV	0.131	0.442	-0.286	0.202	0.477	0.246	0.16	0.104	0.318	0.054	0.236

Table B19. fyb=241 ksi nail hysteretic parameters for 1/2 in. plywood

Sample	K_o lb/in	r_1	r_2	r_3	r_4	F_0 lb	F_1 lb	Δ_u in	α	β	F_u+ lb
8-1	3571	0.072	-0.030	3.5	0.060	348	31.5	0.283	0.05	1.1	394
8-2	3538	0.084	-0.030	3.7	0.050	337	40.5	0.439	0.36	1.0	463
8-3	2896	0.117	-0.030	3.9	0.045	247	16.9	0.316	0.15	1.1	345
8-5	3383	0.033	-0.045	3.6	0.030	382	32.6	0.552	0.20	1.1	441
8-6	3817	0.028	-0.030	2.6	0.045	348	29.2	0.363	0.15	1.1	380
8-7	3399	0.058	-0.200	3.1	0.045	405	29.2	0.482	0.18	1.1	491
8-8	2311	0.078	-0.075	5.4	0.063	225	29.2	0.358	0.10	1.1	282
8-9	3054	0.100	-0.065	3.8	0.020	315	6.74	0.205	0.06	1.1	326
Avg	3200	0.071	-0.068	3.73	0.043	323	26.3	0.388	0.171	1.09	390
Std Dev	477.1	0.031	0.058	0.807	0.014	62.2	10.4	0.112	0.098	0.035	71.7
COV	0.149	0.431	-0.856	0.216	0.335	0.193	0.40	0.289	0.577	0.033	0.184

Moisture content and embedment strength (Table B20) were determined for all materials used in the connection tests. All materials used in the connection tests were also tested for moisture contents and embedment strengths (Table B20). The moisture contents were measured in accordance with D 4444 (ASTM 2002b). The embedment strengths for the lumber and the sheathing materials were found in conjunction with D 5764 (ASTM 2002c).

Table B20. Average embedment properties and moisture contents.

Material	Grade	n	F_e lb	MC %
Doug-fir Larch 2×4	No. 1 and better	20	939	9.6
Doug-fir Larch 2×4	Std. and better	41	912	8.7
OSB sheathing 15/32"	Exposure 1	41	259	6.2
OSB sheathing 7/16"	Exposure 1	43	267	7.1
Plywood sheathing 1/2"	CDX	42	300	7.0

For the dowel bearing strength tests, 0.8-in. holes were drilled in the materials and then the material was cut along the centerline of the hole to create a dimple for nail placement. The minimum height of the specimen below the hole and the minimum width on either side of the hole was 0.452 in., the actual height of the specimens were approximately 2 in. The embedment tests were done to the L-T and R-T planes of the framing and in the minor axes of the sheathing panels. The specimen was clamped in the testing jig and the nail was embedded at a speed of 0.08 in./min. The yield load was calculated at 5-percent of the dowel diameter offset from the linear portion of the curve. The average of the embedment yield loads were used to calculate the design yield modes of connections built with these materials (Table B21).

Table B21. Yield mode calculations for laterally loaded single nail connections constructed with wood materials as described and varying f_{yb} nails.

Yield Mode	OSB thickness	87 ksi	115 ksi	145 ksi	241 ksi
I_m	7/16 in.	415	415	415	415
	15/32 in.	427	427	427	427
I_s	7/16 in.	121	121	121	121
	15/32 in.	121	121	121	121
II	7/16 in.	2455	2455	2455	2455
	15/32 in.	2455	2455	2455	2455
III_m	7/16 in.	145	147	149	155
	15/32 in.	148	150	152	159
III_s	7/16 in.	60	65	71	87
	15/32 in.	60	66	71	88
IV	7/16 in.	73	83	94	121
	15/32 in.	73	84	94	122

Appendix C – Shearwall Tests

Eight 8 × 8-ft. fully anchored shearwalls with hold-downs were constructed with the framing for each wall spaced 16 in. o.c. (Figure C1).

Figure C1. Shearwall test set-up.

The nails with the different f_{yb} values were used only for the sheathing nails, the framing nails were typical construction nails. Two walls at each nail type were tested. The sheathing panels were oriented vertically and attached to the framing using sheathing nails spaced at 4-in. on the perimeter and 12-in. in the field of each panel. The minimum edge distance was 3/8 in. The plate-to-stud connections were end-nailed using 16d common nails at each end; the double top plates were connected with one 16d common every 6 in., the double end studs were connected using two 10d common nails every 8.5 in. except in the areas where hold-downs were located (the bottom 13 in. of the end studs). The hold-downs were Simpson PHDS®. The walls were tested in accordance with E 2126 (ASTM 2002f) following the CUREE loading protocol, with a reference displacement of 3 in. Rather than testing a wall monotonically to determine the reference displacement, it was selected based

on previous studies conducted at Oregon State University, as well as the limitations of the hydraulic actuator. The maximum stroke of the actuator was 10 in. The slip was measured by an actuator-internal LVDT at a rate of 25 Hz. The tests were run at 0.25 Hz.

The test set up is a welded steel fixture heavily bolted to the lab reaction floor. The wall is bolted to the steel top and bottom plates using four 11/16-in. bolts on the bottom in addition to the hold-downs, and six 5/8-in. bolts on the top. The washers used on the bolts were 2-1/2-in. square ¼-in. thick steel plates for the bolts on the ends, and 3-in. square, 3/8-in. thick steel plates for interior bolts. The nuts were tightened to 50 ft·lb. The load is applied at the top of the wall using a 150-kip capacity hydraulic actuator (Fig. C2).

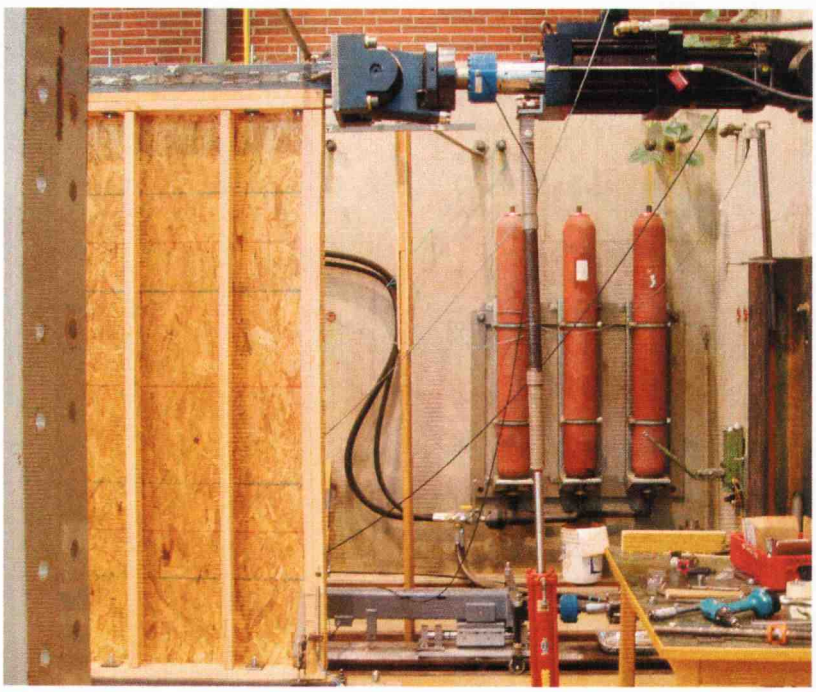

Fig. C2. Hydraulic actuator and set-up.

During the fabrication of the walls, one of the center studs of the 115 ksi walls cracked. The wall was tested with the cracked stud and observed, there were no drastic visual changes to the crack (Fig. C3), and the results (Fig.

C5) were comparable to the other walls (Fig. C4-C11), therefore, it was not replaced with a different wall. The hysteretic loops for the test data are symmetric, and the shape is similar for the different f_{yb} nails.

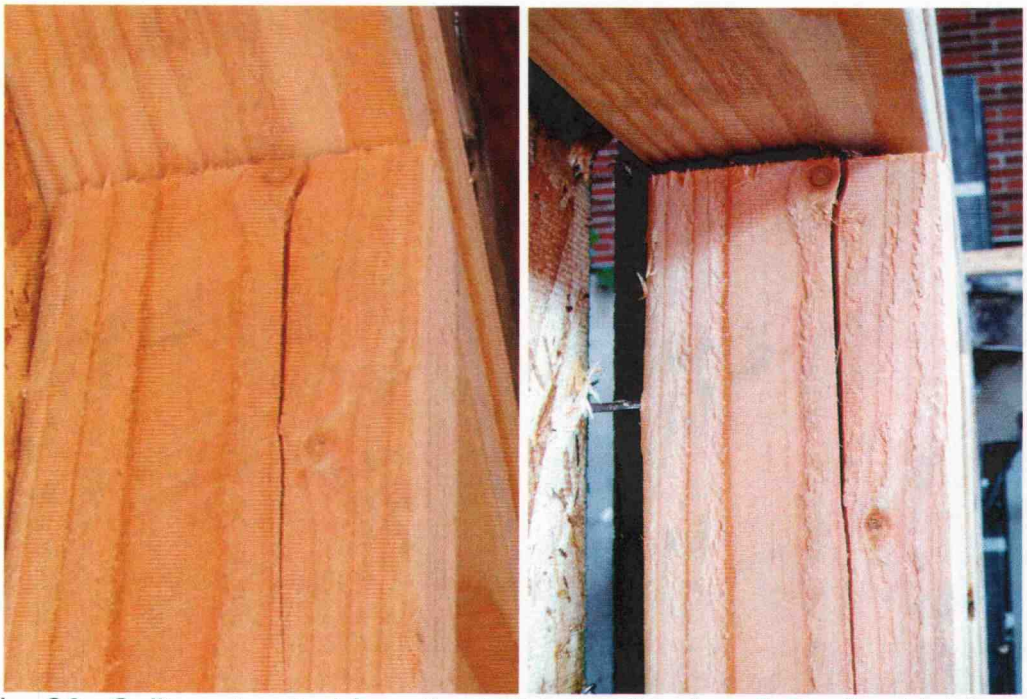

Fig. C3. Split center stud from the 115-ksi wall before (left) after (right).

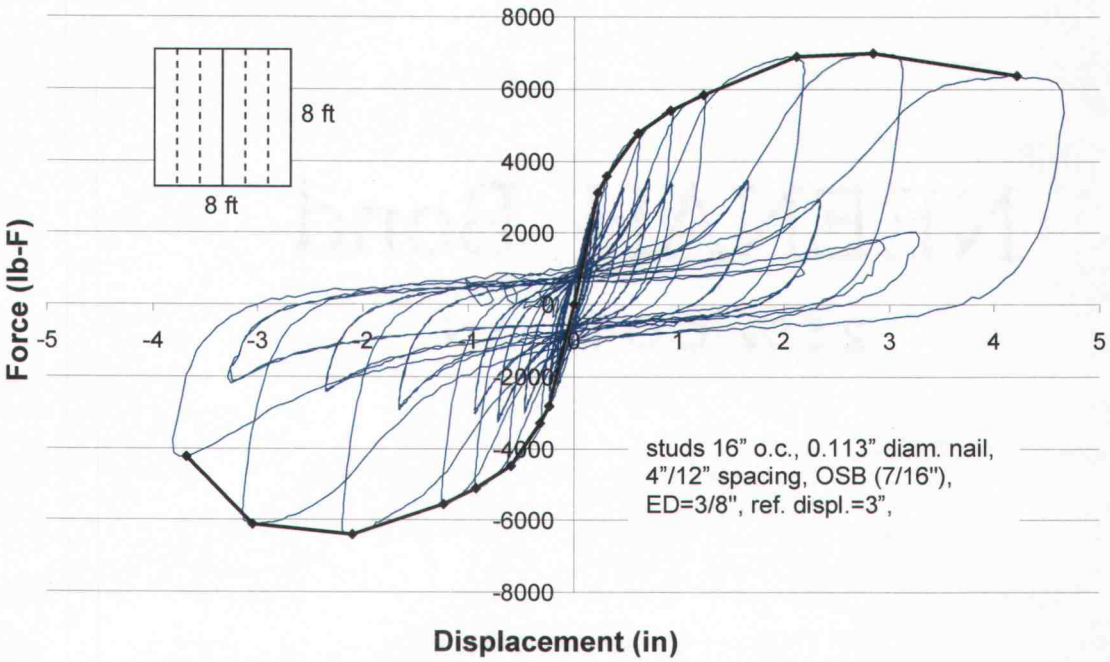

Fig. C4. Wall 1 hysteresis curve f_{yb}=87 ksi.

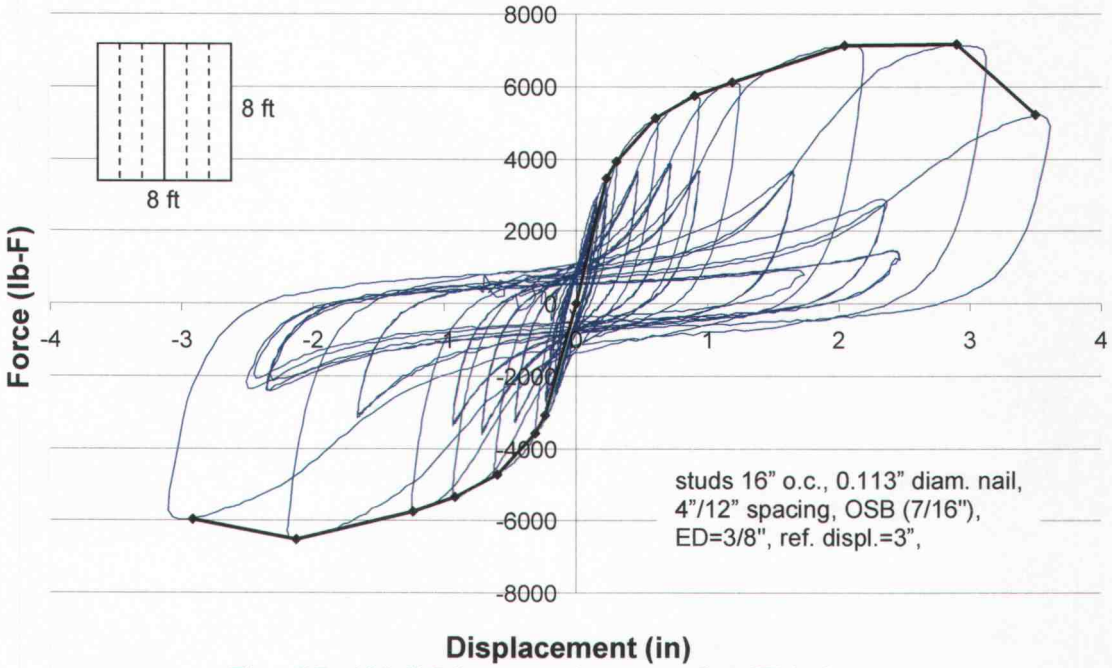

Fig. C5. Wall 2 hysteresis curve f_{yb}=87 ksi.

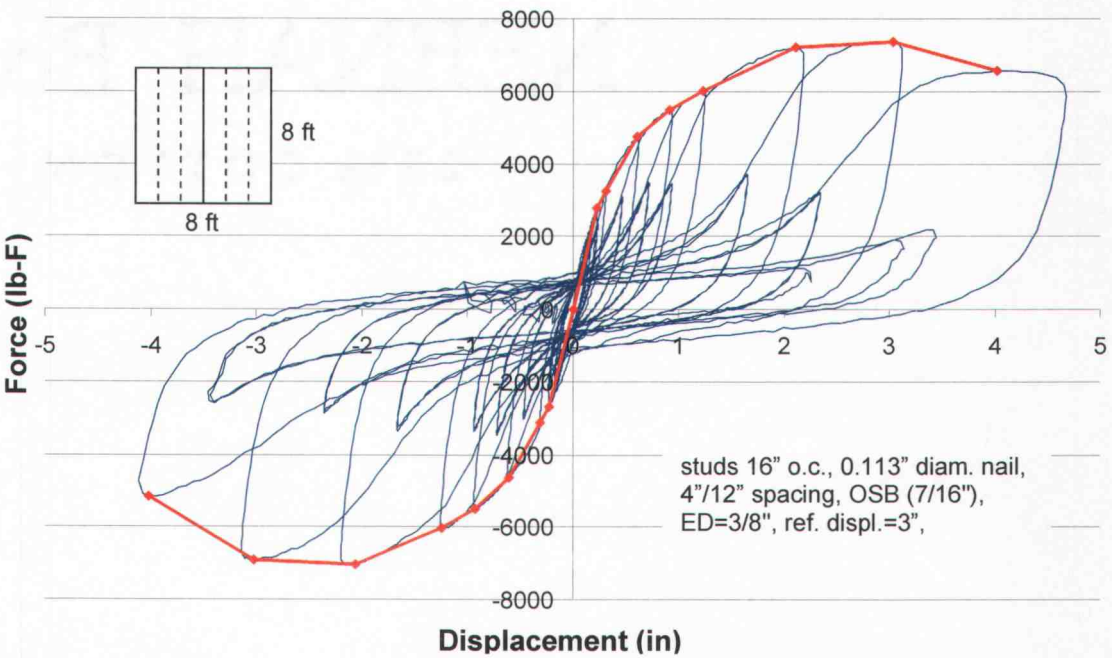

Fig. C6. Wall 3 hysteresis curve f_{yb}=115 ksi, wall with cracked center stud.

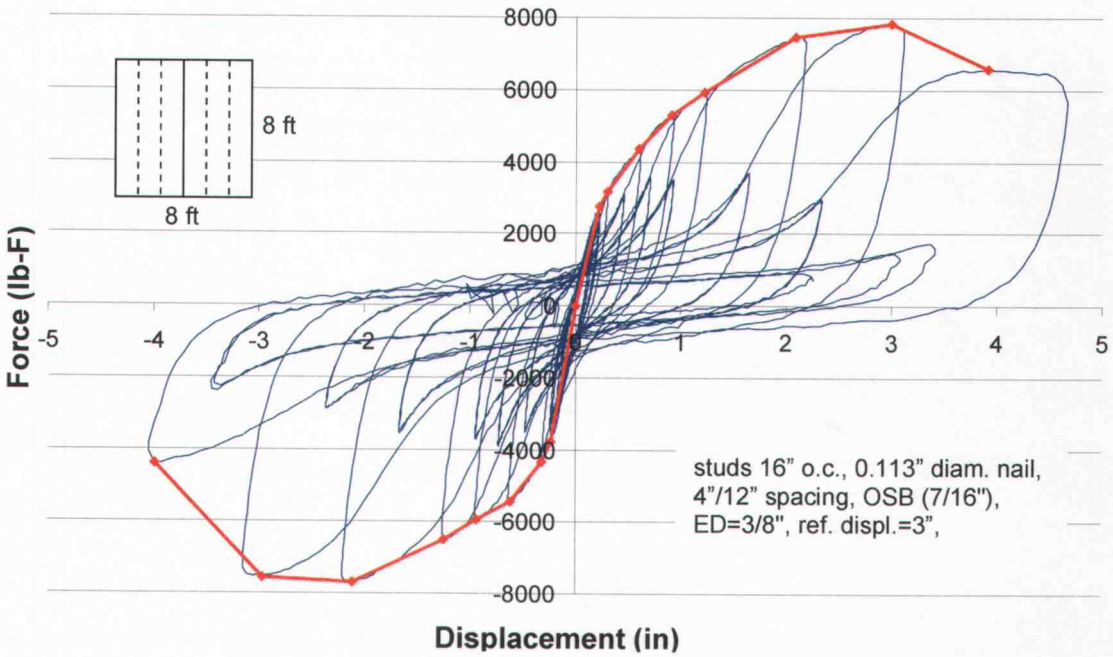

Fig. C7. Wall 4 hysteresis curve f_{yb}=115 ksi.

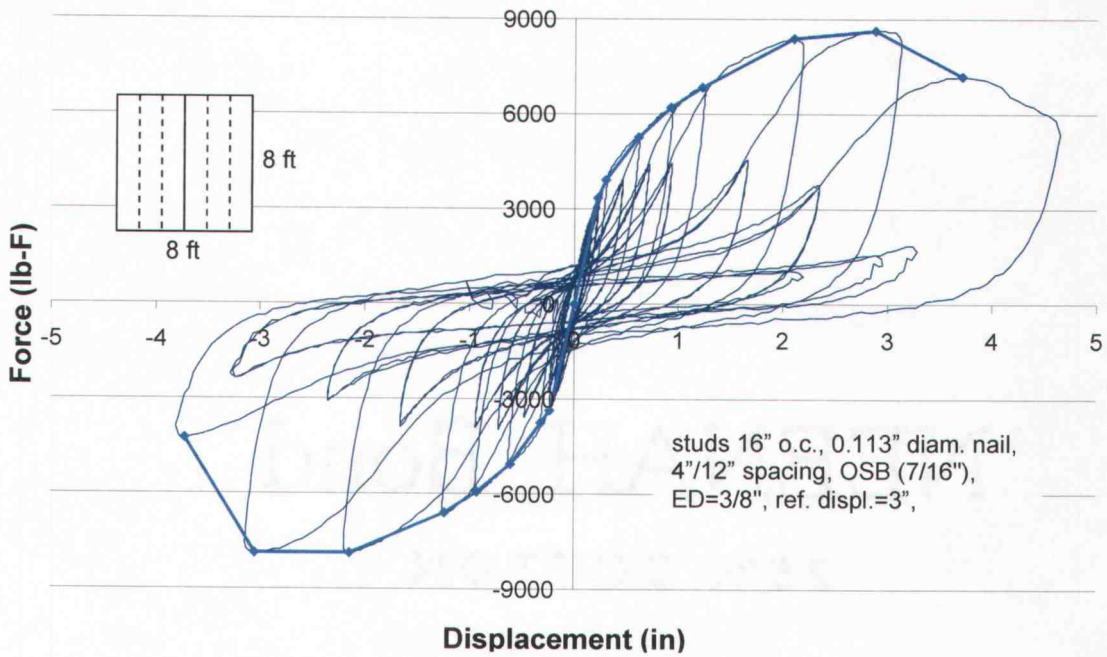

Fig. C8. Wall 5 hysteresis curve f_{yb}=145 ksi.

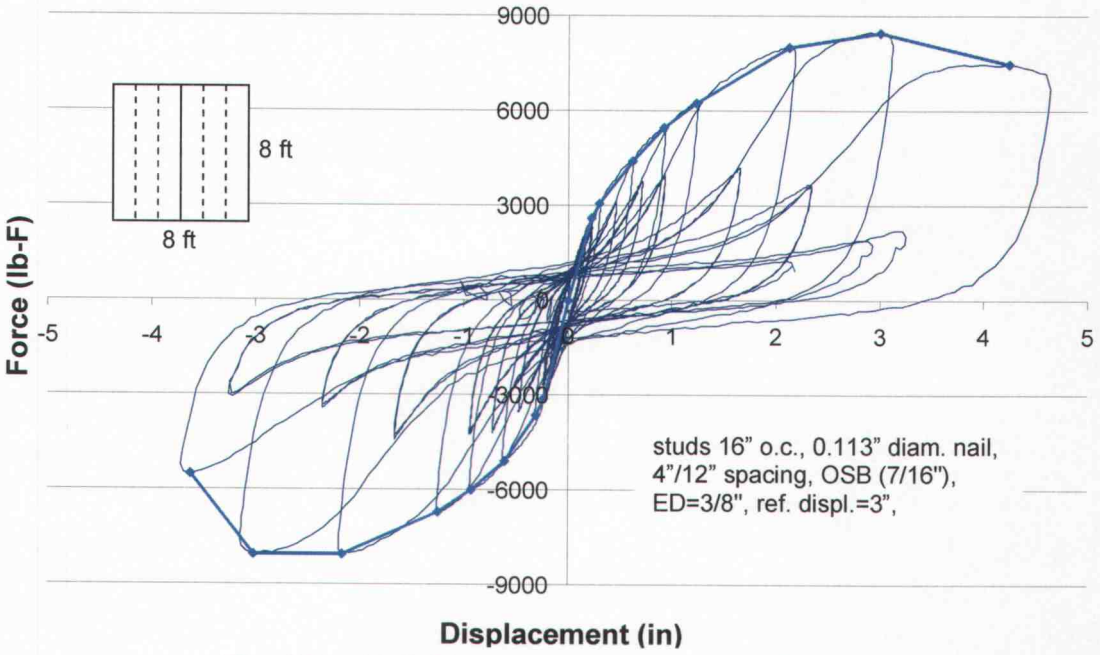

Fig. C9. Wall 6 hysteresis curve f_{yb}=145 ksi.

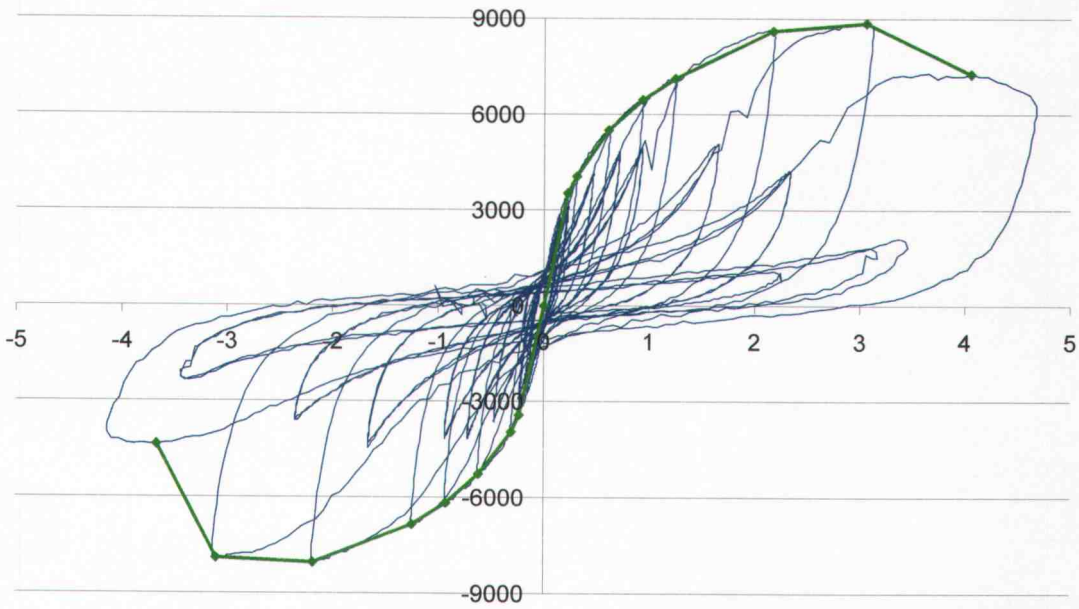

Fig. C10. Wall 7 hysteresis curve f_{yb}=241 ksi.

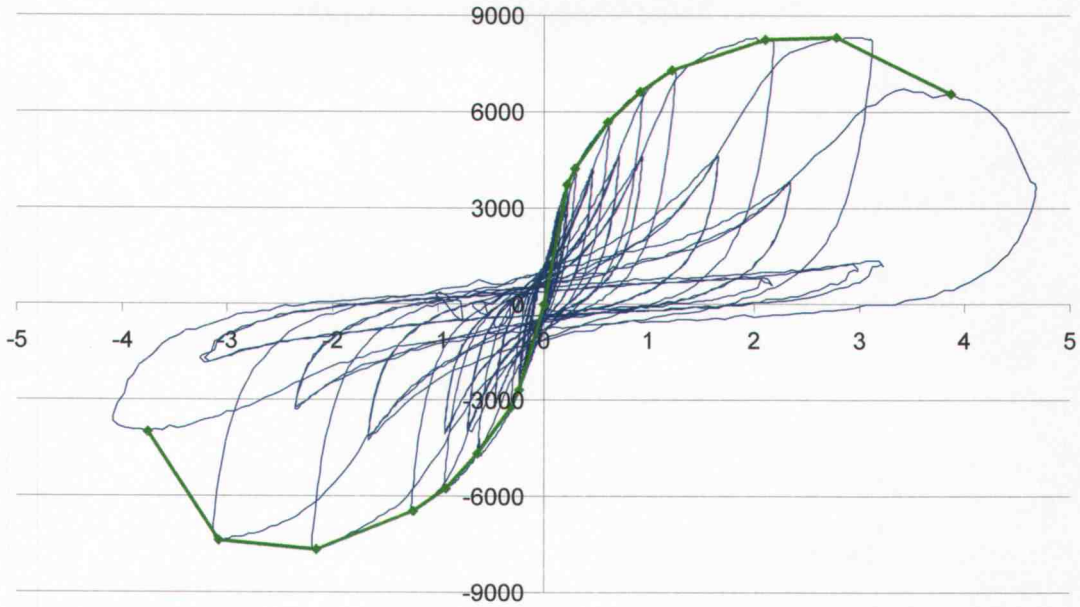

Fig. C11. Wall 8 hysteresis curve f_{yb}=241 ksi.

The nail failure modes common in the wall tests include withdrawal, pull-through, edge tear-out and fatigue. The OSB separated from the framing in several locations, and the top plate also separated from the top of the studs at both ends of the wall (Figure C12).

Fig. C12. Top plate separation from the studs.

Nails along the bottom plate and end studs commonly withdrew, the most common type of failure throughout the wall (Figure C13-a), while the nails along the center stud exhibited all of the failure modes: pull-though, edge tear-out and withdrawal (Figure C13-b) and fatigue (Figure C13-c). The nails also commonly fatigued or tore through the edge at the corners of the sheathing. Pull-through was also common along the top and bottom plates. The field

nails showed no visible signs of any failure. After each wall test, the sheathing nails were examined and the failure modes were recorded. The damage on each wall is shown in Fig. C14-C21; the field nails are not included in the summary. The nail conditions in Fig. C14-C21 are coded as withdrawal (W), pull-through (P), fatigue (F), and edge tear-out (T).

Fig. C13. Nail failure modes (left) OSB separation due to nail withdrawals, (middle) edge tear-out and pull-though (right) fatigue

The energy dissipated by the walls was calculated based on the area under each of the individual hysteresis loops of the test data. The sum of all of the curves is the cumulative energy dissipated by the walls (Table C22). The peak capacity, initial displacement and energy dissipated by the average of each bending yield stress wall are then compared to the CASHEW predicted values based on the connections removed from the walls.

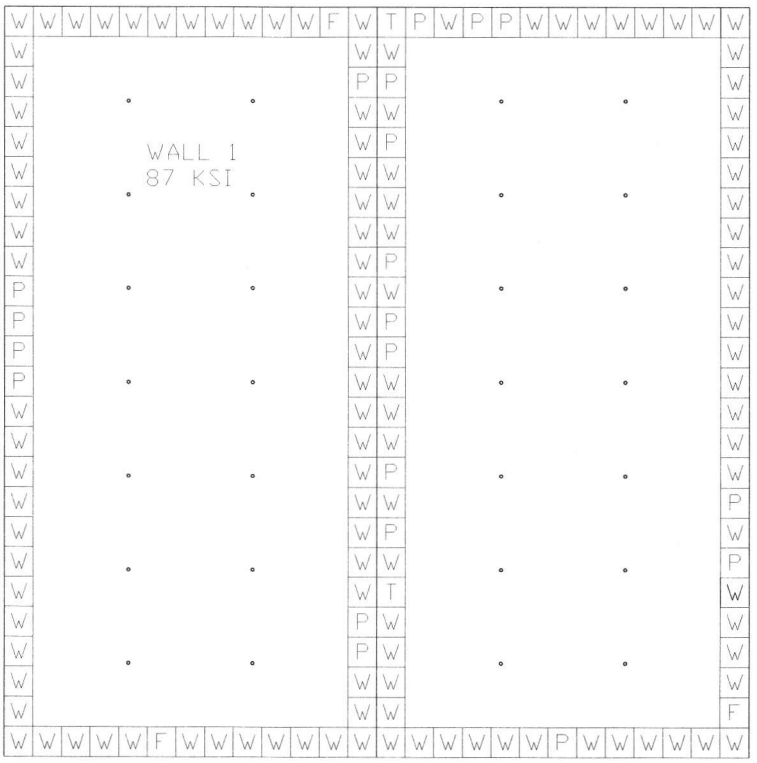

Fig. C14. Sheathing nail failure modes for Wall 1, f_{yb}=87 ksi

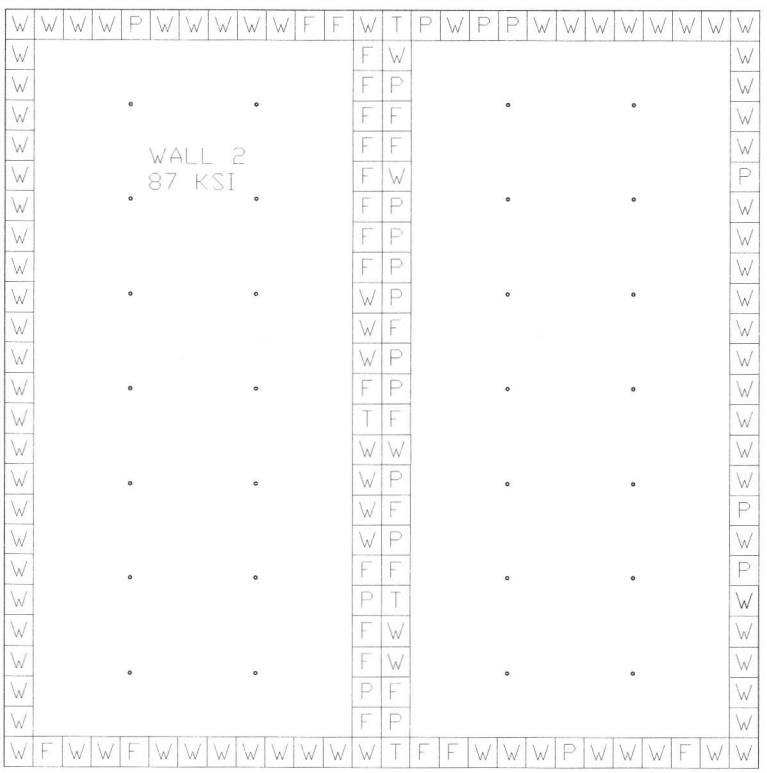

Fig. C15. Sheathing nail failure modes for Wall 2, f_{yb}=87 ksi.

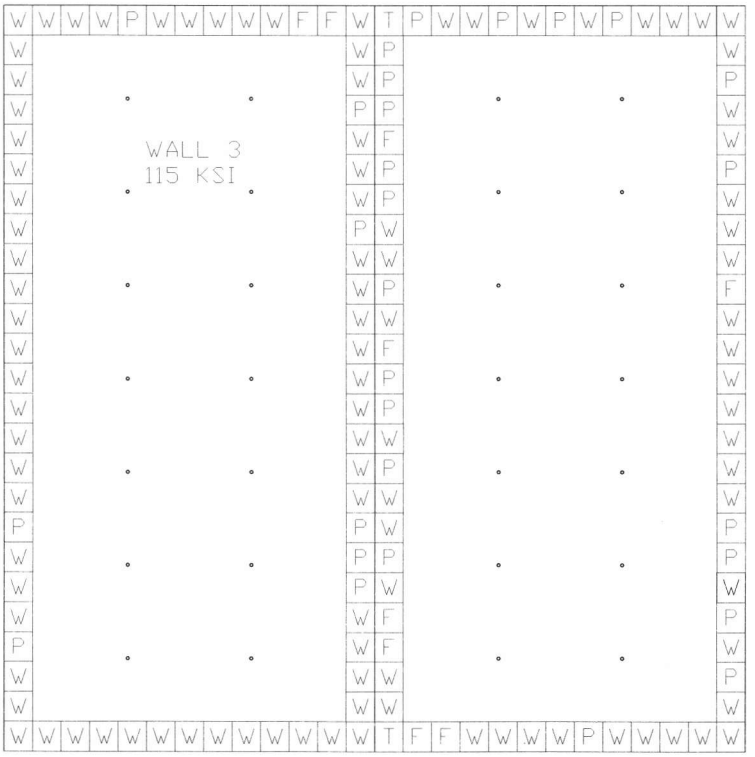

Fig. C15. Sheathing nail failure modes for Wall 2, f_{yb}=87 ksi.

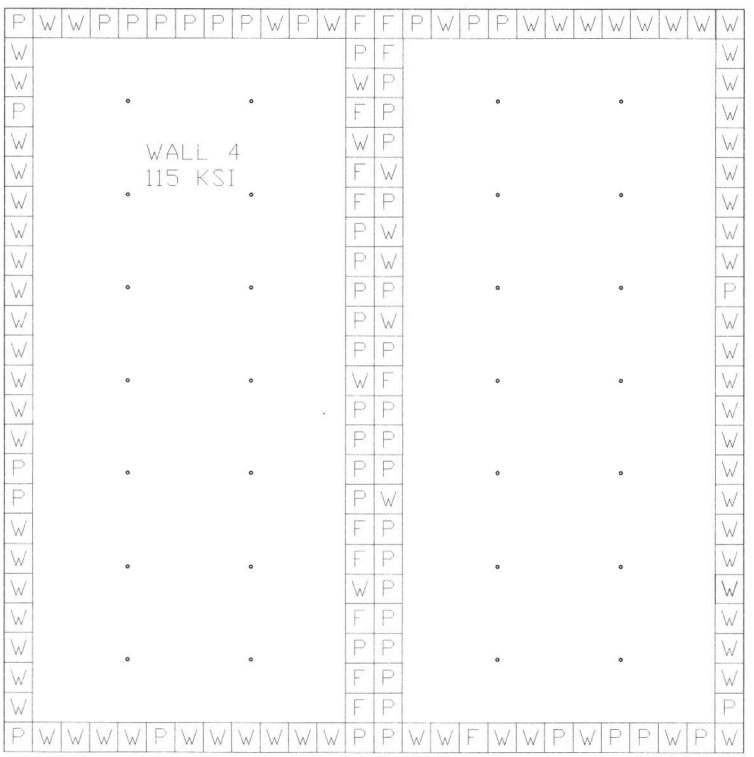

Fig. C17. Sheathing nail failure modes for Wall 4, f_{yb}=115 ksi.

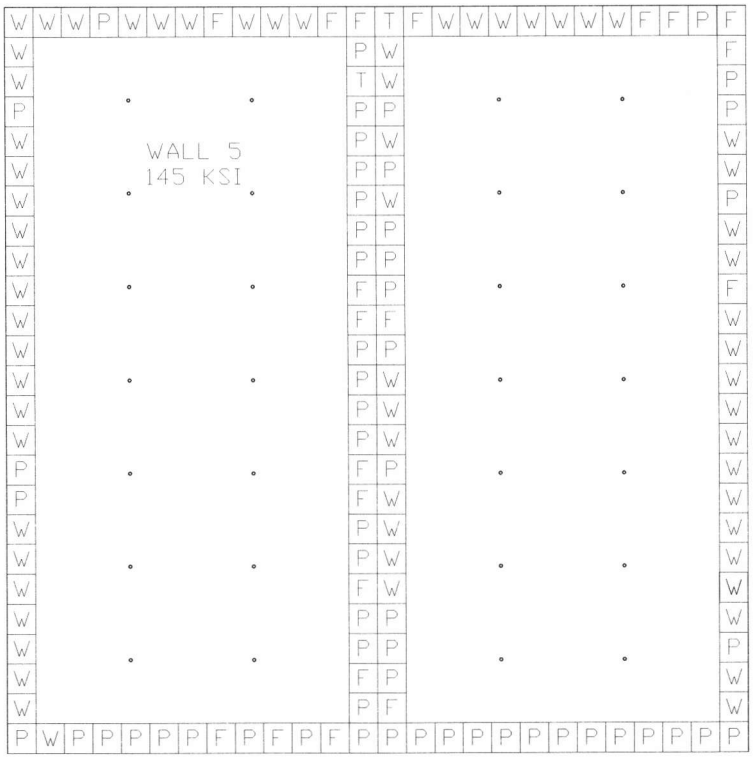

Fig. C18. Sheathing nail failure modes for Wall 5, f_{yb}=145 ksi.

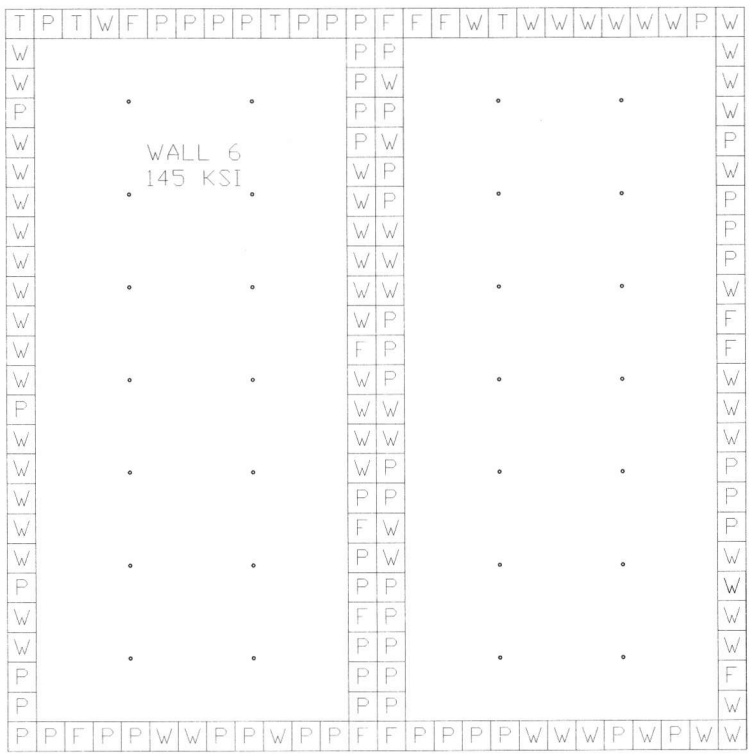

Fig. C19. Sheathing nail failure modes for Wall 6, f_{yb}=145 ksi.

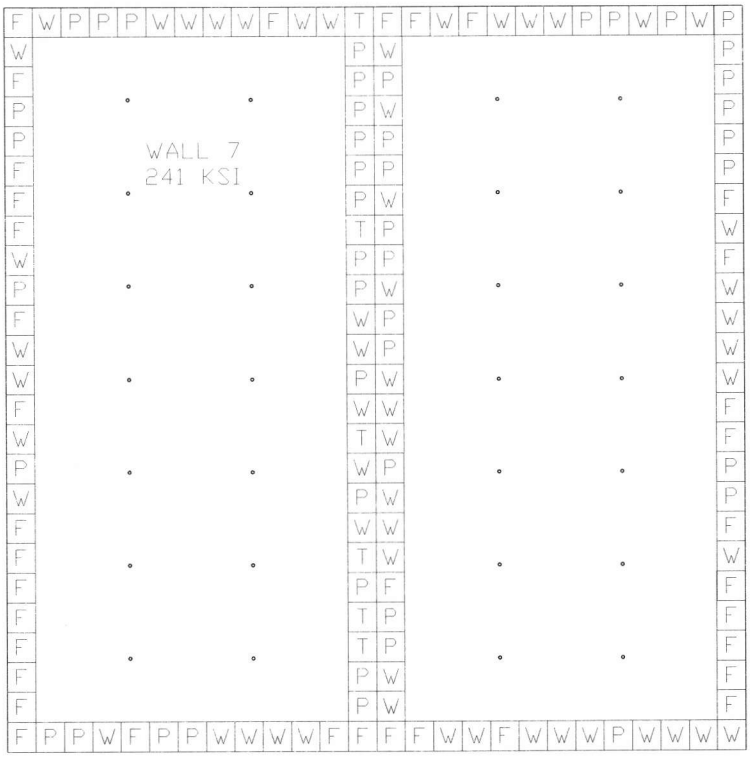

Fig. C20. Sheathing nail failure modes for Wall 7, f_{yb}=241 ksi.

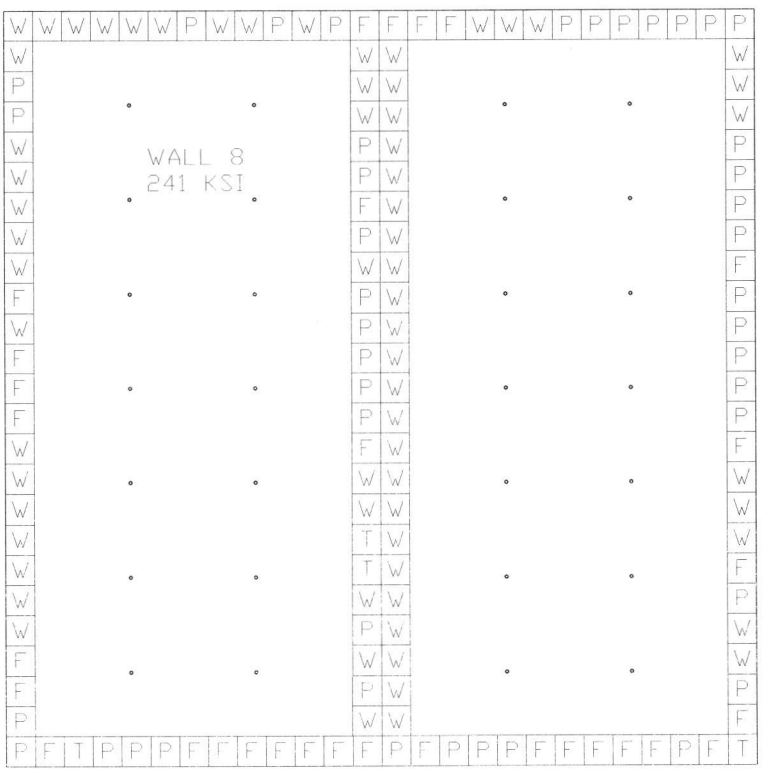

Fig. C21. Sheathing nail failure modes for Wall 8, f_{yb}=241 ksi.

Table C1. Wall Energy Dissipated per Loop (lb·in.)

Loop #	Wall							
	1	2	3	4	5	6	7	8
1.	347	401	346	311	379	336	418	334
2.	295	329	269	293	310	288	362	323
3.	276	314	252	285	295	274	349	312
4.	264	307	243	281	286	267	333	304
5.	260	304	238	280	276	262	335	302
6.	263	303	235	277	280	260	330	297
7.	589	671	532	634	634	570	700	641
8.	321	379	290	352	351	330	412	382
9.	309	360	276	336	431	313	395	367
10.	303	361	275	332	227	311	393	369
11.	304	352	272	332	324	311	389	359
12.	301	354	269	327	322	308	389	359
13.	302	356	272	329	326	309	388	360
14.	942	1081	845	1035	1009	915	1083	1023
15.	500	591	448	563	549	512	622	594
16.	473	559	424	528	521	484	596	565
17.	468	556	421	522	514	482	592	563
18.	462	549	416	515	509	477	588	558
19.	457	547	415	509	505	474	582	553
20.	473	568	429	522	524	495	608	572
21.	3261	3646	2991	3498	3653	3229	3488	3364
22.	1325	1542	1185	1566	1521	1356	1468	1482
23.	1227	1442	1097	1478	1367	1254	1380	1382
24.	1216	1418	1089	1460	1347	1240	1359	1362
25.	5355	5962	5079	5662	6018	5602	5762	5517
26.	2208	2555	1985	2497	2571	2394	2325	2390
27.	2056	2360	1850	2344	2325	2185	2127	2162
28.	2019	2315	1823	2332	2272	2154	2090	2106
29.	7205	7886	6969	7726	8260	7909	7870	7455
30.	2871	3208	2636	3143	3245	3233	2947	2988
31.	2690	3011	2486	3000	3003	3009	2745	2723
32.	17522	18617	17861	19203	20335	19923	19450	18704
33.	5846	6232	5468	6029	6303	6506	5796	5607
34.	5269	5589	4977	5674	5724	5877	5080	4842
35.	22815	22913	23503	25495	27326	27271	25955	24583
36.	7945	7928	7601	8046	8660	8645	7758	7166
37.	7063	6707	6909	7274	7679	7820	6842	6290
38.	25578	11810	27834	26815	26671	29638	28915	25707
39.	7965	5614	8187	7134	6969	8462	6822	5063
40.	8099	5102	8450	7440	7075	8673	6714	4935
41.	1862	1317	1702	1655	1450	1981	1425	1271
Total	149309	136415	148849	158034	162347	166339	158176	146235
Average	142862		153442		164343		152205	

Appendix D –CASHEW Nail Bending-Yield Analysis

The average hysteretic parameters as determined from SASHFIT are listed in Appendix B and are used as the input nail parameters for CASHEW. One wall configuration, the same as the wall tests, was used for each nail type. The set of nail hysteretic parameters are assigned to all of the sheathing nails in the shearwall. The input file for CASHEW (Table D1) is the same for each bending-yield stress wall model with the exception of the connector properties.

Table D1. Typical CASHEW Input File for Bending-Yield Stress

```
96" X 96" OSB Sheathed, Test Shear Wall, Units are kip - in (4/12 spacing)
3,                                      ! Analysis Control Parameter
96,2,                                   ! Height wall, Num of panels
1,48,96,0.4375,24,48,3,4,180,           ! Panel 1 geo& material props.
2,48,96,0.4375,72,48,3,4,180,           ! Panel 2 geo& material props.
1,                                      ! Panel 1 connector properties
0.2485,0.03241,0.425,                   !
2.851,0.037,-0.0694,3.91,0.0277,        !
0.265,1.146,                            !
2                                       ! Panel 2 connector properties
0.24851,0.03241,0.425,                  !
2.851,0.037,-0.0694,3.91,0.0277,        !
0.265,1.146,                            !
1                                       ! Panel 1 connector placement
-48.0,-23.25,24.0,4.0,                  ! Horizontal connector lines
48.00,-23.25,24.0,8.0,                  !
45.75,-20.00,20.0,8.0,                  !
-23.25,-44.0,44.0,4.0,                  !
-8.0,-36.0,36.0,12.0,                   ! Vertical connector lines
8.0,-36.00,36.0,12.0,                   !
24.0,-44.0,44.0,4.0,                    !
2                                       ! Panel 2 connector placement
-48.0,-24.00,23.25,4.0,                 ! Horizontal connector lines
48.00,-24.00,23.25,4.0,                 !
45.75,-20.625,20.,8.0,                  !
```

```
-24.0,-46.00,42.0,4.0,                ! Vertical connector lines
-8.0,-36.00,36.0,12.0,                !
8.0,-36.000,36.0,12.0,                !
23.25,-44.0,44.0,4.0,                 !
3.0                                   ! Reference wall displacement
```

One set of hysteretic parameters was output by CASHEW to represent the cyclic behavior of the shearwalls. The cyclic output is also fitted with a backbone curve to represent the overall cyclic performance of the wall. The backbone curves are drawn starting at zero and connect the peak displacements at each primary cycle. CASHEW predicts the monotonic and hysteretic behavior of the wall, and it also calculates the cumulative energy dissipated by the wall (Table D2). The CASHEW analysis similar to the other tests used the CUREE loading protocol, however, the CASHEW analysis begins after the initiation cycles. The initiation cycles correspond to the fist twenty-one cycles of the CUREE protocol.

Table D2. CASHEW Wall Cumulative Energy Dissipated (lb·in)

Wall Loop #	87 ksi	115 ksi	145 ksi	241 ksi
1.	3398	3521	3485	3546
2.	5094	5255	5114	5194
3.	6779	6981	6737	6839
4.	8465	8708	8360	8484
5.	13992	14441	14076	14502
6.	16633	17148	16615	17093
7.	19258	19842	19149	19682
8.	21883	22537	21682	22272
9.	29399	30317	29510	30679
10.	32932	33939	32887	34121
11.	36443	37545	36257	37563
12.	55502	56745	55831	58670
13.	61587	63089	61599	64390
14.	67607	69412	67362	70109
15.	90239	91642	89364	94595
16.	98795	100607	97488	102618
17.	107254	109548	105607	110641
18 Total	137941	137611	130061	140208

The ten hysteretic parameters predicted by CASHEW were used as input into SASH1. Seismic Analysis of Wood Shear Walls (SASH1) written by Brian Folz at the University of California, San Diego performs a nonlinear dynamic time history analysis of a wood shearwall that is modeled as a nonlinear single degree of freedom system. It performs this analysis based on an earthquake ground motion record and peak ground accelerations obtained from a response spectrum for specific hazard levels. Input for this program includes the hysteretic parameters of the shearwall as output from CASHEW, properties of the wall, the damping ratio, time integration and earthquake properties. The records considered in this study included 20 earthquake ground motions from the Los Angeles area scaled to hazard levels associated with life safety and immediate occupancy as defined by FEMA (2000). A seismic weight of 11.24 kips is applied to the wall, with a damping ratio of 2 percent. The input file for SASH1 is long due to the earthquake record, however, a sample of a SASH1 input file is given in Table D3. The peak displacements from each analysis were ordered and fit with a lognormal distribution. The common distribution function of the lognormal distribution for probability is:

$$f_x(x) = \frac{1}{\sqrt{2\pi}\xi x}\exp\left[-\frac{1}{2}\left(\frac{\ln x - \lambda}{\xi}\right)^2\right]$$

where λ is the average of the natural logs of the peak displacements, while ξ is the standard deviation of the natural logs of the peak displacements. All of the displacements were truncated at 5 in. if they were larger. The ordered data points are listed for Life Safety (Table D4) and for Immediate Occupancy (Table D5).

Table D3. Typical SASH1 Input File for Nail Bending-Yield Stress Models

```
96" x 96" Test Shear Wall, OSB, Nails Spacing @ 4-12, stud 16" o.c.(115 ksi).
0.029116,2.0,                              ! Wall mass & damping ratio (in %)
2,                                         ! Hysteretic element type
11.33,0.03307,-0.07718,2.889,0.01814,      ! Hysteretic element stiffness props.
```

```
7.95,0.9617,2.102,                          ! Hysteretic element strength props.
0.3067,1.164,                               ! Hyst. element degradation props.
0.002,4,21900,5.,2200,204.80,               ! Time integration & earthquake props.
0.020,                                      ! Time increment for EQ record
PACIFIC ENGINEERING AND ANALYSIS STRONG-MOTION DATA  ! Header for record
2200 .02000
  0.1514095E-01  0.3960228E-02  0.4071718E-02  0.8116682E-02  0.1279775E-02
```

Table D4. Cumulative distribution function for peak displacement data points for life-safety

δ_{max} (Life Safety)					
Wall Type		**8 ft. × 8 ft std.**			
Seismic Weight		**50 kN**			
ξ		**2%**			
Edge Distance		**3/8"**			
Nailing Schedule		**4"-12"**			
G (ksi)					
Sheathing		**OSB**			
Thickness		**7/16"**			
yb		**87 ksi**	**115 ksi**	**145 ksi**	**241 ksi**
1	**0.0476**	0.000	0.474	0.453	0.411
2	**0.0952**	0.780	0.932	0.931	0.861
3	**0.1429**	0.780	0.955	0.934	0.868
4	**0.1905**	1.033	0.970	0.937	0.984
5	**0.2381**	1.041	1.248	1.224	1.135
6	**0.2857**	1.108	1.343	1.365	1.281
7	**0.3333**	1.255	1.423	1.418	1.285
8	**0.3810**	1.287	1.560	1.426	1.291
9	**0.4286**	1.437	1.653	1.529	1.302
10	**0.4762**	1.468	1.656	1.607	1.321
11	**0.5238**	1.648	1.664	1.610	1.329
12	**0.5714**	1.696	1.728	1.614	1.453
13	**0.6190**	1.907	1.743	1.651	1.473
14	**0.6667**	1.974	1.783	1.813	1.492
15	**0.7143**	1.988	1.900	1.825	1.594
16	**0.7619**	2.004	2.046	1.837	1.597
		2.500	2.217	1.911	1.611
18	**0.8571**	2.797	2.875	2.370	1.704
19	**0.9048**	3.356	2.985	2.629	2.080
20	**0.9524**	5.000	3.260	3.077	2.265
		1.582	1.640	1.531	1.320
		0.779	0.624	0.512	0.367
		0.61	0.39	0.26	0.13
		0.492	0.381	0.335	0.278
λ					
ξ					

Table D5. Cumulative distribution function for peak displacement data points for immediate-occupancy

δ_{max} (Immediate Occupancy)					
Wall Type		**8 ft. × 8 ft std.**			
Seismic Weight		**50 kN**			
ξ		**2%**			
Edge Distance		**3/8"**			
Nailing Schedule		**4"-12**			
G (ksi)					
Sheathing		**OSB**			
Thickness		**7/16"**			
y					
λ					
ξ					

Appendix E – Decayed Lateral Nail Connection Tests

The connection tests for the decayed connections are similar to those used in the nail bending-yield study. The connections are the same size and are composed of 15/32-in. OSB sheathing and 2×4 Douglas Fir-Larch framing. The difference is that with the exception of the control group, the specimens were inoculated with brown rot fungus and incubated to five different levels of decay. The levels of decay (described by weeks of incubation period) ranged from no damage to extreme damage: 0, 5, 10, 20 and 30 weeks. The connections are tested using the CUREE loading protocol with a reference displacement of 0.43 in. using the first lateral nail test set-up described in Appendix B. Complete information on experimental design, testing methods and materials can be found elsewhere (Kent 2004). The terminology used in the thesis to describe the physical condition of the decayed connection treatments as dry, wet, mild decay, moderate decay, and severe decay correspond to the control, 0, 10, 20, and 30 week treatments, respectively.

The load-displacement curves for the decayed connections were fitted using SASHFIT to find the hysteretic parameters for each specimen (Table E1-E6). The parameters from SASHFIT are used to model decayed walls with CASHEW with the exception of connections from the 5-week inoculation treatment.

Table E1. Connection hysteretic parameters for Control Group

Sample	Ko	r1	r2	r3	r4	F_0	F_I	Δu	α	β	F_u+
	lb/in					lb	lb	in			lb
C1	2861	0.028	-0.55	1.16	0.017	184	24.9	0.865	0.45	1.0	255
C2	3560	0.047	-0.06	1.65	0.025	157	28.2	0.410	0.37	1.1	227
C3	3839	0.100	-0.09	1.75	0.020	171	35.8	0.433	0.42	1.1	255
C4	3887	0.034	-0.06	2.10	0.022	180	27.0	0.437	0.54	1.1	237
C5	5441	0.036	-0.03	1.47	0.016	216	31.7	0.432	0.46	1.1	299
C6	2883	0.037	-0.05	1.00	0.010	153	22.3	0.887	0.58	1.0	248
C7	4321	0.031	-0.04	1.48	0.023	178	33.7	0.412	0.46	1.1	232
C8	3767	0.063	-0.06	1.81	0.024	173	30.9	0.377	0.51	1.1	263
C9	3940	0.026	-0.05	1.32	0.031	191	25.8	0.391	0.49	1.1	231
C10	3826	0.088	-0.04	1.72	0.031	172	30.4	0.428	0.36	1.1	314
Avg	3833	0.049	-0.10	1.55	0.022	177	29.1	0.507	0.464	1.08	256
Std Dev	727.6	0.026	0.158	0.328	0.007	17.6	4.21	0.195	0.070	0.042	29.3
COV	0.190	0.534	-1.53	0.212	0.303	0.099	0.145	0.385	0.150	0.039	0.115

Table E2. Connection hysteretic parameters for 0 Weeks Inoculation

Sample	Ko	r1	r2	r3	r4	F_0	F_I	Δu	α	β	F_u+
	lb/in					lb	lb	in			lb
0-1	2309	0.101	-0.16	1.00	0.018	121	22.5	0.929	0.42	1.0	338
0-2	3169	0.101	-0.05	1.47	0.030	119	30.3	0.423	0.38	1.1	252
0-3	3180	0.068	-0.04	0.90	0.017	180	23.3	0.871	0.49	1.1	368
0-4	3018	0.130	-0.04	0.97	0.016	83	27.7	0.389	0.31	1.1	235
0-5	2812	0.069	-0.05	1.10	0.020	184	23.6	0.919	0.54	1.0	363
0-6	2465	0.092	-0.07	1.10	0.019	133	27.3	0.881	0.43	1.1	332
0-8	1773	0.079	-0.07	1.30	0.016	130	21.6	0.860	0.46	1.1	250
0-9	2495	0.113	-0.08	2.46	0.026	114	22.9	0.612	0.39	1.1	286
0-10	2688	0.070	-0.06	1.16	0.014	198	25.0	0.881	0.44	1.0	363
Avg	2657	0.091	-0.07	1.27	0.020	140	24.9	0.751	0.429	1.07	310
Std Dev	455.1	0.022	0.038	0.477	0.005	38.5	2.91	0.217	0.066	0.050	54.1
COV	0.171	0.239	-0.539	0.375	0.268	0.275	0.117	0.289	0.155	0.047	0.175

Table E3. Connection hysteretic parameters for 5 Weeks Inoculation

Sample	Ko	r1	r2	r3	r4	F_0	F_I	Δu	α	β	F_u+
	lb/in					lb	lb	in			lb
5-1	2556	0.156	-0.055	1.80	0.042	54.8	25.9	0.440	0.34	1.1	230
5-2	2841	0.154	-0.075	1.70	0.018	85.9	25.9	0.427	0.24	1.1	273
5-3	3382	0.127	-0.036	1.44	0.030	103	31.5	0.438	0.33	1.1	292
5-4	3275	0.124	-0.105	2.20	0.020	118	31.5	0.402	0.22	1.1	278
5-5	2973	0.092	-0.060	1.76	0.022	142	25.9	0.592	0.35	1.0	303
5-6	3296	0.164	-0.020	1.80	0.020	101	29.2	0.433	0.26	1.1	335
5-7	3024	0.074	-0.110	2.40	0.028	180	31.3	0.433	0.38	1.1	280
5-8	3314	0.106	-0.043	1.63	0.014	118	31.5	0.621	0.30	1.1	337
5-9	2654	0.114	-0.055	1.74	0.040	101	22.5	0.435	0.33	1.0	233
5-10	3799	0.084	-0.080	1.85	0.026	211	36.4	0.624	0.32	1.1	410
Avg	3111	0.119	-0.065	1.83	0.026	122	29.1	0.484	0.307	1.08	297
Std Dev	374.9	0.031	0.029	0.276	0.009	45.7	4.08	0.089	0.051	0.042	53.3
COV	0.121	0.264	-0.453	0.151	0.355	0.376	0.140	0.184	0.168	0.039	0.180

Table E4.Connection Hysteretic Parameters for 10 weeks Inoculation

Sample	Ko	r1	r2	r3	r4	F_0	F_I	Δu	α	β	F_u+
	lb/in					lb	lb	in			lb
10-1	2443	0.140	-0.033	1.65	0.033	68.5	22.3	0.438	0.29	1.1	218
10-2	2833	0.091	-0.080	1.85	0.022	104	25.9	0.416	0.38	1.1	211
10-3	2597	0.193	-0.067	1.70	0.032	62.9	27.5	0.435	0.24	1.1	280
10-4	3279	0.115	-0.030	1.74	0.026	107	30.5	0.440	0.36	1.1	273
10-5	2566	0.259	-0.040	1.80	0.022	47.2	27.0	0.432	0.22	1.1	334
10-6	2862	0.060	-0.065	1.55	0.047	105	20.2	0.440	0.65	1.1	181
10-7	3716	0.069	-0.031	1.74	0.032	135	28.3	0.415	0.49	1.1	241
10-8	2507	0.050	-0.103	1.66	0.042	86.8	20.2	0.433	0.6	1.1	141
10-9	3101	0.186	-0.060	2.90	0.030	146	28.5	0.415	0.10	1.0	386
10-10	2533	0.122	-0.022	1.20	0.020	98.9	29.2	0.934	0.39	1.1	387
Avg	2844	0.128	-0.053	1.78	0.031	96.2	26.0	0.480	0.372	1.09	265
Std Dev	411.7	0.067	0.026	0.433	0.009	31.0	3.74	0.160	0.1716	0.032	83.5
COV	0.145	0.523	-0.493	0.244	0.286	0.322	0.144	0.334	0.4612	0.029	0.315

Table E5. Connection hysteretic parameters for 20 Weeks Inoculation

Sample	Ko	r1	r2	r3	r4	F_0	F_I	Δu	α	β	F_u+
	lb/in					lb	lb	in			lb
20-1	2110	0.085	-0.040	2.23	0.033	125	27.0	0.439	0.55	1.1	203
20-2	2347	0.092	-0.050	1.78	0.032	113	21.8	0.624	0.45	1.1	247
20-3	1511	0.126	-0.030	1.80	0.052	62.9	20.2	0.460	0.51	1.1	151
20-4	3321	0.041	-0.023	1.48	0.005	139	11.2	0.589	0.54	1.3	219
20-5	2167	0.144	-0.033	2.40	0.052	96.8	25.9	0.430	0.36	1.0	231
20-6	1925	0.081	-0.040	1.86	0.046	73.5	18.0	0.433	0.63	1.1	141
20-7	3183	0.043	-0.080	1.00	0.022	243	22.2	0.924	0.60	1.1	370
20-8	2793	0.106	-0.086	2.00	0.019	157	28.1	0.589	0.33	1.1	331
20-9	2441	0.091	-0.030	1.60	0.036	98.8	18.0	0.424	0.39	1.1	193
20-10	2998	0.072	-0.110	1.30	0.013	229	19.9	0.899	0.60	1.0	423
Avg	2480	0.088	-0.052	1.75	0.031	134	21.2	0.581	0.496	1.10	251
Std Dev	583.9	0.032	0.029	0.420	0.016	60.9	5.02	0.190	0.108	0.082	94.0
COV	0.24	0.368	-0.564	0.241	0.524	0.455	0.236	0.327	0.217	0.074	0.374

Table E6.Connection hysteretic parameters for 30 Weeks Inoculation

Sample	Ko	r1	r2	r3	r4	F_0	F_I	Δu	α	β	F_u+
	lb/in					lb	lb	in			lb
30-1	1713	0.026	-0.064	1.02	0.005	62.9	2.25	0.194	0.61	1.2	71.1
30-2	3216	0.081	-0.048	1.80	0.019	94.4	19.1	0.415	0.49	1.2	134
30-3	1839	0.032	-0.053	1.20	0.058	68.2	11.2	0.407	0.84	1.2	90.7
30-4	2065	0.045	-0.053	1.30	0.030	77.6	14.6	0.417	0.55	1.1	116
30-5	2828	0.101	-0.100	1.20	0.030	79.8	20.2	0.422	0.45	1.2	200
30-6	1812	0.170	-0.060	0.89	0.010	45.0	1.35	0.047	0.53	1.1	50.3
30-7	1299	0.054	-0.040	1.40	0.010	74.8	3.37	0.364	0.46	1.1	99.9
30-8	1967	0.047	-0.050	1.25	0.010	67.4	5.62	0.244	0.64	1.2	115
30-9	1542	0.094	-0.064	1.34	0.042	54.2	12.1	0.399	0.45	1.1	112
30-10	868	0.056	-0.055	2.30	0.015	59.6	3.37	0.599	0.57	1.3	61.7
Avg	1915	0.071	-0.059	1.37	0.023	68.4	9.32	0.351	0.56	1.17	105
Std Dev	685.0	0.043	0.016	0.406	0.017	14.1	7.09	0.152	0.119	0.067	42.6
COV	0.36	0.610	-0.278	0.296	0.740	0.206	0.760	0.435	0.213	0.058	0.405

Appendix F – CASHEW Decay Analysis

CASHEW was altered to allow multiple sets of connection properties to be assigned to different areas in the wall (Appendix H). The wall configuration used for the CASHEW decay analysis is the same configuration as the nail bending-yield stress analyses (Fig. F1).

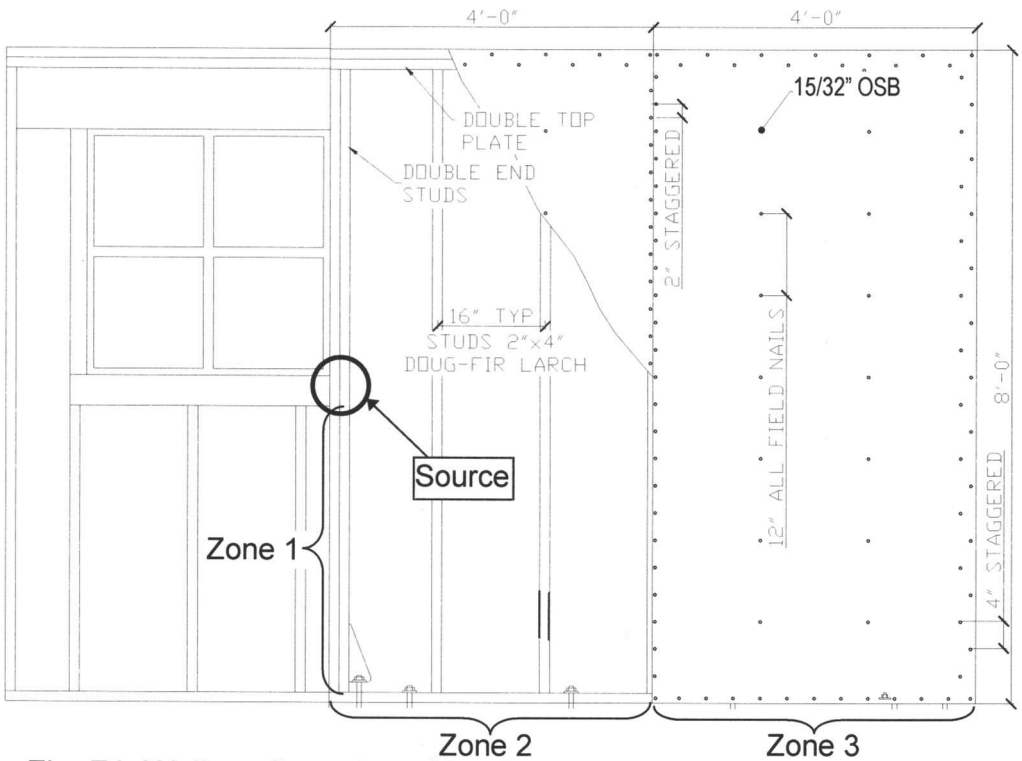

Fig. F1. Wall configuration with adjacent window modeled by CASHEW.

Seven different decay conditions are considered; at each decay condition, 30 walls were analyzed. Connection parameters are assigned to the wall by line based on location. On panel 1, right of and adjacent to the window, there are three horizontal lines of nails: one on the sole plate, and two on the top plate due to the staggering. This is the same for panel 2 on the right. Panel 1 is considered to have seven vertical lines of nails, while panel 2 has five. The vertical lines of nails are on the center stud, the interior studs, and two on the end studs again due to the staggered nail pattern. Panel 1 has two additional lines because the vertical lines on the end stud by the window

are split at midheight, which corresponds to the bottom corner of the window. Nails above the midheight are assigned control parameters while nails below the midpoint are assigned decay parameters. Each line of nails is numbered, starting from bottom to top and then left to the right on each panel. Therefore, 1-1 is the horizontal line of nails on the sole plate of panel one, and 2-4 is the vertical line of nails on the center stud on panel two, and so on. Combining both panels there are 17 lines of nails with assigned parameters, and 4 of these lines are assigned decay parameters. The four decayed lines are 1-4, 1-5, 1-1, 2-1, which correspond to the two vertical lines beneath the window, and the lines of nails on the sole plate of panel one and panel two. At the most severe level of decay, the nails from the decayed lines were removed from the model leaving only 2 horizontal and 5 vertical lines of nails on each panel.

Of the four decayed lines at each decay level, connection parameters with different incubation times were assigned depending on the level of decay. As an example, at decay level 4, lines 1-4 and 1-5 were randomly assigned connection properties at 20 weeks of incubation, while 1-1 was assigned properties at 10 weeks of incubation and 2-1 was assigned properties at 0 weeks of incubation. To make sure that the connection parameters were randomly assigned to all locations in each wall, a random number generator was used to determine which set of parameters would be assigned to each line of nails (Table F1). Next to the connection line number in Table F1. there is a column of numbers designating from which incubation time the parameters should be taken, c indicates the control level. The parameters were generated for thirty-five walls at each decay level on the event that CASHEW encountered an error during the analysis of the first thirty walls. The random number generator served as a guide to assign the connection properties to CASHEW. A sample input file for the decay model in CASHEW is given in Table F2. The file remained the same for each wall, with the exception of the connection properties and the final level of decay.

Table F1. Randomized nail parameters at each decay condition

WALL		1	2	3	4	5	6	7	8	9	10	11	12	13	14	15	16	17	18	19	20	21	22	23	24	25	26	27	28	29	30	31	32	33	34	35
Decay Level 1																																				
1-4	C	2	7	2	9	4	2	10	6	10	7	10	3	8	4	9	5	6	2	9	5	3	7	8	7	4	1	10	3	8	8	8	6	1	10	3
1-5	C	6	3	4	4	1	5	8	3	4	8	1	4	9	8	7	7	8	5	1	10	10	10	5	3	10	9	1	3	4	7	4	4	3	10	2
1-1	C	8	10	9	8	7	7	4	5	9	6	1	6	8	5	1	9	2	5	3	6	7	2	6	2	9	4	6	9	2	10	5	6	2	8	1
2-1	C	10	10	6	7	4	2	9	7	10	5	2	6	5	8	5	2	9	5	1	7	9	2	3	9	1	8	4	7	6	4	5	5	3	1	1
1-2	C	5	3	2	7	10	5	7	2	3	8	9	10	9	2	9	1	9	6	5	5	5	7	10	2	7	7	2	3	1	4	6	3	10	10	2
1-3	C	3	3	2	9	5	8	8	10	9	1	2	10	4	2	4	4	5	2	7	9	5	9	1	2	6	3	1	8	8	9	8	3	4	1	6
1-6	C	10	2	3	9	3	4	5	4	6	2	9	3	7	3	6	3	1	9	10	2	2	5	3	3	4	9	3	1	3	4	6	9	10	4	9
1-7	C	1	2	4	2	4	5	9	7	1	9	1	4	6	10	4	3	4	8	3	3	4	7	10	9	9	8	1	8	1	7	1	1	9	9	5
1-8	C	5	7	9	1	10	9	10	6	3	1	2	2	5	4	10	7	1	6	8	8	6	9	8	6	9	4	8	5	9	10	1	4	8	10	1
2-2	C	1	4	6	4	4	1	7	7	9	1	5	6	2	2	3	6	7	2	5	10	4	7	4	1	4	5	9	8	9	1	3	3	9	1	1
2-3	C	8	6	6	6	1	3	1	3	5	4	2	6	5	7	3	2	4	1	8	8	2	3	8	3	5	10	10	9	3	7	7	2	5	9	2
2-4	C	8	3	10	10	4	7	6	5	9	9	7	4	9	7	4	9	5	5	5	4	5	2	7	9	7	3	8	8	8	5	1	2	10	5	6
2-5	C	2	8	10	2	2	2	4	3	4	1	3	1	5	3	5	7	1	9	9	4	7	10	3	2	3	2	5	9	10	9	10	4	8	8	2
2-6	C	9	1	7	6	4	2	6	1	5	5	5	10	6	2	2	4	3	2	3	5	1	10	2	9	8	9	8	6	10	10	9	7	1	1	5
2-7	C	9	1	5	4	9	5	1	1	7	3	9	9	6	4	8	10	7	6	9	1	10	7	1	10	10	1	10	6	8	9	4	1	2	9	4
2-8	C	4	3	2	9	10	5	4	6	9	1	6	9	5	3	10	10	9	9	1	3	10	10	8	7	6	10	9	7	4	5	10	1	10	9	7
Decay Level 2																																				
1-4	0	1	3	2	3	9	8	9	1	5	2	2	5	9	4	10	1	5	4	6	6	1	2	5	1	5	2	9	9	3	1	4	2	9	1	1
1-5	0	5	7	3	10	1	3	8	2	6	9	6	5	5	5	1	1	9	6	8	8	1	10	4	10	1	4	8	6	2	5	8	2	5	6	8
1-1	C	8	1	10	7	5	4	10	7	10	6	2	1	6	8	10	10	1	8	2	6	3	9	8	3	10	5	4	4	8	3	5	6	1	6	9
2-1	C	1	8	6	7	2	10	2	10	10	8	9	9	1	4	4	8	8	9	5	7	2	3	1	1	7	6	2	2	8	3	7	8	1	3	6
1-2	C	2	1	10	1	8	10	10	5	2	10	3	7	9	1	10	4	7	6	7	8	4	8	8	4	6	5	5	3	10	4	2	7	10	7	9
1-3	C	5	3	5	10	6	5	7	9	4	1	8	2	9	3	8	4	9	6	5	2	4	7	6	5	4	8	4	7	1	2	6	7	3	4	6
1-6	C	3	3	7	4	2	2	4	1	4	6	5	10	6	8	2	5	3	5	10	6	3	7	10	5	10	2	5	8	1	2	7	5	6	3	6
1-7	C	2	5	7	1	2	5	8	2	4	9	4	10	4	1	4	7	2	1	6	1	8	7	5	7	10	4	4	10	7	3	5	7	4	5	2
1-8	C	6	1	9	9	5	2	2	9	6	8	5	7	1	10	7	4	1	6	6	5	10	6	9	5	8	2	6	3	5	7	1	10	8	2	8
1-9	C	10	3	7	9	9	10	9	7	8	8	10	10	10	4	10	4	3	7	6	10	6	7	5	4	3	5	7	7	6	1	4	6	9	3	10
1-10	C	8	8	7	3	7	7	10	1	7	2	8	2	2	5	10	5	10	3	9	6	3	8	9	10	8	9	4	6	6	6	9	4	4	6	9
2-2	C	8	6	2	4	7	2	1	9	1	2	7	4	2	4	5	10	5	9	3	1	5	3	8	4	8	10	2	2	1	3	9	6	1	8	10
2-3	C	7	5	8	2	7	9	2	5	9	1	8	8	7	2	1	9	4	7	7	4	5	9	10	9	10	5	6	9	9	4	7	4	3	6	3
2-4	C	4	4	6	10	6	10	6	9	3	6	6	1	1	7	10	4	4	5	3	3	5	4	9	3	10	1	9	5	1	5	2	2	5	4	6
2-5	C	5	1	5	9	4	7	9	3	6	8	10	1	6	9	5	6	8	8	1	1	6	7	3	9	9	7	9	7	7	5	7	6	4	7	2
2-6	C	3	4	7	10	2	1	2	3	6	7	3	2	4	7	4	9	7	3	1	9	9	1	1	10	4	4	3	2	3	1	7	10	7	3	2
2-7	C	3	6	7	1	9	2	10	1	10	7	2	7	3	6	8	4	6	8	4	6	3	8	5	6	4	2	1	8	6	9	7	5	10	8	4
2-8	C	5	4	2	5	9	2	10	3	1	5	6	2	8	4	6	6	8	9	5	4	3	4	6	10	1	8	2	8	3	6	1	5	10	1	10

Table F1. continued

WALL	1	2	3	4	5	6	7	8	9	10	11	12	13	14	15	16	17	18	19	20	21	22	23	24	25	26	27	28	29	30	31	32	33	34	35
Decay Level 3																																			
1-4	10	7	6	9	1	7	7	8	5	7	7	10	10	8	3	5	6	9	3	4	2	10	10	7	8	5	10	10	9	1	10	10	9	7	3	3
1-5	10	1	9	10	4	8	6	2	7	2	3	4	7	7	5	2	2	2	1	6	2	3	10	2	6	5	4	7	5	5	10	1	1	1	10	4
1-1	0	3	5	5	7	2	4	2	8	1	6	5	8	4	3	1	5	1	3	7	3	7	2	1	9	8	2	9	6	7	5	2	5	4	4	8
2-1	C	3	6	7	7	7	8	4	3	10	10	3	2	2	9	1	8	7	8	4	5	5	10	8	2	5	1	3	10	4	5	8	1	3	7	5
1-2	C	4	7	5	6	8	8	3	8	10	4	8	4	2	2	5	2	9	1	2	7	8	1	9	7	4	10	1	1	10	5	3	9	7	3	5
1-3	C	4	1	5	4	2	4	6	8	10	6	2	7	6	7	7	2	9	7	3	7	8	1	1	10	6	7	4	6	8	4	6	3	7	9	7
1-6	C	8	7	4	5	7	2	3	5	8	3	6	8	10	3	2	2	10	5	2	7	3	7	3	7	6	9	2	4	10	10	5	1	6	8	3
1-7	C	8	9	3	1	8	1	2	3	9	7	6	3	9	10	4	9	9	7	4	4	1	3	4	4	2	2	9	10	6	2	1	3	3	8	9
1-8	C	4	10	4	3	5	2	10	4	8	5	1	10	5	10	1	3	4	2	9	10	5	10	9	9	2	3	4	7	4	5	9	7	4	6	5
1-9	C	7	5	10	9	3	9	2	6	4	4	10	3	2	6	6	6	5	3	1	2	2	9	6	3	5	5	8	1	5	9	4	7	4	5	2
1-10	C	10	10	10	10	10	5	2	3	9	3	1	8	1	2	4	2	10	9	6	8	9	8	5	8	6	8	3	2	8	4	8	5	8	4	4
2-2	C	4	3	8	9	2	1	9	4	5	3	2	6	10	5	10	10	5	6	3	9	8	4	10	1	1	6	2	4	8	4	1	3	3	7	1
2-3	C	4	8	1	10	7	10	8	10	10	3	7	10	2	9	6	8	7	1	3	3	1	7	4	3	9	9	2	8	6	7	9	9	2	8	3
2-4	C	5	4	7	6	5	10	10	4	6	10	2	3	3	3	10	10	9	9	7	3	7	2	10	10	1	7	9	4	4	3	7	4	9	3	3
2-5	C	7	4	7	4	7	1	3	1	7	8	3	9	3	5	2	8	4	8	1	3	2	9	2	5	8	9	1	4	8	5	3	3	2	6	4
2-6	C	4	1	2	5	1	4	8	6	10	3	7	2	4	2	9	8	10	9	8	7	5	5	3	9	2	10	6	3	6	9	3	9	2	9	2
2-7	C	10	8	5	5	3	1	6	8	3	4	4	3	10	9	8	9	3	6	3	7	9	7	10	1	4	8	1	4	9	6	7	6	1	7	2
2-8	C	9	1	10	1	2	2	8	7	5	4	9	2	10	10	3	6	5	8	10	3	8	7	3	6	9	1	3	7	7	7	7	3	5	3	4
Decay Level 4																																			
1-4	20	1	7	9	2	2	5	6	8	9	4	10	2	5	1	8	6	4	7	7	8	7	1	1	4	9	4	4	10	9	1	3	8	1	7	3
1-5	20	9	3	4	1	9	10	3	10	9	5	2	10	8	3	3	9	10	9	3	10	5	7	9	8	7	2	8	3	3	6	5	8	2	2	6
1-1	10	9	3	6	1	3	5	4	9	1	5	3	9	7	1	3	3	6	9	8	4	3	2	1	2	4	5	4	4	8	3	7	2	9	2	9
2-1	0	8	6	5	5	6	6	10	8	6	10	2	8	2	4	3	7	3	9	8	5	8	1	10	4	8	10	4	5	1	2	4	1	2	4	1
1-2	C	8	9	4	1	4	4	5	1	3	4	6	3	9	10	7	5	5	7	2	5	6	8	1	8	10	10	10	5	8	3	9	6	8	4	4
1-3	C	1	6	2	10	9	8	10	6	8	1	7	10	10	5	8	9	4	1	5	9	1	6	6	6	10	5	3	6	6	4	2	2	1	6	4
1-6	C	1	2	3	8	4	3	10	1	3	6	1	3	9	2	4	2	6	5	8	7	5	4	9	1	4	6	1	7	5	6	6	5	10	9	2
1-7	C	6	2	10	8	6	7	9	5	4	5	1	3	2	2	9	2	10	3	10	1	8	6	3	6	10	10	1	7	1	2	9	6	4	2	2
1-8	C	6	1	5	9	6	10	8	6	1	5	1	2	10	7	4	4	10	5	7	2	10	8	8	7	3	4	6	5	10	3	7	6	6	8	7
1-9	C	5	3	1	6	7	2	10	5	8	3	4	5	1	9	5	10	2	4	10	6	3	2	2	4	7	3	3	5	3	2	4	9	1	4	8
1-10	C	2	2	4	6	5	6	1	3	2	5	7	10	1	5	4	2	8	7	9	5	2	5	10	6	2	1	2	5	5	3	7	6	2	6	4
2-2	C	4	3	8	9	2	1	9	4	5	3	2	6	10	5	10	10	5	6	3	9	8	4	10	1	1	6	2	4	8	4	1	3	3	7	1
2-3	C	4	8	1	10	7	10	8	10	10	3	7	10	2	9	6	8	7	1	3	3	1	7	4	3	9	9	2	8	6	7	9	9	2	8	3
2-4	C	5	4	7	6	5	10	10	4	6	10	2	3	3	3	10	10	9	9	7	3	7	2	10	10	1	7	9	4	4	3	7	4	9	3	3
2-5	C	7	4	7	4	7	1	3	1	7	8	3	9	3	5	2	8	4	8	1	3	2	9	2	5	8	9	1	4	8	5	3	3	2	6	4
2-6	C	4	1	2	5	1	4	8	6	10	3	7	2	4	2	9	8	10	9	8	7	5	5	3	9	2	10	6	3	6	9	3	9	2	9	2
2-7	C	10	8	5	5	3	1	6	8	3	4	4	3	10	9	8	9	3	6	3	7	9	7	10	1	4	8	1	4	9	6	7	6	1	7	2
2-8	C	9	1	10	1	2	2	8	7	5	4	9	2	10	10	3	6	5	8	10	3	8	7	3	6	9	1	3	7	7	7	7	3	5	3	4

Table F1. continued

WALL	1	2	3	4	5	6	7	8	9	10	11	12	13	14	15	16	17	18	19	20	21	22	23	24	25	26	27	28	29	30	31	32	33	34	35
Decay Level 5																																			
1-4	30	2	1	8	4	6	7	9	8	9	8	2	8	9	9	4	4	8	4	9	4	7	7	8	5	1	5	3	4	1	8	1	4	5	6	8
1-5	30	2	5	1	2	5	6	3	6	6	8	6	7	2	3	7	3	3	8	9	6	6	8	5	1	8	1	6	7	5	3	9	6	3	2	7
1-1	20	7	7	10	1	8	10	7	3	5	1	1	5	4	10	2	4	10	2	6	2	3	7	6	9	4	4	2	8	10	5	4	9	7	1	1
2-1	10	3	7	8	4	8	5	3	4	9	1	4	2	8	7	4	9	7	1	5	9	1	5	3	9	5	5	3	1	7	7	10	9	5	10	10
1-2	C	6	6	4	6	6	8	2	10	9	5	1	9	6	8	9	5	2	5	2	9	10	9	8	3	8	6	4	9	1	7	8	1	1	6	7
1-3	C	4	5	5	3	8	5	9	4	8	2	2	7	9	8	9	9	8	8	2	9	4	9	10	9	4	5	1	5	1	7	9	6	1	4	9
1-6	C	9	8	4	6	9	3	6	5	3	5	8	9	7	4	7	6	3	8	4	1	3	1	8	7	1	9	2	8	10	5	4	6	7	6	2
1-7	C	10	5	8	3	9	2	5	10	8	5	3	6	5	9	6	1	4	7	5	8	3	3	10	7	3	6	9	5	5	3	1	3	10	7	4
1-8	C	9	8	1	3	7	6	8	8	10	10	6	9	6	7	10	3	6	8	3	1	6	4	7	4	4	6	6	7	9	3	5	2	9	5	10
1-9	C	7	5	8	5	6	7	4	6	1	6	10	2	4	8	7	4	6	7	4	1	3	7	8	1	5	7	9	5	2	5	9	9	4	8	8
1-10	C	4	4	3	2	9	7	9	5	2	4	7	3	5	10	8	9	2	9	1	5	4	8	9	5	7	8	4	9	7	2	6	3	7	8	9
2-2	C	9	3	8	6	6	5	3	7	7	8	5	6	4	6	8	6	8	6	5	7	6	8	8	9	5	6	4	5	4	6	6	8	1	4	9
2-3	C	8	10	3	4	4	3	7	4	7	7	8	3	7	2	3	2	8	7	5	10	1	4	2	7	6	3	7	10	8	2	10	7	5	4	2
2-4	C	8	7	8	3	6	4	4	9	3	9	2	8	1	8	4	1	4	6	9	2	7	1	7	5	1	6	4	10	7	8	5	6	1	3	4
2-5	C	4	7	5	7	8	3	8	4	2	8	5	7	3	3	2	3	9	7	10	1	8	4	4	6	2	3	2	10	9	2	5	8	10	2	9
2-6	C	8	10	9	10	5	2	10	9	1	3	4	1	2	3	3	4	1	5	8	4	10	4	6	5	9	4	9	2	2	1	3	8	8	6	7
2-7	C	10	7	10	2	9	5	6	7	1	4	4	9	5	5	7	4	6	6	8	8	3	4	5	7	3	3	4	5	1	1	2	7	2	9	3
2-8	C	4	7	6	1	1	7	10	7	3	2	3	10	10	4	3	8	10	7	8	10	6	4	4	9	3	2	5	8	1	9	7	9	7	1	4
Decay Level 6																																			
1-4	30	10	4	5	9	8	5	5	1	1	10	1	8	7	8	8	7	5	4	10	5	9	1	9	10	10	3	2	10	7	7	7	1	7	2	8
1-5	30	2	4	5	1	4	1	4	2	4	1	1	2	3	3	1	4	7	4	3	4	3	7	5	2	7	9	10	9	10	2	5	1	5	5	4
1-1	30	2	9	1	8	9	3	5	6	2	5	8	8	2	8	4	9	9	9	9	7	7	8	3	3	2	6	7	1	7	8	2	9	9	9	5
2-1	20	8	4	5	1	6	6	8	8	4	4	3	2	8	8	7	3	9	8	7	9	9	4	7	3	8	6	6	1	10	6	4	4	4	3	5
1-2	C	7	6	1	7	9	4	7	1	2	8	5	2	10	10	2	4	6	1	5	2	3	4	2	9	6	6	5	10	1	2	3	4	10	10	5
1-3	C	8	8	1	3	6	9	1	5	8	7	5	3	5	3	6	5	5	5	4	9	1	9	3	7	5	3	6	10	7	6	5	10	2	9	3
1-6	C	3	6	9	1	7	8	2	10	8	5	6	4	7	3	3	2	7	3	3	6	4	1	6	7	7	10	7	7	3	8	8	8	5	3	1
1-7	C	9	6	5	5	9	7	7	2	10	6	1	4	9	5	7	8	2	10	7	4	5	3	5	6	4	3	1	10	1	10	6	3	9	10	3
1-8	C	6	5	2	5	1	9	8	2	4	7	6	4	4	7	3	1	5	4	5	2	8	1	7	1	8	7	1	5	5	1	7	4	1	9	8
1-9	C	4	2	4	5	3	10	8	9	3	9	2	3	2	1	4	4	7	9	9	6	5	10	8	1	6	9	5	1	4	2	4	3	1	2	9
1-10	C	3	2	8	3	8	4	2	7	7	2	7	5	4	10	7	7	4	6	5	9	4	5	3	9	7	8	8	5	4	2	10	6	6	1	8
2-2	C	3	9	5	2	4	5	6	5	2	4	3	9	2	2	9	8	3	6	1	4	8	8	1	4	4	9	7	3	1	1	2	7	6	2	2
2-3	C	4	9	2	3	8	5	8	9	5	5	2	5	9	3	7	6	5	8	1	1	6	2	1	9	9	1	3	7	8	1	4	7	3	9	2
2-4	C	6	6	2	4	6	4	1	1	7	7	4	8	4	1	8	5	2	8	1	1	3	7	5	6	1	2	4	9	9	7	7	1	3	3	4
2-5	C	5	6	5	3	4	5	7	5	2	4	2	9	9	4	6	2	9	9	6	8	6	3	3	6	1	9	4	9	2	8	2	9	2	2	7
2-6	C	8	1	1	4	7	1	7	3	4	2	8	1	2	6	1	4	4	2	6	9	6	5	4	6	1	1	9	6	8	9	7	5	4	7	9
2-7	C	7	9	7	7	4	7	8	5	5	6	8	4	3	3	1	7	1	2	4	1	7	6	3	2	8	1	1	7	4	1	4	6	8	6	9
2-8	C	8	2	2	9	2	8	2	6	5	8	2	5	1	7	3	3	3	8	9	8	1	8	7	5	8	8	6	9	1	4	2	1	8	6	4

Table F1. continued

WALL		1	2	3	4	5	6	7	8	9	10	11	12	13	14	15	16	17	18	19	20	21	22	23	24	25	26	27	28	29	30	31	32	33	34	35
Decay Level 7																																				
1-1	C	8	10	9	8	7	7	4	5	9	6	1	6	8	5	1	9	2	5	3	6	7	2	6	2	9	4	6	9	2	10	5	6	2	8	1
1-2	C	5	3	2	7	10	5	7	2	3	8	9	10	9	2	9	1	9	6	5	5	5	7	10	2	7	7	2	3	1	4	6	3	10	10	2
1-4	C	2	7	2	9	4	2	10	6	10	7	10	3	8	4	9	5	6	2	9	5	3	7	8	7	4	1	10	3	8	8	8	6	1	10	3
1-5	C	6	3	4	4	1	5	8	3	4	8	1	4	9	8	7	7	8	5	1	10	10	10	5	3	10	9	1	3	4	7	4	4	3	10	2
1-3	C	3	3	2	9	5	8	8	10	9	1	2	10	4	2	4	4	5	2	7	9	5	9	1	2	6	3	1	8	8	9	8	3	4	1	6
1-6	C	10	2	3	9	3	4	5	4	6	2	9	3	7	3	6	3	1	9	10	2	2	5	3	3	4	9	3	1	3	4	6	9	10	4	9
1-7	C	1	2	4	2	4	5	9	7	1	9	1	4	6	10	4	3	4	8	3	3	4	7	10	9	9	8	1	8	1	7	1	1	9	9	5
2-1	C	10	10	6	7	4	2	9	7	10	5	2	6	5	8	5	2	9	5	1	7	9	2	3	9	1	8	4	7	6	4	5	5	3	1	1
2-2	C	1	4	6	4	4	1	7	7	9	1	5	6	2	2	3	6	7	2	5	10	4	7	4	1	4	5	9	8	9	1	3	3	9	1	1
2-3	C	8	6	6	6	1	3	1	3	5	4	2	6	5	7	3	2	4	1	8	8	2	3	8	3	5	10	10	9	3	7	7	2	5	9	2
2-4	C	8	3	10	10	4	7	6	5	9	9	7	4	9	7	4	9	5	5	5	4	5	2	7	9	7	3	8	8	8	5	1	2	10	5	6
2-5	C	2	8	10	2	2	2	4	3	4	1	3	1	5	3	5	7	1	9	9	4	7	10	3	2	3	2	5	9	10	9	10	4	8	8	2
2-6	C	9	1	7	6	4	2	6	1	5	5	5	10	6	2	2	4	3	2	3	5	1	10	2	9	8	9	8	6	10	10	9	7	1	1	5
2-7	C	9	1	5	4	9	5	1	1	7	3	9	9	6	4	8	10	7	6	9	1	10	7	1	10	10	1	10	6	8	9	4	1	2	9	4

Table F2. Typical CASHEW Input File for Decayed Wall

```
Level 6 Decay Decayed, OSB(15/32"), .113" diam @4"-12", 16"o.c. studs kips-in
4,                                          ! Analysis Control Parameter
96,2,                                       ! Height wall, Num of panels
1,48,96,.46875,24,48,3,7,180,               ! Panel 1 geo& material props.
2,48,96,.46875,72,48,3,5,180,               ! Panel 2 geo& material props.
1,1,                                        ! 1-1 Sole Plate connector prop
0.1529,0.02228,0.887,                       ! (DECAY)
2.8834,0.0372,-0.05,1.0,0.010,              !
0.58,1.0,                                   !
1,2,                                        ! 1-2 connector properties
0.1776,0.0371,0.412,                        !
4.3213,0.0306,-0.04,1.48,0.023,             !
0.46,1.1,                                   !
1,3,                                        ! 1-3 connector properties
0.1798,0.02698,0.437,                       !
3.8868,0.0336,-0.058,2.1,0.022,             !
0.54,1.1,                                   !
1,4,                                        ! 1-4 connector properties
0.121,0.02255,0.929,                        ! (DECAY)
2.309,0.101,-0.16,1.00,0.018,               !
0.42,1.0,                                   !
1,5,                                        ! 1-5 connector properties
0.1326,0.02731,0.881,                       ! (DECAY)
2.465,0.092,-0.065,1.10,0.019,              !
0.43,1.1,                                   !
1,6,                                        ! 1-6 connector properties
0.17985,.02825,0.865,                       !
2.859,0.0303,-0.2,0.99,0.0168,              !
0.55,1.10,                                  !
1,7,                                        ! 1-7 connector properties
0.21556,0.03173,0.4317,                     !
5.441,0.0356,-0.0335,1.47,0.016,            !
0.46,1.1,                                   !
1,8,                                        ! 1-8 connector properties
0.1574,.02825,0.4104,                       !
3.5597,0.0473,-0.06,1.654,0.025,            !
0.37,1.1,                                   !
1,9,                                        ! 1-9 connector properties
0.17985,.02825,0.865,                       !
2.859,0.0303,-0.2,0.99,0.0168,              !
0.55,1.10,                                  !
1,10,                                       ! 1-10 connector properties
0.1529,0.02228,0.887,                       !
2.8834,0.0372,-0.05,1.0,0.010,              !
0.58,1.0,                                   !
2,1,                                        ! 2-1 sole plate connector prop
0.17985,.02825,0.865,                       ! (DECAY)
2.859,0.0303,-0.2,0.99,0.0168,              !
0.55,1.10,                                  !
2,2,                                        ! 2-2 connector properties
0.1574,.02825,0.4104,                       !
3.5597,0.0473,-0.06,1.654,0.025,            !
0.37,1.1,                                   !
2,3,                                        ! 2-3 connector properties
0.1911,0.02582,0.391,                       !
3.940,0.0258,-0.046,1.32,0.031,             !
0.49,1.1,                                   !
2,4,                                        ! 2-4 connector properties
0.17985,.02825,0.865,                       !
```

```
2.859,0.0303,-0.2,0.99,0.0168,          !
0.55,1.10,                              !
2,5,                                    ! 2-5 connector properties
0.1574,.02825,0.4104,                   !
3.5597,0.0473,-0.06,1.654,0.025,        !
0.37,1.1,                               !
2,6,                                    ! 2-6 connector properties
0.1776,0.0371,0.412,                    !
4.3213,0.0306,-0.04,1.48,0.023,         !
0.46,1.1,                               !
2,7,                                    ! 2-7 connector properties
0.1529,0.02228,0.887,                   !
2.8834,0.0372,-0.05,1.0,0.010,          !
0.58,1.0,                               !
2,8,                                    ! 2-8 connector properties
0.1529,0.02228,0.887,                   !
2.8834,0.0372,-0.05,1.0,0.010,          !
0.58,1.0,                               !
1                                       ! Panel 1 connector placement
-47.625,-20.00,23.625,4.0,              ! Horizontal connector lines
47.625,-23.625,23.625,8.0,              !
45.750,-20.00,20.00,8.0,                !
-23.625,-47.625,4.00,8.0,               ! Vertical connector lines
-21.750,-44.00,-4.00,8.0,               !
-23.600,8.0000,40.00,8.0,               !
-21.700,-4.000,44.00,8.0,               !
-8.000,-36.00,36.00,12.0,               !
8.000,-36.000,36.00,12.0,               !
23.625,-44.00,44.00,4.0,                !
2                                       ! Panel 2 connector placement
-47.625,-23.625,23.625,4.0,             ! Horizontal connector lines
47.625,-23.625,23.625,8.0,              !
45.750,-20.00,20.00,8.0,                !
-23.625,-46.00,42.0,4.0,                ! Vertical connector lines
21.750,-40.00,40.00,8.0,                !
-8.000,-36.00,36.00,12.0,               !
8.000,-36.000,36.00,12.0,               !
23.625,-44.000,44.00,8.0,               !
9900                                    ! Number of Step Sizes
0.0    . . .                            ! Input Load Protocol
```

CASHEW output hysteretic parameters for each wall, as well as the cumulative energy dissipated by each of the walls. The hysteretic parameters for the walls are listed in Table F3-F9. The initial stiffnesses and peak capacities of each of the walls are ordered and fit with a normal distribution to create a distribution curve fit to the data. The common distribution function of the normal distribution for probability is:

$$f_x(x) = \frac{1}{\sqrt{2\pi}\sigma} \exp\left[-\frac{1}{2}\left(\frac{x-\mu}{\sigma}\right)^2\right]$$

where μ is the mean variable, and σ is the standard deviation of the variable. The ordered data points are listed for initial stiffness (Table F10) and for peak capacity (Table F11).

Table F3. Wall hysteretic parameters for decay condition 1.

Sample	K_o lb/in	F_u+ lb	Δ_u in	r_1	r_2	r_3	r_4	F_0 lb	F_l lb
1-1	15.87	6.79	1.89	0.057	-0.044	0.911	0.034	5.14	0.846
1-2	15.01	6.78	2.02	0.062	-0.059	0.907	0.042	5.01	0.826
1-3	14.89	6.46	1.86	0.045	-0.094	0.893	0.039	5.31	0.819
1-4	15.40	6.82	1.90	0.060	-0.099	0.935	0.036	5.12	0.832
1-5	16.70	6.65	1.83	0.045	-0.051	0.858	0.036	5.26	0.895
1-6	15.73	7.10	2.00	0.070	-0.063	0.939	0.040	4.92	0.898
1-7	14.75	6.77	3.35	0.032	-0.070	0.766	0.024	5.42	0.787
1-8	14.87	6.56	2.04	0.042	-0.037	0.847	0.038	5.36	0.812
1-9	14.19	6.33	1.89	0.037	-0.146	0.789	0.032	5.35	0.758
1-10	14.52	6.33	1.95	0.053	-0.055	0.830	0.035	4.90	0.821
1-11	14.21	6.24	2.02	0.045	-0.082	0.827	0.035	4.99	0.767
1-12	17.69	6.97	1.69	0.042	-0.047	0.860	0.035	5.71	0.858
1-13	15.40	6.53	2.03	0.047	-0.059	0.874	0.033	5.11	0.878
1-14	15.95	6.81	1.85	0.051	-0.062	0.921	0.038	5.39	0.853
1-15	16.24	6.59	1.85	0.047	-0.054	0.859	0.040	5.22	0.910
1-16	15.25	6.42	1.86	0.034	-0.111	0.826	0.032	5.50	0.781
1-17	15.64	6.69	1.80	0.043	-0.108	0.838	0.036	5.51	0.811
1-18	16.46	7.33	2.01	0.066	-0.055	0.890	0.035	5.24	0.908
1-19	15.57	6.65	1.79	0.060	-0.055	0.903	0.041	5.00	0.884
1-20	15.19	6.74	1.90	0.061	-0.055	0.899	0.035	5.03	0.892
1-21	15.02	6.65	2.15	0.048	-0.055	0.873	0.035	5.21	0.825
1-22	15.23	6.98	1.91	0.068	-0.069	0.920	0.037	5.06	0.839
1-23	15.76	6.63	2.08	0.036	-0.030	0.846	0.034	5.58	0.876
1-24	15.02	6.70	1.90	0.060	-0.065	0.935	0.040	5.04	0.825
1-25	17.00	7.22	1.86	0.057	-0.052	0.907	0.036	5.48	0.900
1-26	14.66	6.68	1.86	0.050	-0.160	0.855	0.031	5.35	0.774
1-27	14.48	6.28	2.01	0.047	-0.083	0.800	0.031	4.91	0.764
1-28	14.74	7.12	1.97	0.076	-0.071	0.905	0.038	5.03	0.849
1-29	16.01	7.42	2.04	0.064	-0.071	0.934	0.040	5.51	0.863
1-30	13.46	6.08	2.07	0.043	-0.106	0.783	0.028	4.93	0.747
Avg	15.36	6.71	1.98	0.052	-0.072	0.871	0.035	5.22	0.836
Std Dev	0.894	0.320	0.278	0.011	0.030	0.049	0.004	0.227	0.048
COV	0.058	0.048	0.140	0.218	-0.416	0.056	0.111	0.043	0.058

Table F4. Wall hysteretic parameters for decay condition 2.

Sample	K_o lb/in	F_u+ lb	Δ_u in	r_1	r_2	r_3	r_4	F_0 lb	F_l lb
2-1	15.13	6.78	1.80	0.061	-0.101	0.836	0.031	5.18	0.825
2-2	15.02	6.75	1.80	0.059	-0.068	0.889	0.035	5.22	0.825
2-3	16.08	6.55	1.89	0.048	-0.038	0.837	0.035	5.12	0.909
2-4	14.55	6.86	2.47	0.038	-0.045	0.778	0.029	5.66	0.851
2-5	16.13	6.64	1.87	0.058	-0.054	0.876	0.035	4.88	0.912
2-6	14.17	6.99	2.03	0.074	-0.116	0.912	0.035	4.95	0.825
2-7	14.39	6.42	1.97	0.048	-0.141	0.823	0.031	5.08	0.774
2-8	16.04	6.91	1.91	0.051	-0.056	0.836	0.030	5.36	0.880
2-9	16.22	6.83	2.00	0.051	-0.066	0.953	0.033	5.21	0.876
2-10	15.48	6.61	1.88	0.052	-0.058	0.883	0.037	5.14	0.856
2-11	15.87	6.83	1.92	0.054	-0.063	0.951	0.036	5.26	0.887
2-12	14.37	6.56	1.95	0.058	-0.191	0.813	0.033	5.00	0.770
2-13	15.49	7.24	2.12	0.067	-0.044	0.928	0.038	5.22	0.918
2-14	16.24	7.17	2.00	0.064	-0.046	0.932	0.032	5.16	0.869
2-15	14.69	6.53	2.05	0.055	-0.053	0.829	0.030	5.01	0.826
2-16	15.64	6.51	1.91	0.053	-0.060	0.856	0.036	4.99	0.877
2-17	15.28	6.42	2.15	0.046	-0.017	0.820	0.029	5.04	0.876
2-18	14.31	6.39	2.21	0.041	-0.035	0.865	0.033	5.23	0.808
2-19	14.83	6.60	1.93	0.052	-0.078	0.842	0.034	5.19	0.895
2-20	15.07	6.57	2.01	0.043	-0.068	0.827	0.036	5.43	0.822
2-21	16.24	7.52	2.25	0.063	-0.041	0.855	0.031	5.38	0.850
2-22	15.72	6.88	1.93	0.060	-0.065	0.883	0.038	5.19	0.898
2-23	15.46	6.44	2.00	0.045	-0.022	0.801	0.032	5.14	0.837
2-24	14.90	6.58	2.03	0.050	-0.150	0.917	0.032	5.10	0.777
2-25	13.82	6.50	3.32	0.026	-0.170	0.856	0.030	5.56	0.789
2-26	14.83	6.66	2.00	0.057	-0.032	0.895	0.029	5.04	0.810
2-27	15.80	6.50	1.91	0.049	-0.054	0.853	0.038	5.12	0.828
2-28	15.41	6.46	1.87	0.042	-0.078	0.895	0.035	5.25	0.850
2-29	14.10	6.49	2.00	0.053	-0.056	0.811	0.032	5.07	0.819
2-30	15.40	6.47	2.40	0.027	-0.033	0.819	0.028	5.64	0.823
Avg	15.22	6.69	2.05	0.052	-0.070	0.862	0.033	5.19	0.845
Std Dev	0.708	0.270	0.286	0.011	0.043	0.046	0.003	0.191	0.042
COV	0.047	0.040	0.140	0.204	-0.615	0.053	0.090	0.037	0.049

Table F5. Wall hysteretic parameters for decay condition 3.

Sample	K_o lb/in	F_u+ lb	Δ_u in	r_1	r_2	r_3	r_4	F_0 lb	F_i lb
3-1	16.58	6.76	1.90	0.048	-0.034	0.855	0.034	5.33	0.940
3-2	14.81	6.62	2.04	0.064	-0.099	0.912	0.035	4.75	0.779
3-3	15.91	6.76	1.91	0.065	-0.061	0.922	0.037	4.86	0.954
3-4	14.54	6.56	2.00	0.055	-0.071	0.934	0.031	5.11	0.790
3-5	16.22	6.57	1.95	0.051	-0.050	0.906	0.034	5.08	0.880
3-6	14.19	6.61	1.90	0.075	-0.074	0.877	0.034	4.71	0.788
3-7	14.58	6.57	1.87	0.067	-0.025	0.924	0.042	4.90	0.829
3-8	14.56	6.54	2.04	0.062	-0.068	0.940	0.036	4.85	0.858
3-9	15.30	6.85	2.04	0.074	-0.070	0.875	0.034	4.62	0.832
3-10	14.87	6.69	1.90	0.073	-0.057	0.908	0.042	4.70	0.843
3-11	14.89	6.29	1.96	0.052	-0.051	0.884	0.040	4.88	0.797
3-12	14.34	6.58	2.02	0.065	-0.061	0.905	0.033	4.78	0.811
3-13	14.11	6.73	2.04	0.074	-0.073	0.887	0.041	4.79	0.834
3-14	15.05	7.02	2.05	0.066	-0.053	0.918	0.034	5.30	0.856
3-15	15.60	7.26	2.29	0.067	-0.039	0.945	0.037	5.17	0.879
3-16	14.39	6.66	2.05	0.060	-0.068	0.887	0.036	5.03	0.795
3-17	15.91	7.15	1.80	0.077	-0.057	0.937	0.039	5.01	0.861
3-18	15.04	6.57	2.16	0.042	-0.042	0.883	0.037	5.37	0.849
3-19	14.80	7.07	1.92	0.077	-0.056	0.928	0.041	4.98	0.893
3-20	13.27	7.10	3.43	0.040	-0.183	0.827	0.032	5.57	0.831
3-21	15.19	6.95	1.85	0.079	-0.068	0.964	0.037	4.82	0.888
3-22	14.34	6.34	2.03	0.064	-0.050	0.890	0.033	4.60	0.809
3-23	14.75	6.89	2.59	0.047	-0.058	0.893	0.034	5.35	0.805
3-24	15.45	6.97	1.93	0.071	-0.037	0.928	0.035	4.90	0.839
3-25	13.87	6.57	2.00	0.068	-0.170	0.875	0.037	4.88	0.791
3-26	14.47	6.50	1.87	0.060	-0.052	0.825	0.034	4.95	0.813
3-27	14.49	6.56	1.94	0.057	-0.059	0.840	0.037	4.99	0.814
3-28	14.83	6.84	1.94	0.052	-0.066	0.919	0.039	5.50	0.810
3-29	14.67	6.58	1.96	0.074	-0.046	0.853	0.034	4.58	0.867
3-30	14.59	6.70	1.97	0.073	-0.072	0.982	0.037	4.75	0.866
Avg	14.85	6.73	2.05	0.063	-0.066	0.901	0.036	4.97	0.840
Std Dev	0.700	0.237	0.300	0.011	0.033	0.038	0.003	0.266	0.043
COV	0.047	0.035	0.147	0.172	-0.510	0.042	0.078	0.053	0.052

Table F6. Wall hysteretic parameters for decay condition 4.

Sample	K_o lb/in	F_u+ lb	Δ_u in	r_1	r_2	r_3	r_4	F_0 lb	F_1 lb
4-1	13.49	6.49	2.17	0.069	-0.063	0.915	0.032	4.61	0.778
4-2	14.73	6.76	1.91	0.074	-0.066	0.903	0.037	4.74	0.837
4-3	14.53	6.43	2.00	0.060	-0.090	0.888	0.035	4.73	0.761
4-4	13.28	6.32	2.04	0.060	-0.101	0.833	0.030	4.76	0.733
4-5	13.24	6.55	2.47	0.060	-0.022	0.856	0.030	4.77	0.783
4-6	14.19	6.32	1.97	0.054	-0.080	0.843	0.041	4.89	0.755
4-7	14.08	6.82	2.17	0.054	-0.032	0.929	0.033	5.41	0.831
4-8	13.77	6.21	2.04	0.061	-0.052	0.856	0.041	4.58	0.788
4-9	16.10	7.13	2.10	0.060	-0.045	0.898	0.033	5.29	0.818
4-10	13.94	6.34	2.10	0.048	-0.112	0.816	0.036	5.08	0.788
4-11	14.41	6.93	1.85	0.065	-0.091	0.886	0.034	5.30	0.804
4-12	15.42	6.64	1.92	0.053	-0.141	0.890	0.035	5.19	0.824
4-13	15.97	6.71	1.92	0.054	-0.079	0.874	0.037	5.18	0.847
4-14	14.50	6.74	2.11	0.065	-0.044	0.891	0.034	4.85	0.846
4-15	13.83	6.32	1.96	0.067	-0.138	0.891	0.036	4.58	0.766
4-16	14.59	6.59	1.93	0.054	-0.122	0.813	0.032	5.16	0.731
4-17	15.37	6.91	1.89	0.064	-0.056	0.939	0.038	5.18	0.888
4-18	15.22	6.60	1.80	0.048	-0.021	0.849	0.038	5.36	0.822
4-19	16.12	7.19	1.89	0.054	-0.106	0.852	0.029	5.64	0.834
4-20	13.68	6.33	1.90	0.064	-0.084	0.884	0.036	4.83	0.782
4-21	14.58	6.87	1.94	0.075	-0.045	0.976	0.039	4.84	0.843
4-22	13.33	6.18	2.11	0.053	-0.123	0.770	0.024	4.81	0.715
4-23	13.96	6.58	1.97	0.071	-0.161	0.901	0.038	4.75	0.790
4-24	15.69	7.03	2.06	0.057	-0.123	0.847	0.030	5.26	0.780
4-25	14.92	6.50	1.95	0.068	-0.058	0.863	0.032	4.61	0.784
4-26	16.16	7.17	2.18	0.046	-0.043	0.842	0.035	5.69	0.848
4-27	15.63	6.78	2.33	0.044	-0.043	0.846	0.034	5.40	0.819
4-28	13.27	6.16	2.20	0.055	-0.033	0.818	0.029	4.61	0.781
4-29	14.38	6.16	2.01	0.064	-0.057	0.869	0.040	4.38	0.838
4-30	14.03	6.41	2.16	0.059	-0.067	0.924	0.033	4.77	0.791
Avg	14.55	6.61	2.04	0.059	-0.076	0.872	0.034	4.97	0.800
Std Dev	0.93	0.31	0.15	0.008	0.038	0.043	0.004	0.34	0.040
COV	0.06	0.05	0.07	0.134	-0.497	0.049	0.112	0.07	0.050

Table F7. Wall hysteretic parameters for decay condition 5.

Sample	K_o lb/in	F_u+ lb	Δ_u in	r_1	r_2	r_3	r_4	F_0 lb	F_I lb
5-1	15.25	6.83	2.02	0.072	-0.068	0.951	0.037	4.68	0.811
5-2	15.16	6.44	1.88	0.058	-0.055	0.958	0.034	4.91	0.788
5-3	14.07	5.92	1.99	0.034	-0.062	0.867	0.033	5.09	0.724
5-4	13.19	5.97	2.10	0.055	-0.087	0.838	0.033	4.59	0.769
5-5	13.37	5.84	2.19	0.043	-0.094	0.839	0.035	4.73	0.686
5-6	14.27	6.18	2.05	0.051	-0.048	0.912	0.031	4.83	0.753
5-7	14.53	6.43	2.04	0.063	-0.063	0.935	0.041	4.69	0.768
5-8	15.78	6.38	1.84	0.047	-0.054	0.927	0.036	5.13	0.768
5-9	12.85	6.07	2.31	0.050	-0.047	0.927	0.038	4.82	0.765
5-10	14.92	6.30	1.90	0.065	-0.051	0.874	0.034	4.55	0.835
5-11	13.47	5.97	1.85	0.053	-0.045	0.908	0.038	4.77	0.751
5-12	14.95	6.22	1.92	0.051	-0.146	0.857	0.034	4.94	0.748
5-13	14.59	6.72	1.98	0.065	-0.058	0.912	0.041	5.02	0.844
5-14	13.79	5.98	1.85	0.049	-0.091	0.844	0.035	4.83	0.705
5-15	14.47	6.07	1.99	0.046	-0.066	0.915	0.038	4.83	0.733
5-16	14.11	5.89	2.09	0.043	-0.061	0.887	0.035	4.81	0.749
5-17	14.06	6.20	1.92	0.068	-0.054	0.888	0.039	4.50	0.756
5-18	14.64	6.30	1.87	0.056	-0.076	0.955	0.037	4.96	0.767
5-19	12.84	5.85	2.20	0.048	-0.042	0.913	0.032	4.65	0.697
5-20	13.59	5.98	2.09	0.029	-0.141	0.914	0.031	5.30	0.683
5-21	14.61	6.29	1.93	0.061	-0.064	0.987	0.040	4.66	0.784
5-22	16.36	7.17	1.91	0.053	-0.032	0.858	0.034	5.54	0.880
5-23	13.70	5.46	2.05	0.016	-0.114	0.804	0.029	5.08	0.688
5-24	14.65	5.92	2.03	0.043	-0.091	0.983	0.041	4.75	0.747
5-25	15.22	6.83	2.13	0.061	-0.065	0.955	0.041	5.08	0.815
5-26	14.84	6.26	1.88	0.052	-0.088	0.881	0.038	4.87	0.772
5-27	14.47	6.37	1.85	0.050	-0.052	0.923	0.039	5.02	0.839
5-28	14.99	6.10	1.88	0.043	-0.057	0.813	0.029	4.96	0.723
5-29	12.86	5.90	2.20	0.049	-0.048	0.820	0.031	4.67	0.712
5-30	14.52	6.70	2.00	0.077	-0.155	0.862	0.039	4.58	0.820
Avg	14.34	6.22	2.00	0.052	-0.072	0.897	0.036	4.86	0.763
Std Dev	0.858	0.364	0.125	0.012	0.031	0.050	0.004	0.232	0.050
COV	0.060	0.059	0.062	0.241	-0.431	0.055	0.102	0.048	0.066

Table F8. Wall hysteretic parameters for decay condition 6.

Sample	K_o lb/in	F_u+ lb	Δ_u in	r_1	r_2	r_3	r_4	F_0 lb	F_I lb
6-1	13.49	6.11	2.47	0.044	-0.062	0.824	0.029	4.86	0.724
6-2	13.15	5.55	2.38	0.040	-0.032	0.828	0.030	4.47	0.670
6-3	14.85	6.46	2.02	0.072	-0.075	0.927	0.037	4.45	0.807
6-4	13.36	5.67	1.85	0.041	-0.051	0.867	0.036	4.75	0.732
6-5	13.38	5.34	2.03	0.026	-0.061	0.909	0.034	4.77	0.693
6-6	13.96	6.30	2.04	0.071	-0.138	0.898	0.035	4.38	0.791
6-7	14.80	5.96	1.87	0.034	-0.111	0.838	0.028	5.18	0.692
6-8	14.97	5.89	1.91	0.037	-0.139	0.876	0.031	4.94	0.729
6-9	14.44	5.94	1.99	0.050	-0.054	0.919	0.032	4.66	0.728
6-10	13.99	5.16	1.75	0.022	-0.054	0.866	0.032	4.68	0.692
6-11	15.87	6.20	1.85	0.039	-0.070	0.904	0.033	5.18	0.754
6-12	14.41	5.92	1.99	0.038	-0.089	0.973	0.037	4.94	0.719
6-13	13.60	5.90	1.94	0.037	-0.140	0.908	0.035	5.05	0.710
6-14	13.84	5.65	2.11	0.024	-0.053	0.806	0.031	5.03	0.736
6-15	14.39	6.44	1.98	0.049	-0.034	0.888	0.036	5.06	0.849
6-16	13.60	6.09	2.00	0.061	-0.048	0.894	0.034	4.57	0.755
6-17	13.97	5.90	2.15	0.029	-0.151	0.804	0.032	5.18	0.679
6-18	13.52	6.11	2.01	0.060	-0.181	0.855	0.038	4.56	0.715
6-19	12.84	5.62	2.07	0.041	-0.090	0.853	0.036	4.69	0.692
6-20	14.46	5.63	1.63	0.027	-0.056	0.856	0.028	5.11	0.686
6-21	14.08	6.25	2.09	0.041	-0.035	0.823	0.033	5.21	0.780
6-22	13.54	5.69	2.34	0.041	-0.044	0.796	0.031	4.55	0.667
6-23	13.72	5.90	2.04	0.046	-0.128	0.870	0.031	4.76	0.717
6-24	13.19	5.74	1.93	0.061	-0.074	0.920	0.046	4.31	0.745
6-25	13.97	5.95	1.94	0.060	-0.055	0.857	0.033	4.46	0.725
6-26	14.75	6.05	1.86	0.045	-0.043	0.864	0.040	4.90	0.735
6-27	13.59	5.83	1.89	0.037	-0.062	0.891	0.037	4.97	0.658
6-28	13.90	5.95	2.04	0.060	-0.073	0.934	0.039	4.36	0.755
6-29	14.79	6.11	1.96	0.055	-0.049	0.922	0.037	4.68	0.782
6-30	13.93	5.97	1.96	0.043	-0.092	0.868	0.033	4.93	0.705
Avg	14.01	5.91	2.00	0.044	-0.078	0.875	0.034	4.79	0.727
Std Dev	0.658	0.294	0.171	0.013	0.040	0.043	0.004	0.273	0.044
COV	0.047	0.050	0.086	0.301	-0.508	0.049	0.113	0.057	0.060

Table F9. Wall hysteretic parameters for decay condition 7.

Sample	K_o lb/in	F_u+ lb	Δ_u in	r_1	r_2	r_3	r_4	F_0 lb	F_1 lb
X-1	12.24	5.10	1.96	0.050	-0.069	0.924	0.034	4.01	0.653
X-2	11.60	5.08	2.09	0.046	-0.086	0.890	0.042	4.17	0.650
X-3	11.32	4.81	1.85	0.041	-0.069	0.886	0.043	4.11	0.626
X-4	11.70	4.91	1.76	0.051	-0.072	0.956	0.037	4.04	0.637
X-5	12.18	5.06	2.10	0.039	-0.082	1.001	0.041	4.23	0.706
X-6	11.07	5.23	3.02	0.042	-0.086	0.759	0.025	3.90	0.593
X-7	11.35	4.78	1.79	0.042	-0.047	0.852	0.041	4.02	0.625
X-8	11.34	4.68	1.83	0.042	-0.047	0.803	0.035	3.92	0.641
X-9	11.15	4.74	2.11	0.034	-0.088	0.877	0.038	4.09	0.605
X-10	13.62	5.00	1.75	0.015	-0.075	0.866	0.038	4.76	0.660
X-11	11.45	4.62	2.16	0.014	-0.072	0.835	0.036	4.38	0.678
X-12	12.15	4.93	1.94	0.031	-0.101	0.982	0.040	4.33	0.661
X-13	12.32	4.91	1.86	0.040	-0.055	0.867	0.041	4.13	0.701
X-14	11.91	4.87	1.87	0.026	-0.117	0.859	0.035	4.43	0.611
X-15	12.18	4.83	1.70	0.039	-0.053	0.830	0.037	4.09	0.613
X-16	12.56	5.04	1.74	0.035	-0.115	0.880	0.036	4.40	0.640
X-17	11.98	5.13	2.07	0.045	-0.049	0.918	0.036	4.18	0.653
X-18	12.89	5.68	2.15	0.059	-0.053	0.906	0.034	4.18	0.708
X-19	12.10	5.16	1.88	0.061	-0.054	0.943	0.042	3.90	0.687
X-20	11.88	4.98	1.89	0.048	-0.061	0.943	0.037	4.06	0.702
X-21	11.15	4.63	2.03	0.037	-0.050	0.830	0.039	3.89	0.635
X-22	11.77	4.85	2.20	0.031	-0.068	0.856	0.037	4.17	0.652
X-23	11.41	4.91	2.36	0.023	-0.128	0.894	0.037	4.41	0.638
X-24	11.85	5.10	1.79	0.055	-0.083	0.908	0.037	4.09	0.662
X-25	12.00	5.02	1.88	0.049	-0.050	0.874	0.033	4.01	0.671
X-26	11.61	5.04	2.06	0.033	-0.104	0.986	0.040	4.40	0.651
X-27	10.50	4.81	1.95	0.033	-0.248	0.900	0.036	4.30	0.586
X-28	10.90	4.71	2.12	0.040	-0.104	0.843	0.035	3.86	0.595
X-29	11.58	4.91	1.97	0.037	-0.203	0.819	0.032	4.16	0.619
X-30	11.98	5.12	2.45	0.021	-0.073	0.908	0.036	4.63	0.688
Avg	11.79	4.96	2.01	0.039	-0.085	0.886	0.037	4.17	0.648
Std Dev	0.619	0.212	0.264	0.012	0.045	0.056	0.004	0.218	0.035
COV	0.052	0.043	0.131	0.302	-0.523	0.063	0.098	0.052	0.053

Table F10. Cumulative distribution function data points for initial stiffness.

Initial Stiffness								
Wall Type		Standard Shearwall						
Edge Distance		3/8"						
Nailing Schedule		4"-12						
G (ksi)		180						
Sheathing		OSB						
Thickness		15/32"						
Decay Condition		1	2	3	4	5	6	7
Unit		kips/in						
Fx(x)		Normal Distribution						
1	0.0323	13.4632	13.8158	13.269	13.243	12.842	12.8371	10.4971
2	0.0645	14.1923	14.0974	13.871	13.272	12.849	13.1530	10.9009
3	0.0968	14.2069	14.1713	14.113	13.283	12.857	13.1882	11.0688
4	0.1290	14.4819	14.3058	14.194	13.331	13.193	13.3645	11.1469
5	0.1613	14.5212	14.3736	14.339	13.486	13.368	13.3809	11.1544
6	0.1935	14.6637	14.3949	14.340	13.682	13.465	13.4915	11.3158
7	0.2258	14.7438	14.5466	14.391	13.771	13.591	13.5153	11.3428
8	0.2581	14.7467	14.6909	14.466	13.835	13.704	13.5410	11.3523
9	0.2903	14.8723	14.8260	14.487	13.942	13.789	13.5925	11.4129
10	0.3226	14.8924	14.8261	14.541	13.961	14.065	13.5970	11.4519
11	0.3548	15.0146	14.8993	14.561	14.028	14.066	13.6000	11.5781
12	0.3871	15.0170	15.0243	14.578	14.081	14.109	13.7184	11.5968
13	0.4194	15.0249	15.0749	14.592	14.195	14.271	13.8426	11.6138
14	0.4516	15.1854	15.1320	14.666	14.383	14.472	13.8956	11.7041
15	0.4839	15.2285	15.2799	14.755	14.413	14.472	13.9323	11.7687
16	0.5161	15.2507	15.4032	14.798	14.497	14.523	13.9564	11.8468
17	0.5484	15.3988	15.4059	14.806	14.531	14.528	13.9655	11.8847
18	0.5806	15.4038	15.4580	14.833	14.584	14.591	13.9710	11.9149
19	0.6129	15.5663	15.4753	14.871	14.593	14.609	13.9915	11.9757
20	0.6452	15.6407	15.4942	14.890	14.732	14.637	14.0844	11.9842
21	0.6774	15.7331	15.6390	15.039	14.916	14.646	14.3870	12.0038
22	0.7097	15.7594	15.7215	15.053	15.225	14.840	14.4146	12.0989
23	0.7419	15.8660	15.8006	15.189	15.372	14.924	14.4383	12.1475
24	0.7742	15.9541	15.8651	15.299	15.423	14.946	14.4569	12.1766
25	0.8065	16.0127	16.0369	15.453	15.630	14.991	14.7474	12.1794
26	0.8387	16.2391	16.0765	15.598	15.692	15.158	14.7923	12.2432
27	0.8710	16.4557	16.1264	15.907	15.974	15.222	14.7981	12.3179
28	0.9032	16.7004	16.2218	15.914	16.098	15.247	14.8515	12.5585
29	0.9355	16.9957	16.2352	16.215	16.124	15.778	14.9738	12.8918
30	0.9677	17.6864	16.2430	16.576	16.157	16.355	15.8678	13.6212
Mean		15.364	15.222	14.853	14.548	14.337	14.012	11.792
SD		0.894	0.708	0.700	0.925	0.858	0.658	0.619
VAR		0.80	0.50	0.49	0.86	0.74	0.43	0.38
COV		0.058	0.047	0.047	0.064	0.060	0.047	0.052
μ		15.363923	15.222047	14.853463	14.548357	14.336907	14.011547	11.791680
σ		0.894187	0.707853	0.700214	0.925489	0.858439	0.657663	0.618834

Table F11. Cumulative distribution function data points for peak capacity.

Peak Capacity								
Wall Type		Standard Shearwall						
Edge Distance		3/8"						
Nailing Schedule		4"-12						
G (ksi)		180						
Sheathing		OSB						
Thickness		15/32"						
Decay Condition		1	2	3	4	5	6	7
Unit		kips						
Fx(x)		Normal Distribution						
1	0.0323	6.0818	6.3878	6.293	6.156	5.457	5.1566	4.6191
2	0.0645	6.2365	6.4161	6.338	6.159	5.842	5.3392	4.6296
3	0.0968	6.2840	6.4208	6.498	6.184	5.849	5.5521	4.6831
4	0.1290	6.3262	6.4365	6.542	6.209	5.891	5.6192	4.7109
5	0.1613	6.3324	6.4635	6.559	6.315	5.897	5.6301	4.7385
6	0.1935	6.4159	6.4668	6.563	6.318	5.920	5.6513	4.7840
7	0.2258	6.4551	6.4946	6.566	6.318	5.924	5.6677	4.8130
8	0.2581	6.5268	6.5038	6.566	6.333	5.968	5.6906	4.8145
9	0.2903	6.5586	6.5039	6.569	6.342	5.972	5.7435	4.8311
10	0.3226	6.5935	6.5105	6.573	6.413	5.978	5.8331	4.8512
11	0.3548	6.6256	6.5275	6.577	6.429	5.983	5.8856	4.8689
12	0.3871	6.6496	6.5515	6.579	6.487	6.066	5.9005	4.9051
13	0.4194	6.6502	6.5600	6.610	6.495	6.072	5.9014	4.9062
14	0.4516	6.6518	6.5693	6.622	6.549	6.097	5.9020	4.9081
15	0.4839	6.6847	6.5815	6.659	6.579	6.176	5.9183	4.9126
16	0.5161	6.6865	6.5994	6.694	6.593	6.203	5.9404	4.9309
17	0.5484	6.7027	6.6095	6.700	6.601	6.215	5.9462	4.9827
18	0.5806	6.7450	6.6386	6.728	6.639	6.259	5.9493	5.0016
19	0.6129	6.7677	6.6646	6.761	6.706	6.288	5.9584	5.0208
20	0.6452	6.7844	6.7511	6.761	6.743	6.297	5.9694	5.0368
21	0.6774	6.7851	6.7836	6.839	6.761	6.299	6.0463	5.0444
22	0.7097	6.8107	6.8304	6.847	6.785	6.365	6.0903	5.0627
23	0.7419	6.8239	6.8324	6.894	6.816	6.376	6.1059	5.0800
24	0.7742	6.9724	6.8575	6.950	6.870	6.428	6.1087	5.0954
25	0.8065	6.9763	6.8797	6.967	6.911	6.444	6.1110	5.1043
26	0.8387	7.0972	6.9060	7.023	6.929	6.700	6.2015	5.1209
27	0.8710	7.1169	6.9928	7.069	7.025	6.723	6.2509	5.1327
28	0.9032	7.2208	7.1737	7.103	7.134	6.828	6.3009	5.1568
29	0.9355	7.3325	7.2370	7.146	7.168	6.835	6.4354	5.2265
30	0.9677	7.4192	7.5153	7.263	7.194	7.169	6.4593	5.6839
Mean		6.710	6.689	6.729	6.605	6.217	5.909	4.955
SD		0.320	0.270	0.237	0.308	0.364	0.294	0.212
VAR		0.10	0.07	0.06	0.09	0.13	0.09	0.05
COV		0.048	0.040	0.035	0.047	0.059	0.050	0.043
μ		6.710463	6.688849	6.728704	6.605397	6.217389	5.908838	4.955217
σ		0.320359	0.270369	0.237111	0.307586	0.364120	0.293808	0.212308

The energy dissipated by each wall is averaged at each cycle to provide the cumulative energy dissipated at each level of decay (Table F12). Showing the energy dissipated by each wall is somewhat too cumbersome, and the overall effect of decay can be seen though the average cumulative energy dissipated. The energy is calculated by CASHEW at each step size based on the area under the curve, which is the height of the curve times the difference between the current and past step size.

Table F12. Cumulative wall energy dissipated (lb·in.), parenthetical values are coefficients of variation.

Cyclic Loop #	Level 1	Level 2	Level 3	Level 4	Level 5	Level 6	Level 7
1	1333	1295	1290	1231	1247	1195	1008
	(0.093)	(0.083)	(0.079)	(0.083)	(0.097)	(0.084)	(0.086)
2	2041	1993	1992	1894	1905	1818	1547
	(0.093)	(0.08)	(0.077)	(0.078)	(0.094)	(0.082)	(0.084)
3	2750	2694	2697	2559	2565	2441	2087
	(0.092)	(0.079)	(0.076)	(0.076)	(0.093)	(0.082)	(0.083)
4	3459	3394	3401	3224	3225	3065	2627
	(0.092)	(0.078)	(0.076)	(0.075)	(0.092)	(0.082)	(0.083)
5	5807	5694	5684	5413	5401	5142	4387
	(0.086)	(0.074)	(0.072)	(0.072)	(0.089)	(0.077)	(0.078)
6	7020	6897	6889	6558	6525	6210	5308
	(0.085)	(0.073)	(0.071)	(0.07)	(0.087)	(0.076)	(0.077)
7	8234	8102	8096	7704	7652	7278	6230
	(0.084)	(0.072)	(0.07)	(0.069)	(0.086)	(0.076)	(0.077)
8	9448	9308	9302	8850	8778	8347	7152
	(0.084)	(0.071)	(0.07)	(0.068)	(0.085)	(0.075)	(0.076)
9	12872	12686	12648	12080	11948	11379	9725
	(0.078)	(0.067)	(0.066)	(0.065)	(0.081)	(0.07)	(0.071)
10	14613	14426	14382	13738	13561	12914	11050
	(0.077)	(0.066)	(0.065)	(0.064)	(0.08)	(0.07)	(0.07)
11	16355	16166	16118	15397	15174	14451	12376
	(0.076)	(0.065)	(0.064)	(0.063)	(0.079)	(0.069)	(0.07)
12	25471	25228	25057	24142	23618	22578	19264
	(0.064)	(0.054)	(0.054)	(0.057)	(0.069)	(0.058)	(0.059)
13	28781	28578	28384	27344	26674	25497	21797
	(0.063)	(0.053)	(0.053)	(0.056)	(0.068)	(0.057)	(0.058)
14	32091	31927	31710	30546	29729	28415	24331
	(0.062)	(0.052)	(0.053)	(0.055)	(0.067)	(0.057)	(0.057)
15	44272	44152	43891	42454	41068	39257	33545
	(0.055)	(0.046)	(0.047)	(0.052)	(0.062)	(0.052)	(0.051)
16	49106	49071	48771	47165	45511	43505	37249
	(0.055)	(0.045)	(0.047)	(0.051)	(0.062)	(0.051)	(0.051)
17	53938	53987	53649	51875	49952	47751	40952
	(0.054)	(0.045)	(0.047)	(0.05)	(0.061)	(0.051)	(0.05)
18 (total)	71577	72570	72353	69672	66803	63359	53911
	(0.064)	(0.048)	(0.046)	(0.055)	(0.065)	(0.054)	(0.059)

APPENDIX G – Hysteretic Parameters

The ten hysteretic parameters K_o, r_1 r_2 r_3, r_4, F_o, F_I, Δ_u, alpha (α) and beta (β). The parameters F_o, F_I, K_o, r_1 and r_2 define the backbone curve that encompasses the hysteretic loops; while r_3, r_4, Δ_u, alpha (α) and beta (β) define the hysteretic nature of the curves.

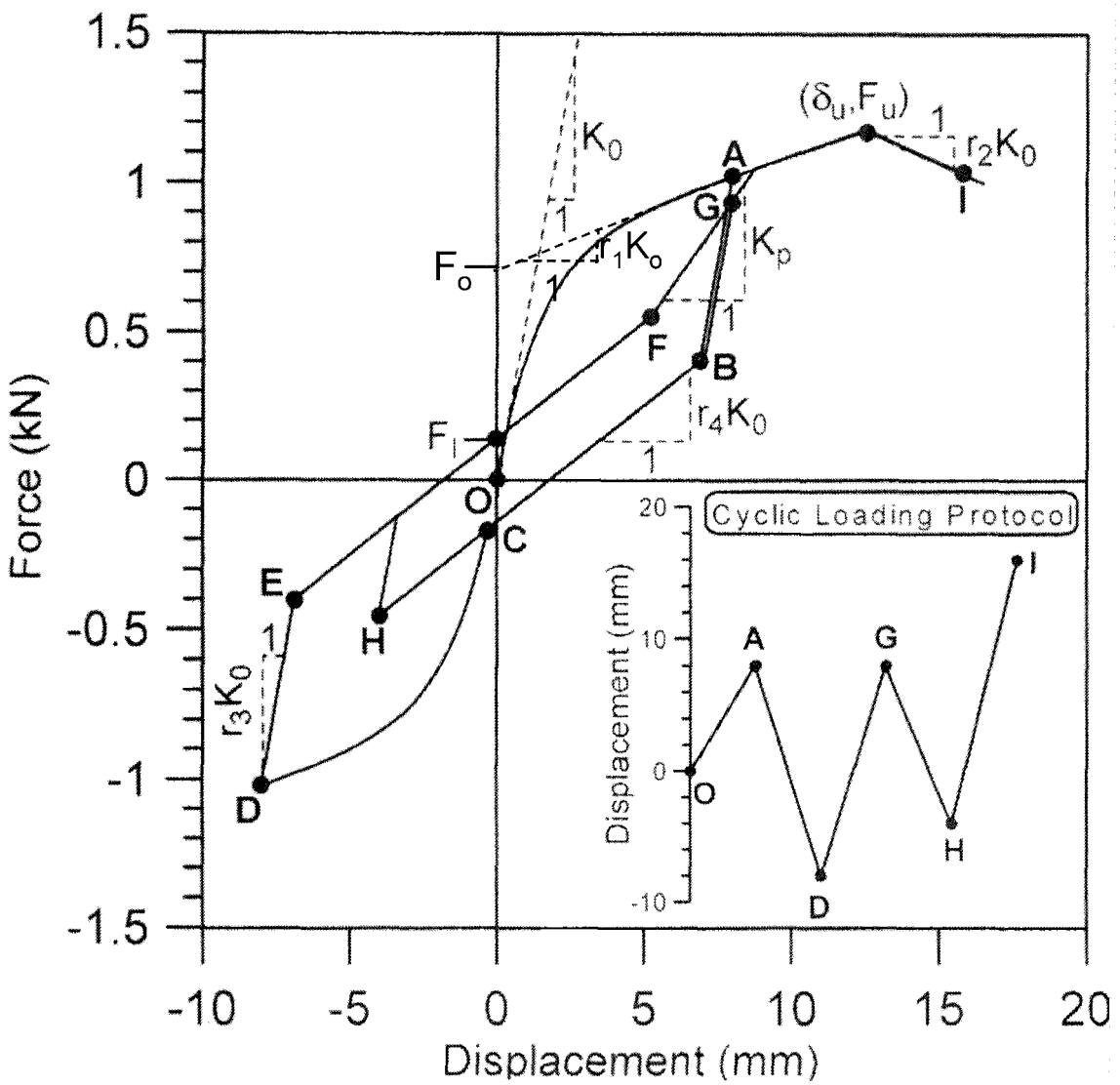

Fig. G1. Hysteretic parameters for connections and walls (modified from Folz and Filiatrault 2000).

Δ_u the displacement at peak capacity (F_u)

K_o the initial stiffness (the slope of the ascending branch of the first primary cycle between 2% and 40% of the maximum load)

r_1K_o the asymptotic stiffness (secondary stiffness)

r_2K_o the post ultimate capacity stiffness

r_3K_o the unloading stiffness

r_4K_o the pinching stiffness

F_I intercept for zero displacement

F_o force intercept of the asymptotic line

α stiffness degradation factor

β strength degradation factor.

In Fig. G1, the paths from OA and CD represent the pre-peak monotonic curve. Leading up to the peak from point A, the line tangent to the curve represents the secondary stiffness. The path from the peak (δ_u, F_u) to I represents the degradation stiffness. Unloading the specimen from A and D is represented by the paths DE and BG (the unloading stiffness), which are assumed to be elastic, followed by the pinching response. The paths EF and BH represent the pinching stiffness, which passes through the y-axis where the intercept is F_I (Folz and Filiatrault 2004a). The pinching stiffness (path BC) has a very low stiffness due to the previously induced crushing done to the framing members and sheathing panels around the connectors. Path FG represents the degrading K_p, which is less than K_o. K_p is defined as:

$$K_p = K_o \times \left(\frac{F_o / K_o}{\delta_{\max}} \right)^{\alpha} \qquad [1]$$

$$\delta_{\max} = \beta \delta_{un} \qquad [2]$$

K_p is a function of the previous loading history though the last unloading displacement δ_{un} (point A) with a corresponding force F_{un}. If in an additional cycle the connector reaches δ_{un}, then the corresponding load

will be less then F_{un} due to the strength and stiffness degradations α and β, which is seen by the difference between points A and G. At the same displacement, G has a lower strength and stiffness. Additional information can be found elsewhere (Folz and Filiatrault 2000, 2001, Filiatrault 1999, Dolan and Madsen 1991, Foschi 1970). The ten parameters provide the summary of the hysteretic response of a fastener and of a wall. The hysteretic parameters are found in this study by using SASHFIT (Elkins and Kim 2003), and are then used as input into CASHEW to determine the hysteretic parameters of a wall.

SASHFIT, developed by Jun Hee Kim at Oregon State University, is an excel spreadsheet that fits the primary loops of the load-slip curves created by the CUREE loading protocol. On any pinched hysteresis loop, there are 10 key points, with the exception of the maximum loop, which has 13 key points. By plotting the points, a fitted curve can be plotted through the points creating the fitted loop. The closer the points are to the actual values the better the curve will fit. To calculate these points, a series of equations are solved using eight of the hysteretic parameters with α and β to shape the curve.

Appendix H – Revisions to CASHEW

Cyclic Analysis of SHEar Walls (CASHEW) (Folz and Filiatrault 2000, 2001) is a program that predicts the load-displacement and energy dissipation of a shearwall subjected to a cyclic load, in this case the CUREE loading protocol. CASHEW uses the geometry of the wall, along with the shear modulus of the panels and the connection hysteresis parameters to predict the behavior of the walls. It is expected that due to an assumption that represents the nail as two uncoupled nonlinear springs CASHEW will slightly overestimate the force and stiffness developed by the connector, thus the shearwall. The output from CASHEW produces the hysteretic response of a full-scale shearwall subjected to the CUREE loading protocol based on the user-defined input consisting of the wall geometry, nailing schedule, material properties, and the sets of hysteretic parameters for the nailed connections. Other output includes the monotonic response, energy absorbed, and the load-displacement response when the wall is modeled as an equivalent single-degree of freedom system.

The original version of CASHEW was modified twice for this study. The original only allows one set of hysteretic connector properties to be assigned to the sheathing nails in a panel. The first modifications allowed for multiple sets of hysteretic connector properties to be assigned to the sheathing nails so different areas of the wall can have different properties. As this study progressed, CASHEW encountered three errors numerous times making the simulations very difficult to complete. The three errors included:

1. Global stiffness matrix not positive definite
2. Convergence not achieved
3. Step-size too large

The step-size error was the most common. In order to compensate for this, which would improve the success rate, the step-size was reduced until the

number of steps was tripled. To triple the step size, the CUREE protocol was expanded and entered as a user defined protocol using IANALY = 4.

By entering the CUREE protocol as a user defined loading protocol the output parameters were limited to only the first five parameters that describe the backbone response, but the parameters that describe the hysteretic behavior were not output. The source code was changed so the user defined protocol would call the entire 'hyster subroutine' rather than the first half. With this revision, eight of the parameters were output, but the α and β parameters were excluded. Since α and β are only shape parameters, they were deemed unnecessary for this study. Using the twice-modified CASHEW, different sets of nail parameters were incorporated into the program to allow the wall to experience decay and successfully complete the analysis, which was not possible with the original program.

Appendix I – Notation

A	cross-sectional area
D	global displacement vector
Ductility	Δ at P_{max} divided by Δ at P_{yield}
E	modulus of elasticity
d_a	anchorage slip
e_n	nail deformation
F	global force vector
F_I	zero displacement load-intercept
F_o	force intercept of the asymptotic line
F_u^+	maximum load in the positive quadrant
F_{un}	unloading force of a sheathing-connection in a previous cycle
f_{yb}	bending yield stress
G	modulus of rigidity
g	acceleration due to gravity
h	height of the wall
h/b	height-to width ratio of a shearwall
IO	immediate occupancy limit state (50 percent in 50 years)
K_o	initial stiffness of the hysteresis
K_p	re-loading degrading stiffness of a sheathing-connection
K_s	global secant stiffness matrix
LS	life safety limit state (10 percent in 50 years)
n	number tested samples
P_{max}	maximum load, peak capacity
P_{yield}	maximum load of the second primary cycle
R	response modification factor
r_1K_o	the asymptotic stiffness (secondary stiffness)
r_2K_o	the post ultimate capacity stiffness
r_3K_o	the unloading stiffness

r_4K_o	the pinching stiffness
S_{DS}	design spectral response acceleration
t	thickness
v	shear force at the top of the wall (lb/ft)
V	base shear
W	effective seismic weight
α	stiffness degradation factor
β	strength degradation factor
δ_{un}	unloading deformation of a sheathing-connection in a previous cycle
δ_{max}	maximum deformation of a sheathing-connector at a given cycle
Δ_a	deflection of a shearwall due to anchorage slip and rotation
Δ_b	bending deflection of the shearwall
Δ_m	displacement at which the applied load drops for the first time below 0.8 of the maximum load
Δ_n	deflection of a shearwall due to nail slip
Δ_{ref}	reference displacement for the CUREE load protocol, $0.6\Delta_m$
Δ_s	shearwall deflection
Δ_u	the displacement at the ultimate load
Δ_v	shear deflection of a shearwall
ξ	damping coefficient